UNIVERSIDADE DE LISBOA

FACULDADE DE CIÊNCIAS

DEPARTAMENTO DE QUÍMICA E BIOQUÍMICA

THEORETICAL STUDY OF THE REACTIVITY AND ENERGETICS OF ORGANIC RADICALS

Filipe Miguel Peres Agapito

DOUTORAMENTO EM QUÍMICA

(Química-Física)

2010

UNIVERSIDADE DE LISBOA

FACULDADE DE CIÊNCIAS

DEPARTAMENTO DE QUÍMICA E BIOQUÍMICA

THEORETICAL STUDY OF THE REACTIVITY AND ENERGETICS OF ORGANIC RADICALS

Filipe Miguel Peres Agapito

Tese orientada por

Prof. Dr. Benedito José Costa Cabral
Prof. Dr. José Artur de Sousa Martinho Simões

DOUTORAMENTO EM QUÍMICA

(Química-Física)

2010

to L. & B.

Resumo

Os radicais orgânicos são espécies importantes em quase todos os domínios da química e bioquímica. Contudo, apesar da sua existência ter sido documentada há mais de uma centena de anos, uma fracção significativa da energética destas espécies é ainda desconhecida. Uma propriedade termoquímica crucial no estudo de um radical é a entalpia associada à quebra da ligação (BDE) que dá origem a esse radical. Estas BDEs podem ser obtidas experimentalmente através de calorimetria fotoacústica (PAC). A química computacional também pode ser utilizada para fazer previsões rigorosas desta propriedade termoquímica. Os métodos teóricos permitem ainda o acesso directo à estrutura de radicais e compostos pais. Neste trabalho, PAC e química computacional foram utilizadas conjuntamente para estudar a energética de radicais orgânicos. A entalpia de formação padrão do radical ciclopentadienilo e a BDE C—H para o 1,3-ciclopentadieno foram reexaminadas. Foi avaliada a precisão de extrapolações para base completa de CCSD(T) e a de métodos de optimização com base na teoria do funcional da densidade. De seguida foi efectuado um estudo detalhado da energética do grupo alilo. Finalmente, foi estudado o efeito da tensão de anel em hidrocarbonetos cíclicos com cinco e seis membros e respectivos radicais.

Abstract

Organic radicals are important species in virtually every domain of chemistry and biochemistry. However, even though they have been known for more than 100 years, the energetic data for radicals typically have large uncertainties or are missing. One crucial thermochemical property in the study of a radical is the enthalpy associated with the bond cleavage (BDE) which originates that radical. BDEs can be obtained experimentally with photoacoustic calorimetry (PAC). Computational chemistry also provides reliable estimates of this thermochemical property. In addition, theoretical methods provide direct access to the structure of radicals and their parent compounds. In this work both PAC and computational chemistry were used to study the energetics of organic radicals. The standard enthalpy of formation for the cyclopentadienyl radical and the 1,3-cyclopentadienyl C—H BDE were re-examined. We proceeded to assess the accuracy of cost-efficient CCSD(T) complete basis set extrapolation schemes and density functional theory optimization methods for radicals. A detailed analysis of the energetics of the allyl moiety was then conducted. Finally, the effect of ring strain on five- and six-membered ring hydrocarbons and respective radicals was discussed.

Preface

In the first months of graduate work I took part in a study of the energetics of the cyclopentadienyl radical [J. Phys. Chem. A **110**, 5130 (2006)], an important ligand in organometallic chemistry. While doing this research it became apparent to us that the energetics of radicals in the vicinity of double bonds had not been thoroughly studied. In addition, some (unpublished) calculations performed for the 1,2,3,4,5-pentamethylcyclopenta-2,4-dien-1-yl radical at that time revealed that the interaction between the allylic moiety and methyl groups was not trivial. By that time we were aware that some terpenes (*viz.* terpinolene, α-terpinene, and γ-terpinene) had relevant antioxidant activity. This activity was related to the formation of terpenyl radicals featuring the allylic moiety near alkyl groups. In addition, the body of this terpenes comprises unsaturated rings, and energetic data for such radicals was both scarce and inaccurate.

In order to understand the antioxidant capabilities of these compounds a stepwise research program was designed. Initially we investigated if the theoretical methods used for the study of cyclopentadienyl could be improved, while remaining cost-effective for large molecules [THEOCHEM **811**, 361 (2007)]. We then proceeded to study small compounds containing the allylic moiety [J. Org. Chem. **72**, 8770 (2007)], followed by a work on the bond dissociation enthalpies in five- and six-membered ring hydrocarbons [J. Org. Chem. **73**, 6213 (2008)]. This is still an ongoing project, and we continue to work on this line, comparing the stabilizing effect of allyl and benzyl groups in organic radicals, and analyzing the structure and energetics of terpenes. Along the way we evaluated critical thermochemical data and gained a deeper understanding of the energetics of carbon radicals.

The timeline of this research is recovered in the present dissertation, which therefore collects the main body of my graduate work, performed between October 2005 and November 2009. Chapter 1 is a general introduction to radical energetics and to the methods used in its study, preeminently photoacoustic calorimetry. Theoretical methods are then discussed in Chapter 2. Chapters 3, 4, 5, and 6 comprise commented facsimiles of the aforementioned articles.

All research was conducted at the Molecular Energetics Group (MEG) and the Group of Mathematical Physics (GFM) of the University of Lisbon, under the supervision of Prof. José Artur Martinho Simões and Prof. Benedito José Costa Cabral, in close collaboration with other members of MEG, namely, Dr. Paulo M. Nunes and Prof. Rui M. Borges dos Santos.

F.A.

Lisbon
December 2009

Acknowledgements

First of all I want to thank Prof. Benedito José Costa Cabral and Prof. José Artur Martinho Simões who have always been there to help me and to steer me in the right direction. It has been a privilege to work with both of them during all these years. They have deeply influenced my perception of science and teaching and I will always treasure the lessons they have taught me.

I was very lucky to share my time in CIUL and FCUL with so many wonderful people to whom I am thankful. They are too many to name all (fortunately) but I wish to thank Hugo Martiniano, Margarida Mateus, Nuno Galamba, Paulo Couto, Rui Borges, Rui Centeno, Rafael Barreto, Ricardo Mata, and Sílvia Estácio particularly for being good colleagues and even better friends.

Special thanks to my longtime friends Bruno Pedras, Eva Lourenço, and João Tiago for always being there for me, and to my parents, brother, and family for supporting me and making all this possible in the first place.

Last but definitely not least, my deepest thanks to my dear wife Marina for her unlimited and unconditional support, for putting up with me, for making me laugh when I'm down, and for all the precious good times together.

Thank you all!
F.A.

Contents

CHAPTER 1

Radical energetics

1.1 Organic radicals

Radicals (often referred to as free radicals) are species that have unpaired electrons.[1] The first organic radical ever reported, triphenylmethyl, was discovered in 1900 by Moses Gomberg while he attempted to synthesize hexaphenyletane using triphenylcloromethane as a starting point.[2] Although the existence of free radicals, was initially received with some scepticism,[3] we are now well aware of the ubiquity and importance of such species. They provide valuable synthetic pathways[4](*viz.* radical polymerization, radical addition to alkenes, radical rearrangement, radical cyclization, radical halogenation, etc.) and are fundamental in several biochemical reactions.[5] Moreover, radicals produced within cells, either as byproducts of normal metabolism or due to external stimuli (*e.g.*, by UV light), react with DNA and other cell structures producing lesions directly related to mutagenesis, carcinogenesis, and aging.[6] Organic radicals are of the utmost importance in atmospheric chemistry, where their role in stratospheric ozone depletion is well known.[7] They are also important in food chemistry, since radical initiated oxidation is a major cause for lipid degradation.[8]

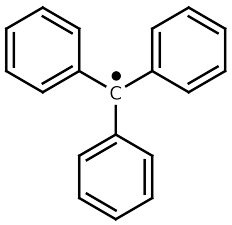

Triphenylmethyl *was discovered in 1900 by Moses Gomberg.*

The latter half of the 20th century witnessed the development of electron spin resonance (ESR), which soon became the quintessential method for detection and structural characterization of organic radicals.[9] This technique provided a valuable insight into the chemistry of these elusive and important species, and a significant fraction of our knowledge of radicals is rightfully owed to ESR. Stable and persistent (*i.e.*, long-lived) radicals do exist but, because of their open-shell configuration, most radicals are highly reactive and have very short lifetimes.[10] Consequently, their experimental study is gener-

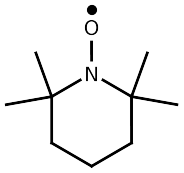

2,2,6,6-tetrameth-ylpiperidine-1-oxyl (TEMPO) is a stable and commercially available organic radical, which is often used as a spin trap.

ally a daunting and technically demanding task. Fortunately, radicals with lifetimes well bellow 1 s have been observed with ESR,[4] and short-lived radicals can be combined with other species (spin traps), yielding stabler radicals that can be studied with this technique.[9] Nevertheless, even today, over 100 years after Moses Gomberg reported his discovery of a free radical, there are still large gaps in our knowledge of these species, particularly concerning their energetics: while the standard enthalpy of formation, $\Delta_f H°$, is known with a great degree of accuracy for a large number of organic and inorganic species, the data for organic radicals are often obscured by large uncertainties or is altogether missing.[11,12] Such lacunae deeply hinder our knowledge of radicals and of the phenomena in which they take part.

1.2 Bond dissociation enthalpies

A bond dissociation enthalpy (BDE), $DH°_T$, is defined as the standard reaction enthalpy of the gas-phase homolytic cleavage of a chemical bond at temperature T.[13] From its definition, it is obvious that BDEs provide a valuable insight into the nature of chemical bonding. This thermochemical property is particularly important for radicals, since it is related with their stability.[10,13] Moreover, the connection between BDE and standard reaction enthalpy, $\Delta_r H°_T$, can be used to derive enthalpies of formation for radicals. For instance, given a generic molecule R_1R_2, its R_1—R_2 bond dissociation enthalpy will correspond to the standard reaction enthalpy of

$$R_1R_2 \longrightarrow R_1^\bullet + R_2^\bullet \tag{1.1}$$

thus,

$$\begin{aligned} DH°(R_1\text{—}R_2) &= \Delta_r H°(1.1) \\ &= \Delta_f H°(R_1^\bullet) + \Delta_f H°(R_2^\bullet) - \Delta_f H°(R_1R_2) \end{aligned} \tag{1.2}$$

The standard enthalpy of formation of $R_1^\bullet$, $R_2^\bullet$, or R_1R_2 can be easily obtained from (1.2) if the remaining data are known.* Carbon—hydrogen bond dissociation enthalpies are particularly useful. In this case one of the radicals formed upon bond cleavage is the hydrogen atom, whose enthalpy of formation is extremely well known.[14] Hence, rearranging (1.2), the reaction enthalpy of

$$RH \longrightarrow R^\bullet + H^\bullet \tag{1.3}$$

* A temperature of 298.15 K has become the *de facto* standard for such thermochemical properties, and unless otherwise noted, all thermochemical data refers to it. Consequently, the temperature subscript was omitted in the above formulae. For species in the gas-phase the state (g) will also be omitted.

can be used to derive

$$\Delta_f H^\circ(R^\bullet) = DH^\circ(R{-}H) + \Delta_f H^\circ(RH) - \Delta_f H^\circ(H^\bullet) \tag{1.4}$$

provided $\Delta_f H^\circ(RH)$ is known.

1.3 Experimental determination of bond dissociation enthalpies

Since C—H bond dissociation enthalpies have a critical importance in the study of organic radicals several experimental techniques have been used to study this property (*e.g.*, radical kinetics, photoionization mass spectrometry, acidity/electron affinity cycles, photoacoustic calorimetry, etc).[13,15] A thorough discussion of these methods is beyond the scope of this work. Nevertheless, since data obtained by photoacoustic calorimetry[16,17] (PAC) will be used in later chapters, a brief description of this technique shall be provided.

Photoacoustic calorimetry

PAC relies on the detection and analysis of an acoustic wave, produced when a solution is struck by a laser pulse. A simplified photoacoustic calorimeter is represented in fig. (1.2). If suitable photoreactive species are present in solution a fraction of the energy in the pulse initiates a chemical reaction, whose reaction enthalpy we shall refer to as $\Delta_r H$, while the remaining energy, $\Delta_{obs} H$, is deposited in the medium as heat.[16] In the absence of any energy loss through other pathways (*e.g.*, fluorescence) we can write that[16]

$$E_m = \Delta_{obs} H + \Phi_r \ \Delta_r H \tag{1.5}$$

or rather,

$$\Delta_r H = \frac{E_m - \Delta_{obs} H}{\Phi_r} \tag{1.6}$$

Since the molar energy of the laser pulse, $E_m = N_A E = N_A h\nu$, is known, the desired $\Delta_r H$ can be obtained provided that its quantum yield, Φ_r, is also known, and that the amount of energy deposited in the solution as heat, $\Delta_{obs} H$, can be determined.

The localized heating of the solution due to the laser pulse leads to a sudden volume change, which generates an acoustic wave. The amplitude of this wave is proportional to the total volume change, Δv:[17]

$$S = K_d \Delta v \tag{1.7}$$

K_d is a proportionality constant and S is the amplitude of the photoacoustic wave as illustrated in fig. (1.2). The volume change is in turn related to the

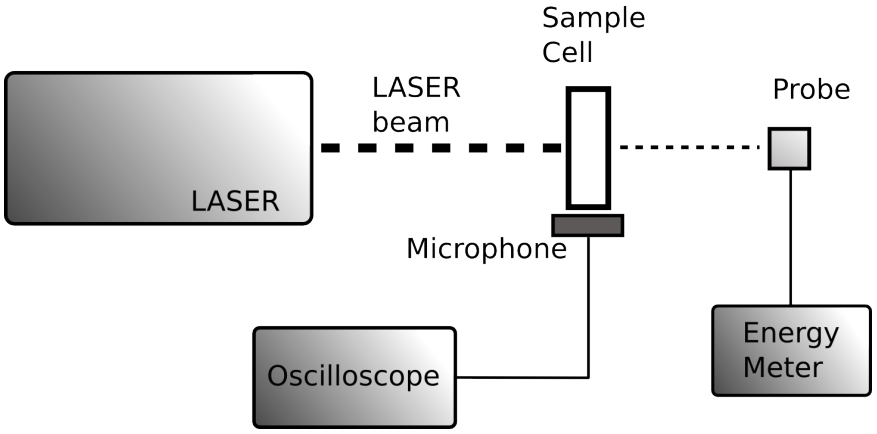

Figure 1.1 A simplified schematic representation of a photoacoustic calorimeter. The LASER beam strikes a solution in the sample cell. The microphone (typically a piezoelectric transducer) detects an acoustic wave generated by the localized heating of the solution, which is then amplified and recorded for measurement in the oscilloscope. The probe and the energy meter are used to determine the sample transmittance.

incident photon laser energy, E, by[16]

$$\Delta v = \chi \phi_{\text{obs}}(1-\mathscr{T})E \tag{1.8}$$

Here $\mathscr{T}$ is the sample transmittance, χ is the adiabatic expansion coefficient of the solution, and ϕ_{obs} is fraction of the laser energy released as heat. Combining (1.7) and (1.8) leads to

$$\begin{aligned} S &= [K_{\text{d}}\chi]\phi_{\text{obs}}(1-\mathscr{T})E \\ &= K\phi_{\text{obs}}(1-\mathscr{T})E \end{aligned} \tag{1.9}$$

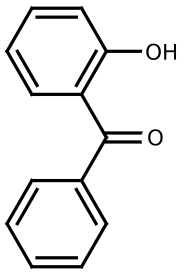

Since $\phi_{\text{obs}} = 1$ for ***o-hydroxybenzophenone*** *it can be used as a thermochemical calibrant.*

Since the solutions used are typically very diluted, χ depends on the thermoelastic properties of the solvent alone, and hence,[16]

$$\chi = \frac{\alpha_p}{\rho C_p} \tag{1.10}$$

where α_p and C_p are, respectively, the isobaric expansion coefficient and heat capacity of the solvent, and ρ is its density. The proportionality constant in (1.7), K_{d}, is characteristic of each calorimeter, but repeating each experiment with a photoacoustic calibrant (*e.g.*, *o*-hydroxybenzophenone) for which ϕ_{obs} is known, K can be canceled out. Using (1.9) we can now obtain ϕ_{obs}, from which the apparent amount of energy dissipated as heat in the solution is calculated:

$$\Delta_{\text{obs}}H = \phi_{\text{obs}}E_{\text{m}} \tag{1.11}$$

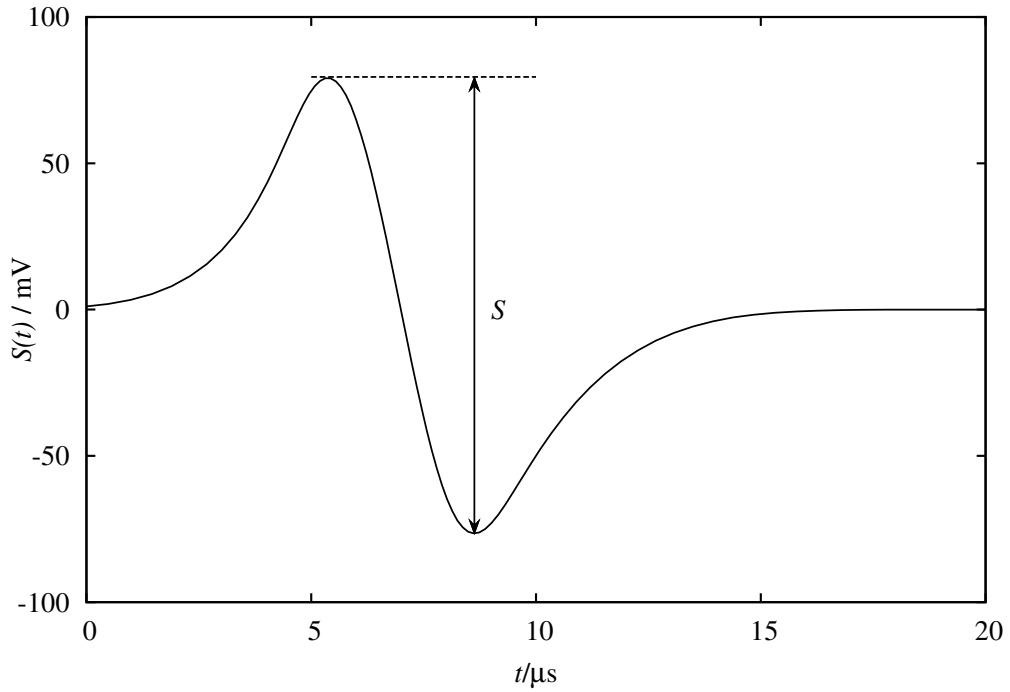

Figure 1.2 A schematic representation of a photoacoustic signal with amplitude S.

Two main problems arise from the formulae above: (1) the total volume change comprises, not only the expansion due to heating, but also the difference between the volumes of reactants and products; and (2) the measurement of S, the amplitude of the photoacoustic wave, depends on the characteristic frequency of the microphone used.[13,16] The former is readily solved by accounting for the volume change due to the chemical reaction taking place in the medium, $\Delta_r V$. This leads to the inclusion of a correction factor in (1.6), resulting in[16]

$$\Delta_r H = \frac{E_m - \Delta_{obs} H}{\Phi_r} + \frac{\Delta_r V}{\chi} \tag{1.12}$$

from which $\Delta_r H$ is ultimately obtained. Regarding the second of the aforementioned complications, it is known that (1.9) is valid only if the photoacoustic signal is much faster than the microphone response (*i.e.*, its characteristic frequency), which is typically an ultrasonic piezoelectric transducer.[18] This is a serious restriction, since it means that only reactions occurring at the nanosecond time-scale can be studied with this technique. Auxiliary reactions can be used to avoid this limitation, but this requires the knowledge of additional kinetic and thermochemical data.[19] Time-resolved PAC, a recent

development of the original technique, allows to bypass the problem.

Time-resolved photoacoustic calorimetry

An extremely useful photoinduced chemical reaction is the production of *tert*-butoxy radical, *t*-BuO$^\bullet$, from di-*tert*-butylperoxide (reac. 1.13). A *t*-BuO$^\bullet$ radical can readily abstract an hydrogen atom from RH, thus leading to the formation of R$^\bullet$ and *tert*-butanol (reac. 1.14).[20]

$$t\text{-BuO—OBu-}t\ (\text{sln}) \xrightarrow{h\nu} 2\ t\text{-BuO}^\bullet(\text{sln}) \tag{1.13}$$

$$2\ t\text{-BuO}^\bullet(\text{sln}) + 2\ \text{RH}\ (\text{sln}) \longrightarrow 2\ t\text{-BuOH(sln)} + 2\ \text{R}^\bullet(\text{sln}) \tag{1.14}$$

Taking into account the definition of bond dissociation enthalpy, eq. (1.2), we have for the reaction enthalpy of reac. (1.14) that

$$\begin{aligned}\Delta_r H(1.14) &= 2\left[\Delta_f H(t\text{-BuOH}, \text{sln}) + \Delta_f H(\text{R}^\bullet, \text{sln})\right] \\ &\quad - 2\left[\Delta_f H(\text{RH}, \text{sln}) + \Delta_f H(t\text{-BuO}^\bullet, \text{sln})\right] \\ &= 2\left[DH_{\text{sln}}(\text{R—H}) - DH_{\text{sln}}(t\text{-BuO—H})\right]\end{aligned} \tag{1.15}$$

The values of $DH_{\text{sln}}(t\text{-BuO—H})$ in the solvents typically used in PAC experiments (*e.g.*, toluene and benzene) are known.[20,21] We can, therefore, obtain the R—H bond dissociation enthalpy from

$$DH_{\text{sln}}(\text{R—H}) = \frac{\Delta_r H(1.14)}{2} + DH_{\text{sln}}(t\text{-BuO—H}) \tag{1.16}$$

if we can determine $\Delta_r H(1.14)$. Unfortunately, while (1.13) is very fast, (1.14) is generally too slow to be studied accurately with PAC. Indeed, such a reaction leads to a broad signal with low amplitude, overlapped with the much stronger signal for the homolysis of di-*tert*-butylperoxide.[13] This hidden information can be recovered using time-resolved photoacoustic calorimetry (TR-PAC),[18] which uses a least squares iterative deconvolution algorithm[22] to extract the signals for each reaction. In a TR-PAC experiment the overall process

$$\begin{aligned}t\text{-BuO—OBu-}t\ (\text{sln}) + 2\ \text{RH}\ (\text{sln}) \xrightarrow{k_1} 2\ t\text{-BuO}^\bullet(\text{sln}) + 2\ \text{RH}\ (\text{sln}) \xrightarrow{k_2} \\ \xrightarrow{k_2} 2\ t\text{-BuOH(sln)} + 2\ \text{R}^\bullet(\text{sln})\end{aligned} \tag{1.17}$$

yields a signal, $S(t)$, which is the sum of two individual heat decays, $S_1(t)$ and $S_2(t)$, with[13]

$$S_1(t) = \phi_1 k_1 e^{-tk_1} \tag{1.18}$$

$$S_2(t) = \frac{\phi_2 k_1 k_2}{k_2 - k_1}\left(e^{-tk_1} - e^{-tk_2}\right) \tag{1.19}$$

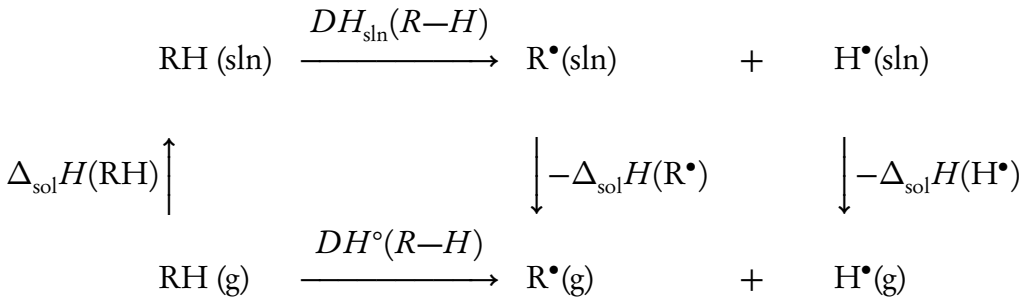

Figure 1.3 Thermodynamic cycle relating the R—H bond dissociation enthalpy in solution, $DH_{sln}(R—H)$, with the standard bond dissociation enthalpy, $DH°(R—H)$, using the solvation enthalpies of reactant and products.

The subscripts 1 and 2 refer to reactions (1.13) and (1.14), respectively, and $S_1(t)$ and $S_2(t)$ have been normalized for the solution transmittance and the laser energy. The rate constants for each reaction, k_1 and k_2 (as indicated in reac. 1.17), and the yields ϕ_1 and ϕ_2, are obtained by fitting $S_1(t)$ and $S_2(t)$ to the experimental signal. The amounts of energy dissipated as heat, $\Delta_{obs}H_1$ and $\Delta_{obs}H_2$, are obtained as before from the multiplication of the yields by the laser molar energy. Inserting these data into the overall energy balance,[13]

$$E_m = (\Delta_{obs}H_1 + \Delta_{obs}H_2) + \Phi_r(\Delta_r H_1 + \Delta_r H_2) - \frac{\Phi_r(\Delta_r V_1 + \Delta_r V_2)}{\chi} \quad (1.20)$$

we can solve for the desired reaction enthalpy, $\Delta_r H_2 \equiv \Delta_r H(1.14)$. The quantities in (1.20) are defined as above, and Φ_r is the (known) quantum yield of di-*tert*-butylperoxide homolysis in the solution.[21]

From solution to gas-phase enthalpies

Bond dissociation enthalpies in solution obtained from PAC or TR-PAC experiments can be used to compute the corresponding gas-phase data. Fig. (1.3) illustrates how this is done by considering the solvation enthalpies, $\Delta_{sol}H$, of the species involved in the reaction. From this thermodynamic cycle we obtain

$$\begin{aligned} DH°(\text{ R—H }) = {} & DH_{sln}(\text{ R—H }) \\ & + \left[\Delta_{sol}H(RH) - \Delta_{sol}H(R^{\bullet}) - \Delta_{sol}H(H^{\bullet})\right] \end{aligned} \quad (1.21)$$

For alkyl radicals in the solvents typically used in TR-PAC (*e.g.*, toluene and benzene) we can consider that $\left[\Delta_{sol}H(RH) - \Delta_{sol}H(R^{\bullet})\right] \approx 0$.[21] Since accurate estimates for the solvation enthalpy of the hydrogen atom in these solvents are available,[23] $DH°(\text{ R—H })$ is readily calculated from (1.21).

1.4 Theoretical study of radicals and their energetics

Quantum theory has certainly gone a long way since the notion of quantization was first proposed by Max Planck.[24] During the last century some of the greatest minds of our time laid the foundations of modern quantum mechanics.[25–40] Subsequent theoretical developments and their implementation in large software packages made the use of quantum theory in the study of chemical species and their reactivity (*i.e.*, quantum chemistry) a common practice.[38–40]

Among other properties, current quantum chemical methods afford very accurate predictions of structures and thermochemical data for a large number of species of chemical interest, including organic radicals.[41] Experimental and theoretical chemistry have a highly synergistic relationship since accurate experimental data are often used to test and/or fine-tune theoretical methods, which can then be used to study systems for which no experimental data are available.

Further details on quantum chemical methods are postponed for the next chapter. Conceptually, the theoretical study of chemical species and their reactions is fairly simple. The energy of a given system (*e.g.*, an atom, a molecule, a cluster of molecules, etc.) at $T = 0$ K is obtained from numerical solution of the non-relativistic time-independent Schrödinger equation.[34,39] Optimized structures correspond to the set of atomic coordinates for which the energy is a minimum.[38] Corrections may be added to the energy to obtain estimates of the enthalpy at the desired temperature.[42] These data can then be used to calculate reaction enthalpies, of which bond dissociation enthalpies are a particular case, and other thermochemical properties.

CHAPTER 2

Quantum chemistry

2.1 Schrödinger equation

According to the Born interpretation of the wavefunction its square modulus, $|\Psi(\boldsymbol{r},t)|^2$, is a probability density which, when multiplied by a volume, $d\boldsymbol{r}$, yields the probability of finding an electron in that region of space at time t.[43] The time-evolution of the wavefunction is given by the Schrödinger equation[34]

$$\hat{H}\,\Psi(\boldsymbol{r},t) = i\,\hbar\frac{\partial\Psi(\boldsymbol{r},t)}{\partial t} \tag{2.1}$$

where $\hat{H}$ is the Hamiltonian operator, $\hbar$ is the reduced Planck constant $[h/(2\pi)]$, and i is the imaginary unit. For stationary states the time dependence of (2.1) may be dropped, resulting in

$$\hat{H}\,\Psi(\boldsymbol{r}) = E\,\Psi(\boldsymbol{r}) \tag{2.2}$$

The eigenvalue of the Schrödinger equation, E, is the system's energy. Equation (2.1) (and (2.2) for that matter) are not in keeping with special relativity.[37] Nevertheless, relativistic effects can be safely neglected for lighter atoms and for molecules composed of such atoms.

For a system composed of M point-like nuclei and N electrons in the absence of external potentials the Hamiltonian operator is defined as[39]

$$\begin{aligned}\hat{H} = &-\sum_{i=1}^{N}\frac{1}{2}\nabla_i^2 - \sum_{A=1}^{M}\frac{1}{2M_A}\nabla_A^2 - \sum_{i=1}^{N}\sum_{A=1}^{M}\frac{\mathrm{Z}_A}{r_{iA}} \\ &+\sum_{i=1}^{N}\sum_{j>i}^{N} r_{ij}^{-1} + \sum_{A=1}^{M}\sum_{B>A}^{M}\frac{\mathrm{Z}_A\mathrm{Z}_B}{r_{AB}}\end{aligned} \tag{2.3}$$

or, using operators to represent each term,*

$$\hat{H} = \hat{T}_e + \hat{T}_n + \hat{V}_{ne} + \hat{V}_{ee} + \hat{V}_{nn} \tag{2.4}$$

In (2.3) Z_A is the atomic number of nucleus A, whose mass is M_A, $\nabla_i = \partial/\partial x_i + \partial/\partial y_i + \partial/\partial z_i$ and $r_{ij} = |\boldsymbol{r}_i - \boldsymbol{r}_j|$ (the other euclidean distances are similarly defined). The terms in (2.3) and (2.4) represent, respectively, the kinetic energy of electrons, the kinetic energy of nuclei, the attraction between electrons and nuclei, the repulsion between electrons, and the repulsion between nuclei. Atomic units[44] (a.u.) were used in (2.3), and the same will be done throughout this work to simplify quantum mechanical formulae. Definitions of some atomic units are given in Table (2.1).

Table 2.1 Definition and S.I. values of some atomic units.

	a.u.	S.I.[a]	symbol
mass	electron mass	$9.109\ 382\ 15(45) \times 10^{-31}$ kg	m_e
charge	electron charge	$1.602\ 176\ 487(40) \times 10^{-19}$ C	e
length	Bohr radius	$0.529\ 177\ 208\ 59(36) \times 10^{-10}$ m	a_0
energy	Hartree energy	$4.359\ 743\ 94(22) \times 10^{-18}$ J	E_h
action	reduced Planck constant	$1.054\ 571\ 628(53) \times 10^{-34}$ J·s	$\hbar$
permittivity[b]	$4\pi\epsilon_0$	$1.112\ 650\ 056\cdots \times 10^{-10}$ F·m^{-1}	

[a] All values were taken from ref. 44. Standard uncertainties given in concise form, *e.g.*, $\hbar = 1.054\ 571\ 628 \times 10^{-34} \pm 0.000\ 000\ 053 \times 10^{-34}$ J·s. [b] exact.

Born-Oppenheimer approximation

The Schrödinger equation cannot be solved analytically for a many-electron system. Much of its complexity stems from the fact that the eigenfunctions of (2.3) depend explicitly on the coordinates of all particles (*i.e.*, all electrons and nuclei) in the system. Significant simplification can be achieved by using a crucial approximation devised by Julius Robert Oppenheimer and Max Born,[45] which allows to treat the motions of electrons and nuclei separately.

A thorough discussion of this approximation is given in ref. 35. From a simplistic and qualitative point of view, this separation is possible because nuclei are much heavier than electrons. Assuming that the particles comprising the system are in equilibrium, their mean kinetic energies will be similar and thus, the ratio of velocities for electrons and nuclei will be roughly proportional to square of their mass ratio.[38] Therefore, in (2.3) the kinetic energy of

* $\hat{T}$ will also be used to denote excitation operators, which we will encounter further down the line, but the distinction will be apparent from the context.

nuclei can be neglected and repulsion between nuclei can be considered constant. Within the framework of the Born-Oppenheimer approximation the total energy of the system, E_{tot}, is then given by

$$E_{\text{tot}} = E_{\text{elec}} + \sum_{A=1}^{M} \sum_{B>A}^{M} \frac{Z_A Z_B}{r_{AB}} \tag{2.5}$$

where the electronic energy, E_{elec}, is obtained solving

$$\hat{H}_{\text{elec}} \Psi_{\text{elec}} = E_{\text{elec}} \Psi_{\text{elec}} \tag{2.6}$$

for the electronic Hamiltonian

$$\begin{aligned} \hat{H}_{\text{elec}} &= \hat{T}_e + \hat{V}_{ne} + \hat{V}_{ee} \\ &= -\sum_{i=1}^{N} \frac{1}{2} \nabla_i^2 - \sum_{i=1}^{N} \sum_{A=1}^{M} \frac{Z_A}{r_{iA}} + \sum_{i=1}^{N} \sum_{j>i}^{N} r_{ij}^{-1} \end{aligned} \tag{2.7}$$

This greatly simplifies the eigenvalue problem, since Ψ_{elec} now only depends explicitly on the coordinates of electrons. The dependence on the position of nuclei is parametric. Because this electronic eigenvalue problem will be our main concern in the remainder of this chapter the label "elec" in (2.6) and the parametrical dependence of Ψ on the atomic coordinates will be omitted. In Dirac notation[37] (2.6) is rewritten as

$$\hat{H} \mid \Psi \rangle = E \mid \Psi \rangle \tag{2.8}$$

where $\mid \Psi \rangle = \Psi(\boldsymbol{r}_1, \boldsymbol{r}_2, \cdots, \boldsymbol{r}_N)$ is the wavefunction for the N of electrons in the system.

Wavefunction

$\hat{H}$ is a second-order linear Hermitian operator, therefore, its eigenvalues are real and its eigenfunctions are orthogonal and form a complete set.[46] Due to the probabilistic interpretation of the wavefunction it must be continuous, single-valued, square integrable (*i.e.*, Ψ is an L^2 function), must not be zero everywhere (if $|\Psi|^2 = 0$ everywhere then there is no system) and must vanish at infinity.[43] In addition, the Laplacian in $\hat{H}$ dictates that the wavefunction must be at least twice-differentiable (*i.e.*, a class C^2 function).

The Schrödinger equation has no dependence on spin, however, the electron spin is an observable property of a system[47] which, according to the Pauli exclusion principle,[48] has a direct influence the on electronic structure. Assuming no spin-orbit coupling, spin can be included *ad hoc* in the wavefunction using the spin functions $\alpha(\omega)$ and $\beta(\omega)$, which represent the two possible spin

states for an electron (*viz.* $1/2$ and $-1/2$), with ω being the spin variable.[39] These functions are orthonormal, therefore*

$$\begin{aligned}\int \alpha^*(\omega)\alpha(\omega)\,d\omega &= \int \beta^*(\omega)\beta(\omega)\,d\omega = 1\\ \int \beta^*(\omega)\alpha(\omega)\,d\omega &= \int \alpha^*(\omega)\beta(\omega)\,d\omega = 0\end{aligned} \tag{2.9}$$

The wavefunction for a many-electron system will depend on the position and spin of all electrons. This is typically represented by writing the wavefunction as $\Psi(\mathbf{x}_1, \mathbf{x}_2, \ldots, \mathbf{x}_N)$, where $\mathbf{x} = \{\boldsymbol{r}, \omega\}$.

Slater determinants

Consider, for now, a system of N non-interacting electrons. Its total energy is just a sum of one-particle energies, ϵ_i^{core}, and the Hamiltonian in (2.7) reduces to a sum of core (one-particle) operators, $\hat{h}_i$. Under these conditions (2.8) becomes

$$\left(\sum_{i=1}^{N}\hat{h}_i\right)|\,\Psi\rangle = \left(\sum_{i=1}^{N}\left[-\frac{1}{2}\nabla_i^2 - \sum_{A=1}^{M}\frac{Z_A}{r_{iA}}\right]\right)|\,\Psi\rangle = \left(\sum_{i=1}^{N}\epsilon_i\right)|\,\Psi\rangle \tag{2.10}$$

Since the quantum states for electrons are decoupled it is tempting to write the total wavefunction as a product of the eigenfunctions of $\hat{h}$,

$$|\,\Psi\rangle = \Psi_{\text{Hartree}}(1,2,\ldots,N) = \chi_i(1)\chi_j(2)\ldots\chi_k(N) \tag{2.11}$$

as Douglas Hartree did to study atoms in the dawn of quantum chemistry.[49–52] Here, the electron variable has been replaced by the electron index in function arguments (*e.g.*, $1 \implies \mathbf{x}_1$). Exchanging $\mathbf{x}_1$ by $\mathbf{x}_2$ in (2.11) the sign of $|\,\Psi\rangle$ would remain the same. This is in clear violation of the Pauli exclusion principle, which states that the wavefunction for electrons (fermions, in general) must be antisymmetric with respect to the exchange of two electrons. We must, therefore, modify (2.11) to account for this antisymmetry while preserving the expectation value for the energy.

If this system had only two non-interacting electrons then $\Psi_{\text{Hartree}}(1,2) = \chi_i(1)\chi_j(2)$. In this case the Pauli exclusion principle requires that $\chi_i(1)\chi_j(2) = -\chi_i(2)\chi_j(1)$. Electrons are undistinguishable, so we cannot ascribe an electron to any given orbital. The wavefunction must, therefore, be written as

$$\Psi(1,2) = 2^{-\frac{1}{2}}[\chi_i(1)\chi_j(2) - \chi_i(2)\chi_j(1)] \tag{2.12}$$

* Unless otherwise stated, integration in all space (*i.e.*, in the interval $]-\infty,+\infty[$) is implicit.

where $2^{-\frac{1}{2}}$ normalizes the wavefunction so that

$$\langle \Psi(1,2) \mid \Psi(1,2) \rangle = \iint \Psi^*(1,2)\Psi(1,2)\, d\mathbf{x}_1\, d\mathbf{x}_2 = 1 \tag{2.13}$$

and therefore

$$\begin{aligned} \langle \Psi(1,2) \mid \hat{H} \mid \Psi(1,2) \rangle &= \iint \Psi^*(1,2) \left(\sum_{i=1}^{N} \hat{h}_i \right) \Psi(1,2)\, d\mathbf{x}_1\, d\mathbf{x}_2 \\ &= \iint \Psi^*(1,2)(\epsilon_i + \epsilon_j)\Psi(1,2)\, d\mathbf{x}_1\, d\mathbf{x}_2 \\ &= (\epsilon_i + \epsilon_j) \langle \Psi(1,2) \mid \Psi(1,2) \rangle \\ &= (\epsilon_i + \epsilon_j) \end{aligned} \tag{2.14}$$

Note that, as required, (2.12) changes sign if the coordinates of electrons 1 and 2 are exchanged. For 3 electrons, we would have $3! = 6$ (undistinguishable) ways of distributing the electrons among the three spin-orbitals, whose signal would be given by the parity of the electrons permutation (*viz.* $+$ for an even and $-$ uneven permutations). Proceeding with this reasoning up to N electrons we would obtain

$$\Psi(1,2,\ldots,N) = (N!)^{-\frac{1}{2}} \sum_{n=1}^{N!} \mathrm{sgn}(n)\hat{P}(n)\{\chi_i(1)\chi_j(2)\ldots\chi_k(N)\} \tag{2.15}$$

where $\mathrm{sgn}(n)$ is the sign of the nth permutation of electrons by the spin-orbitals performed by the permutation operator $\hat{P}$. This is called a Slater determinant in honor its discoverer, the American physicist John Slater.[53] In keeping with its name, (2.15) can be arranged into the following determinant:

$$\Psi(1,2,\ldots,N) = \mid ij\ldots k\rangle = (N!)^{-\frac{1}{2}} \begin{vmatrix} \chi_i(\mathbf{x}_1) & \chi_j(\mathbf{x}_1) & \cdots & \chi_k(\mathbf{x}_1) \\ \chi_i(\mathbf{x}_2) & \chi_j(\mathbf{x}_2) & \cdots & \chi_k(\mathbf{x}_2) \\ \cdots & \cdots & \cdots & \cdots \\ \chi_i(\mathbf{x}_N) & \chi_j(\mathbf{x}_N) & \cdots & \chi_k(\mathbf{x}_N) \end{vmatrix} \tag{2.16}$$

Here we have introduced the common shorthand notation for Slater determinants. Each one-electron wavefunction, χ, is the product of a spatial function by a spin function, that is, $\chi_i(\mathbf{x}) = \psi_i(\boldsymbol{r})s(\omega)$, with $s = \alpha$ or $s = \beta$.

We used this ideal non-interacting system to illustrate how a Slater determinant is built, and how a wavefunction thus constructed respects the anti-symmetry principle, but $\{\chi_i\}$ need not be the spin-orbitals for such a non-interacting system. They must, nevertheless, be linearly independent since

otherwise (2.16) is 0, and should adhere to the same constraints imposed on Ψ if they are to be used as trial eigenfunctions for a one-particle second-order linear operator (*e.g.*, the Fock operator, which we will encounter shortly). In addition, because the orthogonalization of spin orbitals in (2.16) is a trivial algebraic problem,[46] they need not be orthogonal.

Variational principle

There are infinitely many solutions of the Schrödinger equation that comply with the aforementioned conditions. Because they form a complete set, any trial wavefunction which adheres to the same constraints can be represented as

$$\Psi_{\text{trial}} = \sum_{i=0}^{\infty} C_i \Psi_i \tag{2.17}$$

where C_i are the expansion coefficients of Ψ_{trial} in the basis basis formed by the eigenfunctions of (2.8), $\{\Psi_i\}$. The energy for this trial wavefunction, E_{trial}, is then computed from*

$$\begin{aligned}
E_{\text{trial}} &= \langle \Psi_{\text{trial}} \mid \hat{H} \mid \Psi_{\text{trial}} \rangle \\
&= \sum_{i=0}^{\infty} \sum_{j=0}^{\infty} \langle \Psi_{\text{trial}} \mid \Psi_i \rangle \langle \Psi_i \mid \hat{H} \mid \Psi_j \rangle \langle \Psi_j \mid \Psi_{\text{trial}} \rangle \\
&= \sum_{i=0}^{\infty} \sum_{j=0}^{\infty} \langle \Psi_{\text{trial}} \mid \Psi_i \rangle \langle \Psi_i \mid \Psi_j \rangle E_j \langle \Psi_j \mid \Psi_{\text{trial}} \rangle \\
&= \sum_{i=0}^{\infty} \sum_{j=0}^{\infty} \langle \Psi_{\text{trial}} \mid \Psi_i \rangle \delta_{ij} E_j \langle \Psi_j \mid \Psi_{\text{trial}} \rangle \\
&= \sum_{i=0}^{\infty} \langle \Psi_{\text{trial}} \mid \Psi_i \rangle E_i \langle \Psi_i \mid \Psi_{\text{trial}} \rangle \\
&= \sum_{i=0}^{\infty} |C_i|^2 E_i
\end{aligned} \tag{2.18}$$

Here we have used, respectively, the completeness of $\{\Psi_i\}$, the fact that they are eigenfunctions of $\hat{H}$ with eigenvalues E_i, their orthogonality, and the expansion in (2.17). δ_{ij} is the Dirac delta, whose value is 1 if and only if $i = j$, and 0 otherwise. We see that E_{trial} reduces to a sum of eigenvalues of $\hat{H}$ weighed by

* Unless otherwise stated all wavefunctions in the subsequent text are assumed to be normalized.

the square of the expansion coefficients, C_i. Let E_0 be the ground-state energy of the system (*i.e.*, $E_0 \leq E_i$ for all $i > 0$), then (2.18) implies that

$$E_{\text{trial}} \geq E_0 \tag{2.19}$$

Moreover, $E_{\text{trial}} = E_0$ when Ψ_{trial} is the ground-state wavefunction of the system, Ψ_0.* This means that solving the Schrödinger equation for a stationary state is a constrained minimization problem (*viz.* constrained to the condition that the wavefunction is normalized, $\langle \Psi_{\text{trial}} \mid \Psi_{\text{trial}} \rangle = 1$). This is a standard optimization problem, which may be solved using the method of Lagrange multipliers.[54]

2.2 Hartree-Fock approximation

A Slater determinant is only the exact wavefunction for a non-interacting system. However, since the antisymmetry of Ψ is assured if (2.16) is used to represent an N-electron wavefunction, we may consider doing so for an interacting system with Hamiltonian (2.7). This is called the Hartree-Fock (HF) approximation,[49–52,55,56] and it is a cornerstone method in electronic structure theory upon which several more accurate methods are built.[35,38–40,43] In (2.16) our variational freedom lies with the set of spin-orbitals $\{\chi_i\}$. Consequently, solving the Schrödinger using this wavefunction ansatz means finding the optimum set of spin-orbitals which, when used to build a single Slater determinant, minimize the energy.

Energy minimization and the Fock operator

The Hamiltonian in (2.7) comprises a one-electron and a two-electron operator. Slater-Condon rules imply that when it operates on a Slater determinant it yields a sum of one- and two-electron terms.[53,57] Thus, allowing (2.7) to operate on (2.16) leads to

$$E_{\text{HF}} = \langle ij\ldots k \mid \hat{H} \mid ij\ldots k \rangle = \sum_{i=1}^{N} \langle i \mid \hat{h} \mid i \rangle + \sum_{i=1}^{N} \sum_{j>i}^{N} \langle ij \parallel ij \rangle \tag{2.20}$$

where

$$\langle i \mid \hat{h} \mid i \rangle = h_i = \int \chi_i^*(1) \left(-\frac{1}{2}\nabla_1^2 - \sum_{A=1}^{M} \frac{Z_A}{r_{1A}} \right) \chi_i(1)\, d\mathbf{x}_1 \tag{2.21}$$

* If the ground state is degenerate then several Ψ_i yield E_0 and $E_{\text{trial}} = E_0$ when Ψ_{trial} is any of these wavefunctions.

and

$$\begin{aligned}\langle ij \parallel ij\rangle &= J_{ij} - K_{ij} \\ &= \langle ij \mid ij\rangle - \langle ij \mid ji\rangle \\ &= \iint \chi_i^*(1)\,\chi_j^*(2) r_{12}^{-1} \chi_i(1)\,\chi_j(2)\, d\mathbf{x}_1\, d\mathbf{x}_2 \\ &\quad - \iint \chi_i^*(1)\,\chi_j^*(2) r_{12}^{-1} \chi_j(1)\,\chi_i(2)\, d\mathbf{x}_1\, d\mathbf{x}_2\end{aligned} \tag{2.22}$$

The first integral on the right hand side (RHS) of (2.22) is the Coulomb integral, representing the classical repulsion between two electrons occupying two spin-orbitals, and the second is the non-classical exchange integral. When $i = j$ Coulomb and exchange integrals cancel (which is physically sound because an electron does not interact with itself), therefore

$$\sum_{i=1}^{N}\sum_{j>i}^{N}\langle ij \parallel ij\rangle = \frac{1}{2}\sum_{i=1}^{N}\sum_{j=1}^{N}\langle ij \parallel ij\rangle \tag{2.23}$$

Since $\langle ij \parallel ij\rangle^* = \langle ji \parallel ji\rangle$ the 1/2 factor in the RHS is introduced to avoid double counting terms.

The set of spin orbitals which minimizes E_{HF} can be found using the Lagrangian[39]

$$L\left[\{\chi_i\}\right] = E_{\mathrm{HF}}\left[\{\chi_i\}\right] - \sum_{i=1}^{N}\sum_{j=1}^{N} l_{ij}\left[\langle i \mid j\rangle - \delta_{ij}\right] \tag{2.24}$$

where the l_{ij} are the Lagrange multipliers. The condition for energy minimization, under the orthonormality constraint, is that the functional derivative of L with respect to $\{\chi_i\}$ is 0. This leads to a set of coupled equations,

$$\hat{F}(1)\chi_j(1) = \left[\hat{h}(1) + \sum_{j=1}^{N}\hat{J}_i(1) - \hat{K}_i(1)\right]\chi_j(1) = \sum_{j=1}^{N} l_{ij}\chi_j(1) \tag{2.25}$$

where $\hat{F}$ is the Fock operator. The Coulomb, $\hat{J}$, and exchange, $\hat{K}$, operators in (2.25) are defined as

$$\hat{J}_i(1)\chi_j(1) = \left[\int \chi_i^*(2)\, r_{12}^{-1}\chi_i^*(2)\, d\mathbf{x}_2\right]\chi_j(1) \tag{2.26}$$

$$\hat{K}_i(1)\chi_j(1) = \left[\int \chi_i^*(2)\, r_{12}^{-1}\chi_j^*(2)\, d\mathbf{x}_2\right]\chi_i(1) \tag{2.27}$$

Note that RHS of (2.25) is a linear combination of all spin orbitals. A unitary transformation may be used to find the set of spin-orbitals for which the matrix of Lagrange multipliers is diagonal, and write

$$\hat{F}(1)\chi_j(1) = \epsilon_j \chi_j(1) \tag{2.28}$$

In (2.28) the eigenfunctions are the canonical HF spin-orbitals, and the eigenvalues, ϵ, are the orbital energies.[39] There are infinitely-many eigenfunctions and eigenvalues of (2.28). In practice, solution of the Fock equations requires the introduction of a finite set of K spatial functions, from which $2K$ spin-orbitals are obtained. The N spin-orbitals of lowest energy are the occupied orbitals. The remaining orbitals $(2K-N)$ are the (unoccupied) virtual orbitals.

The Hartree-Fock energy is related to the Fock operator and the occupied orbital energies by

$$\begin{aligned} E_{\mathrm{HF}} &= \frac{1}{2}\langle ij\ldots k \mid \hat{h} + \hat{F} \mid ij\ldots k\rangle \\ &= \frac{1}{2}\sum_{i=1}^{N}\langle i \mid \hat{h} + \hat{F} \mid i\rangle \\ &= \frac{1}{2}\sum_{i=1}^{N}\left(h_i + \epsilon_i\right) \end{aligned} \tag{2.29}$$

Note in (2.27) that $\hat{K}$ depends explicitly on its operands, the spin-orbitals, and therefore the set of coupled equations (2.28) must be solved iteratively. This is done using a self-consistent field procedure:

1. From a guess of the spin-orbitals construct the Fock operator.
2. Using $\hat{F}$ defined in **1** solve the set of equations (2.28).
3. Using the eigenfunctions obtained in **2** reconstruct the Fock operator.
4. Repeat steps **1–3** until eigenfunctions (and hence, eigenvalues) are numerically stable. This is the case when eigenfunctions obtained from the cycle **1–3** are the same, within a set of predefined numerical convergence criteria, as those obtained from a previous cycle.
5. Use the converged eigenfunctions and eigenvectors to to obtain the energy and other expectation values for the system.

The simplification brought about by the Hartree-Fock approximation is self-evident: it reduces the N-particle problem in (2.8) to a set of coupled equations

(2.28) which can be easily solved by standard algebraic methods. However, this simplification leads to a loss of accuracy. HF is a mean-field theory wherein each electron feels the average electric field due to all other electrons and not their true electric field.[35]

Hartree-Fock-Roothaan method

Using the HF approximation the Schrödinger equation can be simplified and solved for a molecular system, but one crucial problem still remains: we have yet to provide a definition for the spin-orbitals, $\{\chi_i\}$. For a molecule this can be done using a method introduced (independently) by Clemens Roothaan and George Hall in 1951.[58,59]

A spin-orbital is a product of a (molecular) spatial orbital by a spin function. Each such spatial orbital, ψ, can be expanded as a linear combination of atomic orbitals (LCAO), ϕ, a concept familiar to any chemist which is represented mathematically as

$$\psi_i(1) = \sum_{a=1}^{K} C_{ai}\phi_a(1) \tag{2.30}$$

or equivalently, using parenthesis to denote spatial orbitals, as

$$|\, i) = \sum_{a=1}^{K} C_{ai}\,|\, a) \tag{2.31}$$

In these expressions K is the basis set size, that is, the number of atomic orbitals (AOs) used in the expansion. Mathematically, the larger the AO basis set, the more accurate will the expansion in (2.30) be. This basis set size is, therefore, crucial, since errors in spin-orbitals lead to error in expectation values. For an infinite (complete) basis set the energy obtained would be the Hartree-Fock limit energy. Obviously, for practical implementations the basis set must be truncated.

In keeping with the Pauli exclusion principle, two electrons can share a spatial orbital if and only if their spin states are different. If this is the case, the wavefunction is said to be restricted (R) if there are no unpaired electrons (*i.e.*, closed-shell electronic configurations), or restricted open (RO) if some orbitals are partly filled.[35,38–40] Alternatively, if the spatial orbitals of α and β electrons are different, the wavefunction is unrestricted (U).[35,38–40] The orthogonality of spin functions, represented in (2.9), may be used to simplify formulae. Doing so for a restricted wavefunction and expanding the orbitals as (2.30) leads to the Roothaan-Hall equation[58,59]

$$\mathbf{FC} = \epsilon\mathbf{SC} \tag{2.32}$$

which is the matrix representation of

$$\sum_{a=1}^{K} F_{ia} C_{aj} = \epsilon_j \sum_{a=1}^{K} S_{ia} C_{aj} \tag{2.33}$$

where $\{\mathbf{F} : F_{ij} = (i \mid \hat{F} \mid j)\}$ is the Fock matrix, $\mathbf{C}$ is the matrix of (2.30) expansion coefficients and $\{\mathbf{S} : S_{ij} = (i \mid j)\}$ is the AO overlap matrix. For an unrestricted wavefunction a similar reasoning leads the Pople-Nesbet equations,[60]

$$\mathbf{F}^{\alpha}\mathbf{C}^{\alpha} = \epsilon^{\alpha}\mathbf{S}^{\alpha}\mathbf{C}^{\alpha} \tag{2.34}$$

$$\mathbf{F}^{\beta}\mathbf{C}^{\beta} = \epsilon^{\beta}\mathbf{S}^{\beta}\mathbf{C}^{\beta} \tag{2.35}$$

Since in this case spatial orbitals are different for α and β electrons, we obtain two equations which must be solved simultaneously. The matrices in (2.34) and (2.35) are defined as those in (2.32), but here spatial orbitals are either those of α or β electrons.

Note how expanding molecular orbitals as LCAOs further simplifies the solution of (2.28). The variational flexibility in spin orbitals now lies with the matrix of coefficients, $\mathbf{C}$, and solving the coupled Fock equations can now done by matrix diagonalization. The existence of highly efficient matrix multiplication and diagonalization routines in standard software libraries[61] makes the implementation of the Hartree-Fock-Roothaan method fairly straightforward.

Orbital basis sets

We now focus our attention on the atomic orbitals. Ideally, AOs would be Slater-type orbitals (STO), due to their similarity with one-electron orbitals for an hydrogen-like atom.[35] An STO is defined as

$$\phi^{\mathrm{STO}}(r_A, l, m, n, \zeta) = N x_A^l y_A^m z_A^n \exp(-\zeta r_A) \tag{2.36}$$

where ζ is the orbital exponent, N is a normalization constant, $r_A = |\boldsymbol{r} - \mathrm{A}| = (x_A^2 + y_A^2 + z_A^2)^{1/2}$, with $x_A = (x - A_x)$. Similar definitions apply to y_A and z_A. $\mathrm{A} = (A_x, A_y, A_z)$ is the origin (typically, an atom) of the orbital. The quantum numbers $l, m, n = 0, 1, 2, \ldots, N$ determine the radial type (s, p_x, p_y, p_z, d_{xy}, etc.) of the orbital.

Even though STOs describe AOs accurately, their use as basis functions leads to very complex mathematical formulae. This is particularly true for electron repulsion integrals (that is, coulomb and exchange integrals) involving AOs with three or four distinct centers.[38] Significant algebraic simplification results from the use of gaussian-type orbitals (GTO),

$$\phi^{\mathrm{GTO}}(r_A, l, m, n, \zeta) = N x_A^l y_A^m z_A^n \exp(-\zeta r_A^2) \tag{2.37}$$

Unlike an STO, a GTO can be separated as,

$$\begin{aligned}\phi^{\mathrm{GTO}}(r_A,l,m,n,\zeta) &= N x_A^l y_A^m z_A^n \exp(-\zeta r_A^2) \\ &= N x_A^l y_A^m z_A^n \exp[-\zeta(x_A^2+y_A^2+z_A^2)] \\ &= N x_A^l \exp(-\zeta x_A^2)\cdot y_A^m \exp(-\zeta y_A^2)\cdot z_A^n \exp(-\zeta z_A^2)\end{aligned} \tag{2.38}$$

which means that integration over each cartesian coordinate may be performed separately. Moreover, the product of two GTOs yields a GTO, so intricate two-electron integrals reduce to integration of two GTOs divided by the distance between electrons which can be readily evaluated using standard formulae.[38]

In order to accurately describe AOs, while retaining the more tractable mathematical features of GTOs, contracted gaussian functions (CGF) are used in most quantum chemical packages. Each CGF is an linear expansion using a set of P GTOs, which typically share cartesian factors,

$$\begin{aligned}\phi^{\mathrm{CGF}}(r_A,l,m,n,\{\zeta_i\},\{c_i\}) &= N\, x_A^l y_A^m z_A^n \sum_{i=1}^{P} c_i \exp(-\zeta_i r_A^2) \\ &= N\, x_A^l y_A^m z_A^n \sum_{i=1}^{P} c_i\, g_i(\zeta_i, r_A)\end{aligned} \tag{2.39}$$

The $g_i(r)$ are called primitive gaussian functions (PGF). The set of contraction coefficients, $\{c_i\}$, and exponents, $\{\zeta_i\}$, are optimized so that

$$\phi^{\mathrm{CGF}}(r_A,l,m,n,\{\zeta_i\},\{c_i\}) \approx \phi^{\mathrm{STO}}(r_A,l,m,n,\zeta) \tag{2.40}$$

As with any expansion of a function in terms of a set functions, the more complete (*i.e.*, largest) the set is the more accurate the expansion. Note that integrals over CGF, which are designed to behave like STOs, result in a summation of integrals over GTOs.

Several CGF basis sets have been devised, and exact details on most of them may be found in the database described in ref. 62. They are characterized by the type (s, p, d, f, etc.) of CGF used for each atom, the number of PGF used to expand each CGF, and the number of CGF used for each orbital. A minimal basis set comprises a CGF for each occupied atomic orbital (*e.g.*, STO-nG,[63,64] where each CGF is expanded in n PGF). Such a small basis set provides a poor description of AOs. For most problems, an adequate basis set should comprise several CFG for valence orbitals, those most responsible for chemical structure and reactivity.[39] An example is the 6-31G basis set,[65] in which core orbitals are a contraction of 6 PGF, and two functions are used for each valence orbital — one a contraction of three PGF, the other an uncontracted GTO. This is called

a double-ζ basis basis set. Orbitals with higher angular quantum number (*e.g.*, p-type orbitals for hydrogen, d-type orbitals for second row atoms), dubbed polarization functions, and GTOs with small ζ values (diffuse functions) are also important.

Choosing an adequate orbital basis set is a crucial step in any quantum chemical calculation. The computational cost (measured in time, memory, and disk space requirements) and the correct description of AOs are directly dependent on this choice, and these two factors must be carefully weighed.

2.3 Correlation methods

In previous sections we glanced at how the Hartree-Fock approximation is used to obtain an estimate of the energy from a single Slater determinant. Now we a will discuss the main problem of this approach and see what can be done to improve the description of a N-electron system.*

Correlation energy

Inherent to the construction of Slater determinants is the strict adherence to the antisymmetry principle. Two electrons cannot be in the same quantum state, and therefore, two electrons with the same spin cannot occupy the same region in space. Their motion is, therefore, correlated, and around each electron there is a region — the Fermi hole — where the probability of finding an electron with the same spin is small.[35] This is a built-in feature of the Hartree-Fock method, and gives rise to the non-classical exchange operator: because electrons with the same spin are (on average) farther apart their interaction is (on average) weaker, and the exchange term cancels out some of their Coulombic interaction.

The presence of r_{ij}^{-1} in the Hamiltonian leads to a singularities (due to an infinite Coulomb potential) at $r_{ij} = 0$. This implies that near zero r_{ij} the wavefunction must obey the Kato cusp condition,[66–68]

$$\left[\frac{\partial \Psi}{\partial r_{ij}}\right]_{r_{ij}=0} = \left[\frac{\Psi}{2}\right]_{r_{ij}=0} \tag{2.41}$$

Expanding the wavefunction in a (truncated) Maclaurin series and using (2.41) we find that for small r_{ij} the correct wavefunction (say, Ψ') should be

$$\Psi' = \Psi\left[1 + \frac{r_{ij}}{2}\right] + O(r_{ij}^2) \tag{2.42}$$

* To keep this discussion brief we will assume that the wavefunction is that of a single-reference closed shell system.

The amplitude of Ψ' increases with r_{ij}, and therefore, it is less likely to find two electrons at small interelectronic distance. That is, around each electron there is a Coulomb hole.[35] Consequently, the motions of opposite-spin electrons should also be correlated, but nothing in the Hartree-Fock approximation indicates it to be so. The cusp condition is poorly described by a Slater determinant built from a one-electron basis set which does not depend explicitly on the interelectronic distance.[69] A poor wavefunction leads to poor estimates of expectation values. This means that the HF energy, E_{HF}, is always an upper-bound to the exact electronic energy, E in (2.8).* The difference between the two is definition of the correlation energy,

$$E_{\mathrm{corr}} = E_{\mathrm{HF}} - E \tag{2.43}$$

The Hartree-Fock energy accounts for *ca.* 99 % of the total energy, but the correlation energy is vital to virtually all quantum chemical calculations.[70]

Configuration interaction

Slater determinants built from Hartree-Fock orbitals are eigenfunctions of the Hamiltonian operator for an N-electron system, and therefore, they constitute a basis set in the N-particle Hilbert space.[35] As such, they may be used to expand the exact wavefunction, *viz.* Ψ in (2.8), which is a function in the same space. Each Slater determinant, Φ, in the expansion is built from N occupied and/or virtual spin-orbitals. Their relation with the ground-state Slater determinant, which we will here call Φ_0, can be interpreted as an excitation of electrons from occupied to virtual orbitals.[35,38–40] For instance, Φ_i^p is a single excitation of an electron from the occupied spin-orbital χ_i to the virtual spin-orbital χ_p. Similarly, Φ_{ij}^{pq} is a double excitation of the electrons in χ_i and χ_j to the virtual spin-orbitals χ_p and χ_q. Higher excitations, up to the Nth-order where all electrons occupy virtual orbitals, are defined likewise. This technique is called configuration interaction (CI),[71] and the resulting wavefunction ansatz is

$$\begin{aligned}
\Psi_{\mathrm{CI}} &= \Phi_0 + \sum_{i,p} t_i^p \Phi_i^p + \sum_{\substack{p<q \\ i<j}} t_{ij}^{pq} \Phi_{ij}^{pq} + \cdots \sum_{\substack{p<q<\cdots<r \\ i<j<\cdots<k}} t_{ij\cdots k}^{pq\cdots r} \Phi_{ij\cdots k}^{pq\cdots r} \\
&= [1 + \hat{T}_1 + \hat{T}_2 + \cdots + \hat{T}_N]\Phi_0 \\
&= \left[1 + \sum_{e=0}^{N} \hat{T}_e\right] \Phi_0 \\
&= \Phi_0 + \hat{T}\Phi_0
\end{aligned} \tag{2.44}$$

* Except, of course, in the trivial case of a one-electron system.

where the summations span all occupied (indexed i,j,k) and virtual (indexed p,q,r) orbitals. Above we have implicitly defined the excitation operator, $\hat{T}$, as a sum of single ($\hat{T}_1$), double ($\hat{T}_2$), and higher order excitation operators which, when operating on a Slater determinant, generate a summation of all excited determinants of each particular order.

The one-electron orbitals are fixed *a priori* (*i.e.*, they are obtained from a previous HF calculation) and therefore, so are the Slater determinants built from them. Our variational freedom in (2.44) now lies with the set of amplitudes $\{t_i^p, t_{ij}^{pq}, \ldots, t_{ij\ldots k}^{pq\cdots r}\}$, which are optimized variationally in order to minimize the (normalized) total energy,[35,38–40]

$$E_{\mathrm{CI}} = \frac{\langle \Psi_{\mathrm{CI}} \,|\, \hat{H} \,|\, \Psi_{\mathrm{CI}} \rangle}{\langle \Psi_{\mathrm{CI}} \,|\, \Psi_{\mathrm{CI}} \rangle} \tag{2.45}$$

If all Slater determinants are used (full-CI) the exact electronic energy for a given one-particle basis set is obtained.[72] However, the number of Slater determinants obtained for a N-electron system using a basis set with size K is $\binom{2K}{N}$.[39] The sheer number of terms involved in (2.44) means that full-CI can seldom be used,[70] and instead $\hat{T}$ must be truncated. If this is done after the double excitations term (*i.e.*, $\hat{T} = \hat{T}_1 + \hat{T}_2$) we obtain the CISD method,[39] which includes all single and double excitations.

Coupled-cluster

CISD is undoubtedly a significant improvement over HF, but truncated CI methods are not size-consistent.[39,70,71*] Coupled cluster[73,74] (CC) does not suffer from this limitation,[39,70] and therefore, it is often used instead. In CC the wave function ansatz is

$$\Psi_{\mathrm{CC}} = \exp(\hat{T})\,\Phi_0 \tag{2.46}$$

Since[75]

$$\exp(x) = \sum_{n=0}^{\infty} \frac{1}{n!} x^n \tag{2.47}$$

* That is, the energy does not scale linearly with the size of the system, and is not additive for infinitely separated systems. For instance, He has two electrons so CISD comprises all possible excitations and yields the exact energy. However, for two He atoms CISD no longer provides a full description of the system, since it does not include the triple and quadruple excitations due to single and double excitations in each He atom.

even if $\hat{T}$ is truncated after $\hat{T}_2$ like we did in CISD, the resulting CCSD wavefunction[40]

$$\begin{aligned}\Psi_{\text{CCSD}} &= \exp(\hat{T}_1 + \hat{T}_2)\Phi_0 \\ &= [1 + (\hat{T}_1 + \hat{T}_2) + \frac{1}{2}(\hat{T}_1 + \hat{T}_2)^2 + \frac{1}{6}(\hat{T}_1 + \hat{T}_2)^3 + \ldots]\Phi_0\end{aligned} \tag{2.48}$$

still includes 3rd-order and up to Nth-order excitations partially as products (say, as coupled clusters) of single and double excitations, thus insuring that CC is size-consistent. Amplitudes in the excitation operators, are determined by solving a set of coupled equations (one for each amplitude) iteratively until they are self-consistent.

Besides single and double excitations, a more rigorous description of triple excitations is often necessary to obtain accurate chemical properties.[70] Strict CCSDT, for which $\Psi_{\text{CCSDT}} = \exp(\hat{T}_1 + \hat{T}_2 + \hat{T}_3)\Phi_0$, can be performed with some quantum chemical packages, but due to its extremely high computational cost, its application is still limited to small species. A more reasonably priced method consists in the addition to CCSD of an *a posteriori* non-variational treatment of triple excitations based on the third-order Møller-Plesset perturbation theory.[76] The most common way of doing so is using the CCSD(T) method,[77] which is completely accurate up to 4th-order excitations.[78]

Scaling of correlation methods

We have often noted that the basis set is crucial in quantum chemistry calculations. It affects the accurate description of spin-orbitals $\{\chi\}$, via (2.30), and therefore, influences the quality of the ground-state reference wavefunction, Φ_0. Fortunately, the HF energy converges quickly to its complete basis set (CBS) limit.[79] Moreover, due to its modest computational cost, accurate HF energies can be obtained for most species. The problem that remains is, therefore, the influence of the basis set size on the correlation energy.

Theoretically, the exact numerical solution of the non-relativistic time-independent Schrödinger equation, within the Born-Oppenheimer framework, can obtained from full-CI and a complete one-particle basis set.[39,72] Since the number of Slater determinants increases rapidly with the basis set size, even for small molecules the computational cost of a full-CI calculation with a near-CBS basis sets is not affordable. We have illustrated how the computational can be reduced cost by truncating the CI expansion (*e.g.*, CISD, CCSD), but the accuracy of these methods is still dependent on the number of excited Slater determinants, and hence, on the basis set size. Unfortunately, in contrast to HF, the correlation energy obtained from these methods converges slowly to its CBS limit while their computational cost rises very sharply with the basis

set size. For instance, the cost of CISD and CCSD scales as $O(o^2v^4)$ with the basis set size,[78] where o and v are, respectively, the number of occupied and virtual spin-orbitals. This cost is iterative, which means that we pay this computational toll for every step in the single and double amplitudes $\{t_i^p, t_{ij}^{pq}\}$ convergence procedure. The perturbative treatment of triples in CCSD(T) has an additional $O(o^3v^4)$ cost.[78*] Even though this is cost is not iterative, the time required by a one-time perturbative triples calculation often exceeds the time for the whole iterative CCSD calculation. Consequently, smaller basis sets must be used in wavefunction-based correlation treatments, which introduces a basis set incompleteness error.

Complete basis set extrapolation

The basis set incompleteness error can be partially mitigated trough the use of CBS extrapolation methods.[80–91] Using the monotonic convergence of the energy to its CBS value with respect to the basis set size, these methods can provide estimates of CBS energies from data obtained using smaller basis sets. For this purpose it is crucial to use even-tempered, and systematically improved, basis sets. The correlation-consistent polarized valence x-zeta (dubbed cc-pVxZ or VxZ, with x = D, T, Q, 5, 6) and the augmented correlation-consisted polarized valence x-zeta (dubbed aug-cc-pVxZ or AVxZ, with x = D, T, Q, 5, 6) hierarchical basis set families[92–95] fulfill this requirement and have become the *de facto* standard basis sets for CBS extrapolation.[†] The general extrapolation ansatz is

$$E(x) = E(\infty) + f(x) \tag{2.49}$$

where $E(x)$ is the energy obtained using the basis with cardinal x (*e.g.*, $E(2) \Longrightarrow$ VDZ) and $E(\infty)$ is correlation energy obtained with a CBS basis set. $f(x)$ is a non-general function of the basis cardinal, specific of each ansatz. For correlation energies $f(x)$ is commonly defined as[82–84]

$$f(x) = A(x+\alpha)^{-\beta} \tag{2.50}$$

where A is an undetermined constant and α and β are the parameters, which are specific of each method (*e.g.*, $\alpha = 0$ and $\beta = 3$ for the extrapolation method of Halkier *et al.*;[83] and $\alpha = 0$ and $\beta = 2.4$ for the Truhlar CCSD and CCSD(T) correlation energy extrapolation method[82]). From (2.49) and (2.50) the desired

[*] An iterative treatment of triples using CCSDT scales even worse, as $O(o^3v^5)$.

[†] D,T,Q,5,6 stand, respectively, for double, triple, quadruple, quintuple, and sextuple. They denote the number of CGF used for valence orbitals — the basis set cardinal. The difference between VxZ and AVxZ basis sets is that the latter have diffuse functions. For general details on orbitals basis sets see Section 2.2 and ref. 62.

CBS correlation energy can be estimated using, for example, a two-point (x_1,x_2) (*e.g.*, $x_1 = 2$, $x_2 = 3$) extrapolation

$$E_{\text{corr}}(\infty) = \frac{(x_2+\alpha)^{-\beta}E_{\text{corr}}(x_2) - (x_1+\alpha)^{-\beta}E_{\text{corr}}(x_1)}{(x_2+\alpha)^{-\beta} - (x_1+\alpha)^{-\beta}} \tag{2.51}$$

where $E_{\text{corr}}(x_1)$ and $E_{\text{corr}}(x_2)$ are the correlation energies obtained using two basis sets with cardinal x_1 and x_2. Alternatively, an *ad hoc* fitting of energies obtained with several basis sets to (2.49) may be used to retrieve $E(\infty)$. These extrapolation methods provide data which are often close to their CBS limits, and are more cost-efficient than a single calculation with a larger basis set. Consequently, they are broadly used in computational chemistry.

2.4 Density functional theory

Wavefunction methods can be extremely accurate, but that accuracy comes with a high computational cost. An alternative to them is density functional theory (DFT).[35,40,96,97] In DFT the basic variable needed to describe a N-electron system under some external potential* is the electron density, $\rho(\boldsymbol{r})$, which is the number of electrons per unit volume.† The electron density, which can be observed experimentally,[98] is related to the wavefunction by[99,100]

$$\rho(\boldsymbol{r}) = N \sum_{w_1=\alpha,\beta} \int \cdots \int \Psi^*(\mathbf{x}_1,\mathbf{x}_2,\ldots,\mathbf{x}_N)\Psi(\mathbf{x}_1,\mathbf{x}_2,\ldots,\mathbf{x}_N) d w_1 d\mathbf{x}_2 \ldots d\mathbf{x}_N \tag{2.52}$$

Hohenberg-Kohn theorems

The theoretical foundation for using $\rho(\boldsymbol{r})$ as basic variable is given by a theorem, elegantly proved by Pierre Hohenberg and Walter Kohn,[101] which states that, apart from a trivial additive constant, the external potential (say, $v(\boldsymbol{r})$) is determined by the electron density. For a molecular system, in the absence of any other external potential, this $v(\boldsymbol{r})$ is the coulombic attraction between an electron and the M nuclei,

$$v(\boldsymbol{r}_i) = -\sum_{A=1}^{M} \frac{Z_A}{r_{iA}} \tag{2.53}$$

* In DFT jargon it is common to call "external potential" to the electron-nuclei attraction.

† Note that the definition of functional is implicit: the basic variable in DFT is a function, $\rho(\boldsymbol{r})$.

This implies that $\rho(\boldsymbol{r})$ determines the position and charge of all M nuclei. Indeed, the density has a cusp near nuclei with a slope proportional to the nuclear charge.[96] This is a fundamental point in the theory of atoms in molecules developed by Richard Bader.[102] Considering the wavefunction normalized, then

$$\int \rho(\boldsymbol{r}) d\boldsymbol{r} = N \tag{2.54}$$

That is, $\rho(\boldsymbol{r})$ determines the number of electrons. If we now the positions and charges of all nuclei (in general, if we know the external potential $v(r)$) as well as the number of electrons, the Hamiltonian for the system is completely defined, and therefore, so is the wavefunction and all other electronic properties of the system. Consequently, the energy is a functional of ρ, and the exact ground-state energy can be obtained from the exact ground-state electron density, ρ_0.

The electron density, a function in 3 dimensional space, caries all the information held by the cumbersome $4N$ dimensional wavefunction. The problem lies in obtaining such a function without knowing the wavefunction first. In the same ground-braking work,[101] Hohenberg and Kohn also proved that for a given trial density, such that $\rho_{\text{trial}}(\boldsymbol{r}) \geq 0$ and $\int \rho_{\text{trial}}(\boldsymbol{r}) d\boldsymbol{r} = N$,* then

$$E[\rho_{\text{trial}}] \geq E[\rho_0] \tag{2.55}$$

This means that, if we can write E in terms of the electron density, we can obtain ρ_0 by energy minimization, in much the same way as we did for the wavefunction.

For a system with electron density $\rho(\boldsymbol{r})$ and potential $v(\boldsymbol{r})$ the nuclei-electron interaction operator, $\hat{V}_{ne}$, may be written as

$$\hat{V}_{ne} = \sum_{i=1}^{N} v(\boldsymbol{r}_i) \tag{2.56}$$

* In other words, $\rho_{\text{trial}}(\boldsymbol{r})$ is a positive-semidefinite and N-representable function.

Using (2.52) we find that its expectation value for a wavefunction, Ψ, is,

$$\begin{aligned}\langle \Psi \mid \hat{V}_{ne} \mid \Psi \rangle &= \sum_{i=1}^{N} \langle \Psi \mid v(\boldsymbol{r}_i) \mid \Psi \rangle \\ &= \sum_{i=1}^{N} \int \cdots \int \Psi^*(\mathbf{x}_1, \mathbf{x}_2, \ldots, \mathbf{x}_N)\, v(\boldsymbol{r}_i)\, \Psi(\mathbf{x}_1, \mathbf{x}_2, \ldots, \mathbf{x}_N) d\mathbf{x}_1 d\mathbf{x}_2 \ldots d\mathbf{x}_N \\ &= \sum_{i=1}^{N} \int \left[\frac{\rho(\boldsymbol{r}_i)}{N} \right] v(\boldsymbol{r}_i) d\boldsymbol{r}_i \\ &= \int \rho(\boldsymbol{r}) v(\boldsymbol{r}) d\boldsymbol{r}\end{aligned} \tag{2.57}$$

We can then write the energy as

$$E[\rho] = F_{\mathrm{HK}}[\rho] + \int \rho(\boldsymbol{r}) v(\boldsymbol{r}) d\boldsymbol{r} \tag{2.58}$$

where the undetermined functional, $F_{\mathrm{HK}}[\rho]$, is the Hohenberg-Kohn functional,[101] which accounts for the kinetic and electron-electron potential energy of electrons. Minimizing (2.58) under the constraint that ρ is N-representable yields ρ_0.

Kohn-Sham method

We know how to obtain the energy of a system, via minimization of (2.58), but this cannot be done because we do not know $F_{\mathrm{HK}}[\rho]$. In 1965, Walter Kohn and Lu Sham derived a method which partially solved this problem.[103] The main idea is to consider a fictitious non-interacting system, similar to that of (2.10), but which experiences an external potential $v_{\mathrm{eff}}(\boldsymbol{r})$ such that $\rho(\boldsymbol{r}) = \rho_0(\boldsymbol{r})$. For such a system a Slater determinant of N spin orbitals $\{\chi_i\}$ is the exact wavefunction, and

$$\rho(\boldsymbol{r}) = \sum_{i=1}^{N} \sum_{w=\alpha,\beta} \chi_i^*(\boldsymbol{r}, w) \chi_i(\boldsymbol{r}, w) \tag{2.59}$$

Solving a set of one-particle equation equations

$$\left[-\frac{1}{2} \nabla_i^2 + v_{\mathrm{eff}}(\boldsymbol{r}) \right] \chi_i = \epsilon_i \chi_i \tag{2.60}$$

leads to the Kohn-Sham orbtials, $\{\chi_i^{\mathrm{KS}}\}$, from which the exact density ρ_0 can (in principle) be obtained using (2.59). In order to do this we must first define the effective potential in (2.60). The kinetic energy for this fictitious system is

$$T_{\mathrm{S}}[\rho] = -\frac{1}{2}\sum_{i=1}^{N}\langle\chi_i \mid \nabla_i^2 \mid \chi_i\rangle \tag{2.61}$$

and the classical coulomb repulsion is just[96]

$$J[\rho] = \frac{1}{2}\iint \rho(\boldsymbol{r}_1)\, r_{12}^{-1}\, \rho(\boldsymbol{r}_2) d\boldsymbol{r}_1 d\boldsymbol{r}_2 \tag{2.62}$$

We thus know part of $F_{\mathrm{HK}}[\rho]$, and total energy can be rewritten as

$$\begin{aligned} E[\rho] &= F_{\mathrm{HK}}[\rho] + \int \rho(\boldsymbol{r})v(\boldsymbol{r})d\boldsymbol{r} \\ &= T_{\mathrm{S}}[\rho] + J[\rho] + E_{\mathrm{xc}}[\rho] + \int \rho(\boldsymbol{r})v(\boldsymbol{r})d\boldsymbol{r} \end{aligned} \tag{2.63}$$

Here, $E_{\mathrm{xc}}[\rho]$ is the exchange-correlation functional, which gathers the non-classical interelectronic interaction terms due to the Fermi and Coulomb holes, and the difference between the $T_{\mathrm{S}}[\rho]$ and the actual kinetic energy of the system.[97] Note that in (2.63) we do not have an exchange term to prevent the coulomb interaction of the electron with itself like we did in (2.23). Consequently, $E_{\mathrm{xc}}[\rho]$ must also correct this self-interaction error.

The energy is a functional of the electron density which through (2.59) is defined by the spin-orbitals. We can minimize $E[\rho]$ with respect to the choice of spin-orbitals under the constraint that they remain orthonormal, like we did in (2.24). This leads to[35,40,96,97]

$$\begin{aligned} \hat{F}_{\mathrm{KS}}(1)\chi_i(1) &= \left[-\frac{1}{2}\nabla_i^2 + \int r_{12}^{-1}\rho(\boldsymbol{r}_2)d\boldsymbol{r}_2 + v_{\mathrm{xc}}(\boldsymbol{r}) + v(\boldsymbol{r})\right]\chi_i(1) \\ &= \left[-\frac{1}{2}\nabla_i^2 + v_{\mathrm{eff}}(\boldsymbol{r})\right]\chi_i(1) \\ &= \sum_{i=1}^{N} l_{ij}\chi_i(1) \end{aligned} \tag{2.64}$$

where v_{xc} is the functional derivate of $E_{\mathrm{xc}}[\rho]$ with respect to ρ.[96] Orthogonalizing the spin orbitals so that the matrix of Lagrange multipliers is diagonal we obtain the canonical Kohn-Sham orbital equations

$$\hat{F}_{\mathrm{KS}}(1)\chi_i^{\mathrm{KS}}(1) = \epsilon_i^{\mathrm{KS}}\chi_i^{\mathrm{KS}}(1) \tag{2.65}$$

$\hat{F}_{\mathrm{KS}}$ depends explicitly on the density so (2.65) must be solved using a self-consistent field procedure. As before, the spatial orbitals (and hence, the density) can be expanded in a LCAO, and an orbital basis set used to expand AOs. The electron density may be split in the contributions for α and β electrons, which leads two sets of Kohn-Sham equations similar to (2.65) — one set for each spin. The total energy is related to the Kohn-Sham orbital energies by[96]

$$E[\rho_0] = \sum_{i=1}^{N} \epsilon_i^{\mathrm{KS}} - J[\rho_0] + E_{\mathrm{xc}}[\rho_0] - \int v_{\mathrm{xc}}(r)\rho_0(\boldsymbol{r})d\boldsymbol{r} \tag{2.66}$$

These expressions are strikingly similar to the equations obtained for the Hartree-Fock approximation, but now the energy is exact provided, of course, we know the exact $E_{\mathrm{xc}}[\rho]$.

Approximate exchange-correlation functionals

In wavefunction methods we know how to obtain the exact wavefunction from the CI expansion, and therefore, we can assess analytically how good an approximate correlation method is. For DFT the inverse is true: we know nothing about $E_{\mathrm{xc}}[\rho]$, except that that it must account for all those contributions we left out of (2.63).[35,40,96,97] This means that the accuracy of density functionals has, ultimately, to be evaluated by comparison with accurate experimental or theoretical data. Since this accuracy is directly related to the correct description of Coulomb an Fermi holes,[35] obtaining approximate expressions for the unknown $E_{\mathrm{xc}}[\rho]$ functional is the major challenge faced by DFT.

The simplest approximation to $E_{\mathrm{xc}}[\rho]$ is to consider that it is the exchange and correlation of an uniform electron gas, and therefore

$$\begin{aligned} E_{\mathrm{xc}}^{\mathrm{LDA}}[\rho] &= \int e_{\mathrm{xc}}[\rho(\boldsymbol{r})]\rho(\boldsymbol{r})\,d\boldsymbol{r} \\ &= \int e_{\mathrm{x}}[\rho(\boldsymbol{r})]\rho(\boldsymbol{r})\,d\boldsymbol{r} + \int e_{\mathrm{c}}[\rho(\boldsymbol{r})]\rho(\boldsymbol{r})\,d\boldsymbol{r} \\ &= -C_{\mathrm{x}} \int \rho(\boldsymbol{r})^{4/3} d\boldsymbol{r} + \int e_{\mathrm{c}}[\rho(\boldsymbol{r})]\rho(\boldsymbol{r})\,d\boldsymbol{r}, \text{ with } C_{\mathrm{x}} = \frac{3}{4}\left(\frac{3}{\pi}\right)^{1/3} \end{aligned} \tag{2.67}$$

It is common to split the exchange an correlation as above, and treat them separately. The approximation in (2.67), dubbed local density approximation (LDA), was used in the work of Kohn and Sham.[103] The expression for the exchange in (2.67) is the Dirac exchange functional,[104] but it is often called the Slater exchange (S) due to the similarity with a simplification of the Hartree-Fock approximation proposed by John Slater.[105] The correlation part can be

derived using data from numerical simulations, and the most common such correlation functionals are those proposed by Vosko, Wilk, and Nusair (VWN).[106] LDA can be further extended to the unrestricted case, for which the density of electrons with different spins is not the same. This results in the local spin-density approximation (LSDA),[96] represented by

$$E_{\mathrm{xc}}^{\mathrm{LSDA}}[\rho] = \int e_{\mathrm{xc}}[\rho^{\alpha}(\boldsymbol{r}), \rho^{\beta}(\boldsymbol{r})]\rho(\boldsymbol{r})\, d\boldsymbol{r} \tag{2.68}$$

The electron density of a molecule or an atom is certainly not homogeneous, and therefore LDA and LSDA have limited success. Improvement over the local approximation arises if the gradient of the density is also considered. This is done in generalized gradient approximations (GGA),[97] with general formula

$$E_{\mathrm{xc}}^{\mathrm{GGA}}[\rho] = \int f_{\mathrm{xc}}[\rho^{\alpha}(\boldsymbol{r}), \rho^{\beta}(\boldsymbol{r}), \nabla\rho^{\alpha}(\boldsymbol{r}), \nabla\rho^{\beta}(\boldsymbol{r})]\, d\boldsymbol{r} \tag{2.69}$$

where f_{xc} is a functional of the spin-densities and respective gradients. Examples of GGA functionals are Becke's 1988 exchange functional (B),[107] the Pardew and Wang 1991 correlation functional (PW91),[108,109] and the Lee, Yang, and Parr 1988 correlation functional (LYP).[110] This is taken one step further in meta-GGA functionals, which also depend on the Laplacian of the electron density.[97]

In addition there also hybrid approximations, in which a scaled Hartree-Fock exchange term calculated with Kohn-Sham orbitals is included in $E_{\mathrm{xc}}[\rho]$.[111] One such hybrid functional is B3LYP,[112,113] defined as

$$\begin{aligned} E_{xc}^{\mathrm{B3LYP}}[\rho] = (1-a)E_{\mathrm{x}}^{\mathrm{LSDA}}[\rho] + aE_{\mathrm{x}}^{\mathrm{HF}}[\rho] + bE_{\mathrm{x}}^{\mathrm{B}}[\rho] \\ + cE_{\mathrm{c}}^{\mathrm{LYP}}[\rho] + (1-c)E_{\mathrm{c}}^{\mathrm{VWN3}}[\rho] \end{aligned} \tag{2.70}$$

The parameters $a = 0.20$, $b = 0.72$, and $c = 0.81$ were found by fitting to thermochemical data in the G1 test set.[114,115*] The local correlation functional in B3LYP, $E_{\mathrm{c}}^{\mathrm{VWN3}}[\rho]$, is the third functional proposed by Vosko, Wilk, and Nusair in ref. 106.

* This fitting was done by Becke using the PW91 correlation functional (*i.e.*, for B3PW91) in ref. 112. Guided by a considerable amount of physical intuition (and perhaps a bit of serendipity) Stephens *et al.* later argued in ref. 113 that the exact same parameters could be used with the LYP correlation functional. Since LYP cannot be easily separated into local and gradient-corrected terms, the authors included VWN3 to cancel the local term. This was described by M. J. Frish, one of the coauthors of ref. 113, in `ccl.net`, who also noted that this fortunate swap of correlation functional was motivated by the absence of the PW91 functional in the 1992 version of Gaussian (*viz.* G92/DFT).

2.5 Composite methods

Composite methods are multi-step procedures using a predefined set of wavefunction and/or density functional calculations. They are based on the assumption that the effect of basis set and order of correlation treatment can be decoupled. Most composite methods also include include empirical corrections and complete basis set extrapolations. An example are the Gaussian-*n* methods[114–122] (*viz.* G1, G2, G2MP2, G3, G3MP2, G3B3, G3MP2B3,G4, and G4MP2). For instance in G1, the oldest and simplest composite method in the Gaussian-*n* family, the QCISD(T)/6-311+G(2df,p) energy is estimated from

$$\begin{aligned} E[\text{QCISD(T)/6-311+G(2df,p)}] \approx E[\text{MP4/6-311G(d,p)}] + \Delta E(+) \\ + \Delta E(\text{2df}) + \Delta E(\text{QCI}) + \Delta E(\text{HLC}) \end{aligned} \tag{2.71}$$

with

$$\Delta E(+) = E[\text{MP4/6-311+G(d,p)}] - E[\text{MP4/6-311G(d,p)}] \tag{2.72}$$

$$\Delta E(\text{2df}) = E[\text{MP4/6-311G(2df,p)}] - E[\text{MP4/6-311G(d,p)}] \tag{2.73}$$

$$\Delta E(\text{QCI}) = E[\text{QCISD(T)/6-311G(d,p)}] - E[\text{MP4/6-311G(d,p)}] \tag{2.74}$$

and where $\Delta E(\text{HLC})$ is an empirical correction. CBS-*n* methods[123–130] (*viz.* CBS-4, CBS-4M, CBS-q, CBS-Q, CBS-QB3, CBS-APNO, and ROCBS-QB3) are similarly constructed but feature a CBS extrapolation of MP2 pair energies. Complete basis set extrapolations are heavily used in the Weizmann-*n* methods[131–134] (*viz.* W1, W2, W3, and W4), which do not include empirical corrections, and instead rely on high-order correlation energy calculations with large basis sets. A good compromise between computational cost and accuracy is often obtained with CBS-QB3.[130,132]

Since structure optimizations (*i.e.*, minimization of the total molecular energy with respect to the position of nuclei) require several energy calculations to be performed, they often carried out using less computationally demanding methods. This is a common practice in computational chemistry and not reserved to composite methods.

2.6 Recent quantum chemical methods

Quantum chemistry is far from being a static research field, and new methodologies arise very often. Some of the recent advances in DFT are double-hybrid density functional methods, which include a scaled 2nd-order MP2 correction calculated with Kohn-Sham orbitals,[135–138] and long-range corrected functionals.[135,138–140] These methods increase the accuracy of DFT and partially correct

its behaviour for long-range van der Waals electron interactions,[135] and have already found their way into several quantum chemical software packages.

Regarding wavefunction methods, we saw in (2.41) and (2.42) that the wavefunction should depend on the interelectronic distance. However, explicit inclusion of r_{ij} (R12[69] methods) or of some function of r_{ij} (F12[141]*methods) in the wave function leads to intricate three- and four-electron integrals.[142] Nevertheless, accurate and cost-efficient implementations of these explicitly correlated methods do exist. As expected, this leads to a better description of the wavefunction, and consequently, smaller basis sets produce more accurate energies. For instance, CCSD(T)-F12a/AVTZ yields more accurate reaction energies of both open- and closed-shell reactions, atomization energies, electron affinities, ionization potentials, equilibrium geometries, and harmonic vibrational frequencies than CCSD(T)/AV5Z, while having a cost similar to a conventional CCSD(T)/AVTZ calculation.[143] General details on these methods may be found in a recent review, ref. 142.

Another refinement to wavefunction methods is the use of local approximations.[144–149] Using localized molecular orbitals, these methods allow to truncate the virtual space available for excitations, and to disregard or treat at a lower level of theory the interactions of distant electrons. This lowers the cost of correlation methods, making it scale almost linearly with the system size, while recovering a large amount (*ca.* 99 %) of the correlation energy obtained with equivalent non-local methods. A thorough discussion on local methods is given in ref. 149. Local approximations are now being developed for explicitly correlated methods, yielding to extremely accurate treatments of correlation energy with a favourable, near-linear, scaling.[150–154]

One of the newest developments of quantum mechanics is perhaps the two-electron-reduced-density matrix (2-RDM) theory, described in detail in ref. 155. The 2-RDM is defined as,

$$D^2(12,1'2') = \int \cdots \int \Psi^*(\mathbf{x}_1,\mathbf{x}_2,\ldots,\mathbf{x}_N)\Psi(\mathbf{x}'_1,\mathbf{x}'_2,\ldots,\mathbf{x}_N)d\mathbf{x}_3 d\mathbf{x}_4 \ldots d\mathbf{x}_N \quad (2.75)$$

Since the molecular Hamiltonian contains at most a two-electron operator, (2.75) provides all the information needed to obtain the ground-state energy of a system. Therefore, if we can guess D^2, we can determine the energy exactly without having to know the ground-state wavefunction. The problem is the N-representability of the 2-RDM, that is, making sure that the guessed D^2 corresponds to a system of N fermions obeying the Pauli exclusion principle. The conditions it must obey are known,[156] and the theory is already quite ma-

*Some authors refer to F12 as R12 to emphasize the dependence on r_{ij}.

ture.* Obtaining the 2-RDM this way is possible, and several applications have already emerged. Some recent applications of 2-RDM may be found in refs. 157–159. The main impediment to 2-RDM theory is now mathematical and computational. Finding an N-representable 2-RDM is a semidefinite programming† (SDP) problem,[160,161] and while SDP solver algorithms do exist, they are still rather demanding and cumbersome.

2.7 Calculating enthalpies

Until now we have discussed theoretical methods from which the ground-state energy can be obtained. Here we show how that data can be used to calculate enthalpies.

Zero-point energy correction

The molar enthalpy, H, of a system with internal energy U, pressure p, and volume V, at some temperature T is, by definition,[162]

$$H_T = U_T + pV \tag{2.76}$$

For one molecule in vacuum the ideal gas law applies, and therefore the molar enthalpy is

$$H_T = U_T + RT \tag{2.77}$$

where $R = N_A k_B$ is the ideal gas constant, N_A is the Avogadro constant, and k_B is the Boltzmann constant. The total ground-state energy computed by the computational methods above, E_{tot}, is approximately the internal energy at $T = 0$ K, but since we fixed the positions of nuclei, we must correct it for the vibrational motion of nuclei at $T = 0$ K by adding the zero-point energy correction, E_{zp}. H_0 is therefore,

$$\begin{aligned} H_0 &= U_0 + RT \\ &= E_{\text{tot}} + E_{\text{zp}} + RT \end{aligned} \tag{2.78}$$

Assuming the vibrations are harmonic, the molar zero-point energy correction is[163‡]

$$E_{\text{zp}} = N_A \sum_{i=1}^{N_f} \frac{1}{2} h\nu_i \tag{2.79}$$

* In 1955 Löwdin had already pondered the subject of writing the energy in terms of density matrices.[99]

† Programming in the mathematical sense, *i.e.* optimization.

‡ It is also common to find this expression in terms of vibrational temperatures, $\Theta_i = h\nu_i/k_B$, in which case (2.79) is $E_{\text{zp}} = \frac{R}{2}\sum_{i=1}^{N_f} \Theta_i$

In (2.79) N_f are the degrees of freedom, which for a molecule with M atoms are $N_f = 3M - 6$, or $N_f = 3M - 5$ if the molecule is linear. ν_i is the frequency of each molecular vibrational mode.

Thermal correction

We are often more interested in obtaining the enthalpy at some non-zero temperature, particularly $T = 298.15$ K. For this purpose a thermal correction must be added to H_0. To determine this H_{termal} we may consider the expectation value for the internal energy of an independent molecule at temperature T, given by[42]

$$\begin{aligned}\langle\epsilon\rangle &= \sum_{i=1}^{\Omega}\left(\frac{g_i\, e^{-\beta\epsilon_i}}{Z(V,T)}\right)\epsilon_i \\ &= -\left(\frac{\partial \ln Z(V,T)}{\partial\beta}\right)_V \\ &= k_B T^2\left(\frac{\partial \ln Z(V,T)}{\partial T}\right)_V\end{aligned} \tag{2.80}$$

Here, $\beta = (k_B T)^{-1}$ and the molecular partition, $Z(V,T)$, is

$$Z(V,T) = \sum_{i=1}^{\Omega} g_i\, e^{-\beta\epsilon_i} \tag{2.81}$$

The summations in (2.80) and (2.81) are over all Ω unique states with degeneracy g_i and energy ϵ_i. Assuming the energy can be separated in

$$\langle\epsilon\rangle = \langle\epsilon^{\text{trans}}\rangle + \langle\epsilon^{\text{rot}}\rangle + \langle\epsilon^{\text{vib}}\rangle + \langle\epsilon^{\text{elec}}\rangle \tag{2.82}$$

where the terms are the expectation values for, respectively, the translational, rotational, vibrational, and electronic energies, we may be split the partition function as

$$Z(V,T) = Z_{\text{trans}}(V,T)\, Z_{\text{rot}}(V,T)\, Z_{\text{vib}}(V,T)\, Z_{\text{elec}}(V,T) \tag{2.83}$$

and determine the contribution of each term independently.[42]

For translation and rotational motion we may bypass the partition function and estimate their average contribution directly from the equipartition theorem, which is a good approximation at room temperature.[162,163] Therefore, the rotational contribution to the energy is $3k_BT/2$ for a non-linear molecule, k_BT for a linear molecule, and 0 for an atom. The translational contribution is $3k_BT/2$ in all these cases. Further, if we assume that the difference

between the ground state energy and that of the first excited state is much larger than $k_B T$ so that excited states are unavailable, the electronic contribution can be neglected.

All that remains is the vibrational contribution to the thermal correction. The partition function for an harmonic oscillator is[163]

$$\begin{aligned} z(T) &= \sum_{n=0}^{\infty} e^{-\beta \epsilon_n^{\text{vib}}} \\ &= \sum_{n=0}^{\infty} e^{-\beta(n+\frac{1}{2})h\nu} \\ &= e^{-\beta h\nu/2} \sum_{n=0}^{\infty} e^{-\beta n h\nu} \end{aligned} \tag{2.84}$$

This is a geometric series, which therefore converges to[75]

$$z(T) = \frac{e^{-\beta h\nu/2}}{1 - e^{-\beta h\nu}} \tag{2.85}$$

The total vibrational partition function is a product of (2.85) for the N_f vibrational modes,

$$Z_{\text{vib}}(T) = \prod_{i=1}^{N_f} z_i(T) \tag{2.86}$$

Using (2.86) in (2.80) we find that

$$\begin{aligned} \langle \epsilon_{\text{vib}} \rangle &= -\frac{\partial \ln Z_{\text{vib}}(T)}{\partial \beta} \\ &= -\sum_{i=1}^{N_f} \frac{\partial \ln z_i(T)}{\partial \beta} \\ &= \sum_{i=1}^{N_f} \left(\frac{1}{2} + \frac{e^{-\beta h\nu_i}}{1 - e^{-\beta h\nu_i}} \right) h\nu_i \end{aligned} \tag{2.87}$$

The zero point energy correction is included in (2.87) so, the molar enthalpy at temperature T will be

$$\begin{aligned} H_T &= H_0 + H_{\text{termal}} \\ &= H_0 + (N_A \langle \epsilon \rangle - E_{\text{zp}}) \\ &= E_{\text{tot}} + N_A \langle \epsilon \rangle \end{aligned} \tag{2.88}$$

This is how the $H_{298.15}$ used in the following chapters are calculated.

CHAPTER 3

The cyclopentadienyl radical

The cyclopentadienyl radical (C_5H_5) is a key ligand in organometallic chemistry.[164] A sound knowledge of its energetics, particularly of its standard enthalpy of formation, is fundamental to discuss the nature of metal-C_5H_5bonds. Since the standard enthalpy of formation of 1,3-cyclopentadiene (C_5H_6) is well known,[165] $\Delta_f H°(C_5H_5)$ can be computed from the C_5H_5—H bond dissociation enthalpy. Moreover, this BDE conveys insightful information about the stability of radicals in the vicinity of double bonds. Surprisingly, despite their importance, a review of available thermochemical data reveled that values for $\Delta_f H°(C_5H_5)$ and $DH°(C_5H_5—H)$ spanned a range of *ca.* 30 $kJ \cdot mol^{-1}$.[166] Clearly, a reassessment of these important thermochemical data was needed.

In ref. 166 (henceforth referred to as **P1**) we studied the enthalpy of formation of the C_5H_5radical using TR-PAC and computational chemistry.* A facsimile of this work is included in this chapter. TR-PAC results, together with available experimental data, afforded $DH°(C_5H_5—H) = 357.8 \pm 7.1$ $kJ \cdot mol^{-1}$ and $\Delta_f H°(C_5H_5) = 274.1 \pm 7.3$ $kJ \cdot mol^{-1}$. The C—H BDEs in methane, ethane, propene, 1,3-cyclopentadiene, and toluene were calculated with CBS-Q, and CBS-QB3, and CCSD(T) with both cc-pVDZ and cc-pVTZ basis sets. Comparison with experimental data revealed that these methods can lead to significant deviations from experimental data if homolysis reactions (*cf.* **P1**:eq. 3 and

* The author of this dissertation performed all CBS-Q calculations, contributed to the analysis of theoretical data, and actively participated in the writing of the manuscript of **P1**, particularly in the discussion of theoretical data. This smaller participation was justified by the fact that this work was already ongoing, and was concluded in the first few months of the author's graduate work. This article is here included mainly the for sake of completeness, since it sets the tone for subsequent works. CBS-QB3 and CCSD(T) calculations were performed by B. J. Costa Cabral.

P1:tab. 2*) are used. Larger deviations arise when resonance stabilized radicals are formed upon C—H bond cleavage. CBS extrapolation of CCSD(T) data using a method proposed by Truhlar[82] leads to BDEs in very good agreement with experimental data. This is also the case for the C_5H_5—H BDE we aimed to study. Isodesmic and isogyric reactions (*cf.* **P1**:eq. 4) with allyl radical lead to improvement of CBS-Q and CBS-QB3 data, while extrapolated CCSD(T) values remain accurate and virtually unchanged (*cf.* **P1**:tab. 3).

We recommended $DH°(C_5H_5—H) = 355 \pm 8$ kJ·mol^{-1} and $\Delta_f H°(C_5H_5) = 271 \pm 8$ kJ · mol^{-1} based on our TR-PAC and theoretical results. In a subsequent study Ichino *et al.*[167] provided an accurate determination of the adiabatic electron affinity (EA) of the C_5H_5 radical. The authors then determined the C_5H_5—H BDE from a negative ion thermochemical cycle,

$$DH°(C_5H_5—H) = \Delta_{acid}H(C_5H_6) + EA(C_5H_5) - IE(H) \qquad (3.1)$$

In (3.1) IE(H) is the (well known) ionization energy of the hydrogen atom and $\Delta_{acid}H(C_5H_6)$ is the deprotonation enthalpy of 1,3-cyclopentadiene. This yielded $DH°(C_5H_5—H) = 341.0 \pm 6.3$ kJ · mol^{-1} and $\Delta_f H°(C_5H_5) = 264.4 \pm 5.9$ kJ · mol^{-1}. Taking into account the error bars, these thermochemical data are close to our recommended values.

This work revealed that great care must be used when constructing isodesmic reactions, and underlined the importance of performing CBS extapolations. In addition it demonstrated that composite methods like CBS-Q and CBS-QB3 may not always lead to accurate estimates of thermochemical data.

*That is, Paper 1 equation 3 and Paper 1 table 2.

Enthalpy of Formation of the Cyclopentadienyl Radical: Photoacoustic Calorimetry and ab Initio Studies

Paulo M. Nunes,*,† Filipe Agapito,†,‡ Benedito J. Costa Cabral,*,†,‡ Rui M. Borges dos Santos,§ and José A. Martinho Simões†

Departamento de Química e Bioquímica, Faculdade de Ciências, Universidade de Lisboa, 1749-016 Lisboa, Portugal, Grupo de Física Matemática da Universidade de Lisboa, Av. Professor Gama Pinto 2, 1649-003 Lisboa, Portugal, and Centro de Biomedicina Molecular e Estrutural, Universidade do Algarve, Campus de Gambelas, 8005−139 Faro, Portugal

Received: January 17, 2006; In Final Form: March 1, 2006

The gas-phase C−H bond dissociation enthalpy (BDE) in 1,3-cyclopentadiene has been determined by time-resolved photoacoustic calorimetry (TR-PAC) as 358 ± 7 kJ mol^{-1}. Theoretical results from ab initio complete basis-set approaches, including the composite CBS-Q and CBS-QB3 procedures, and basis-set extrapolated coupled-cluster calculations (CCSD(T)) are reported. The CCSD(T) prediction for the C−H BDE of 1,3-cyclopentadiene (353.3 kJ mol^{-1}) is in good agreement with the TR-PAC result. On the basis of the experimental and the theoretical values obtained, we recommend 355 ± 8 kJ mol^{-1} for the C−H BDE of 1,3-cyclopentadiene and 271 ± 8 kJ mol^{-1} for the enthalpy of formation of cyclopentadienyl radical.

Introduction

During the last fifty years cyclopentadienyl (C_5H_5) has been widely used as a ligand in organometallic chemistry.[1−3] Metal−C_5H_5 complexes have been synthesized for all transition and some f-block metals.[3] A key value for evaluating metal−cyclopentadienyl bond dissociation enthalpies (BDEs), and thus for discussing the nature of metal−C_5H_5 bonding, is the standard enthalpy of formation of the C_5H_5 radical.[4−6] An accurate value of $\Delta_fH°(C_5H_5,g)$ is also required to develop kinetic models for the combustion of aromatic compounds.[7,8]

Surprisingly, the enthalpy of formation of the cyclopentadienyl radical is still subject to controversy. In their 1977 review, Tel'noi and Rabinovich listed several estimates for this quantity, ranging from 190 ± 42 to 264 kJ mol^{-1}.[5] They have arbitrarily chosen $\Delta_fH°(C_5H_5,g)$ = 209 kJ mol^{-1} to derive a number of metal−C_5H_5 BDEs; in a recent book, by the same group, that value was updated to 237 kJ mol^{-1}.[9] In 1982, McMillen and Golden recommended $\Delta_fH°(C_5H_5,g)$ = 242 ± 6 kJ mol^{-1},[10] on the basis of a reassessment of a kinetic study of the iodination of 1,3-cyclopentadiene[11] and on a value derived from a proton affinity study of C_5H_5 (264 ± 9 kJ mol^{-1}).[12] This choice was reconfirmed (243 ± 8 kJ mol^{-1}) in a brief analysis of literature data.[13]

Bordwell et al. used a thermodynamic cycle together with the values of pK_a of 1,3-cyclopentadiene and the oxidation potencial of $C_5H_5^-$, both measured in dimethyl sulfoxide, to derive a value of C_5H_5−H gas-phase BDE consistent with $\Delta_fH°(C_5H_5,g)$ = 256 ± 13 kJ mol^{-1}.[14,15] Bordwell's group result was later reevaluated by Parker et al.,[16] leading to $\Delta_fH°(C_5H_5,g)$ = 267 ± 3 kJ mol^{-1}. The ca. 11 kJ mol^{-1} upward correction is due to a kinetic potential shift caused by the fast dimerization reaction of the oxidation product (cyclopentadienyl), which was not considered in Bordwell's work.

Two other experimental results have appeared more recently, both relying on gas-phase high-temperature kinetics, viz. $\Delta_fH°(C_5H_5,g)$ = 273 and 260 ± 4 kJ mol^{-1}.[8,17] The latter involved the third-law determination of the enthalpy of C_5H_5−H homolysis.[8]

The NIST Chemistry WebBook contains gas-phase ion data from which the C_5H_5−H BDE can be extracted by using thermochemical cycles.[18] One cycle involves the proton affinity of C_5H_5 (831.5 kJ mol^{-1}), the adiabatic ionization energy of 1,3-cyclopentadiene (826.9 ± 1.0 kJ mol^{-1}), and the ionization energy of the hydrogen atom (1312.0 kJ mol^{-1}). This leads to $\Delta_fH°(C_5H_5,g)$ = 263 kJ mol^{-1}. The second cycle involves the acidity of 1,3-cyclopentadiene (1481 ± 9 kJ mol^{-1} or 1485 ± 12 kJ mol^{-1}), the adiabatic electron affinity of C_5H_5 (172.3 ± 1.9 kJ mol^{-1}), and the ionization energy of the hydrogen atom, yielding $\Delta_fH°(C_5H_5,g)$ = 258 ± 10 or 262 ± 12 kJ mol^{-1}.

In summary, the literature values for the standard enthalpy of formation of cyclopentadienyl radical span more than 80 kJ mol^{-1}. Even if only the most recent data are considered (Table 1) the variation is about 30 kJ mol^{-1}. Aiming to improve this situation, we have decided to determine the C_5H_5−H BDE (and the corresponding enthalpy of formation) by using time-resolved photoacoustic calorimetry (TR-PAC) and also quantum chemistry calculations. TR-PAC has been successfully used before to probe the energetics of the benzyl, ethylbenzyl, and cumyl radicals and should provide reliable data for cyclopentadienyl.[19]

Experimental Section

Materials. Benzene (Aldrich, HPLC grade, 99.9+%), was used as received. Cyclopentadiene was prepared by cracking dicyclopentadiene (Aldrich, 96%) at 200 °C, distilled using a Vigreux column, collected at 0 °C and used immediately. Di-*tert*-butyl peroxide (Aldrich) was purified according to a

* Corresponding authors. P.M.N: e-mail, panunes@fc.ul.pt; phone, (+351) 217 500 005; fax, (+351) 217 500 088. B.J.C.C.: e-mail, ben@adonis.cii.fc.ul.pt; phone, (+351) 217 904 728; fax, (+351) 217 954 288.

† Departamento de Química e Bioquímica, Universidade de Lisboa.

‡ Grupo de Física Matemática da Universidade de Lisboa.

§ Universidade do Algarve.

10.1021/jp060325n CCC: $33.50
Published on Web 03/25/2006

TABLE 1: Values of the Standard Enthalpy of Formation of Cyclopentadienyl Radical and the Corresponding Gas-Phase C_5H_5-H Bond Dissociation Enthalpy at 298.15 K (Data in kJ mol^{-1})

authors (year)	method[a]	$DH°(C_5H_5-H)$	$\Delta_f H°(C_5H_5^{\bullet},g)$	ref
McMillen & Golden (1982)	Review	326 ± 6[b]	242 ± 6	10
Bordwell et al. (1988)	EChem	340 ± 13	256 ± 13[b]	14, 15
Puttemans et al. (1990)	Review	326 ± 9	243 ± 8[b]	13
Parker et al. (1991)	EChem	351.0 ± 2.1	267.3 ± 2.6[b]	16
Kern et al. (1998)	GPK	356.9[b]	273.2	17
Roy et al. (2001)	GPK	343.9 ± 4.2	260.2 ± 4.5[b]	8
NIST Database (2005)	GPA	341 ± 9	258 ± 10[b]	18
NIST Database (2005)	GPA	345 ± 12	262 ± 12[b]	18
NIST Database (2005)	PA	346	263[b]	18

[a] EChem = electrochemical cycle; GPA = gas-phase acidity cycle; GPK = gas-phase kinetics; PA = proton affinity cycle. [b] Calculated using the enthalpy of formation of 1,3-cyclopentadiene from ref 46 (134.3 ± 1.5 kJ mol^{-1}).

literature procedure.[20] *ortho*-Hydroxybenzophenone (Aldrich) was recrystallized twice from an ethanol−water mixture.

Photoacoustic Calorimetry. The theoretical basis of time-resolved photoacoustic calorimetry has been widely discussed,[21,22] and only a brief outline is given here. The TR-PAC technique involves the measurement of an acoustic wave generated by the sudden volume change that occurs when a laser pulse strikes a solution, initiating a sequence of physicochemical processes. The photoacoustic signal thus measured provides information on the intensity and temporal profile of nonradiative energy released during these processes. Using a deconvolution analysis for the time dependence of the signal, both the magnitudes of each of the signal-inducing events and their lifetimes can be determined.[23] The analysis involves first the normalization of the waveform for its respective absorbance and incident laser energy. Extraction of the observed heat fraction, $\phi_{obs,i}$, and the lifetime, τ_i, for each process is then accomplished by the deconvolution of the normalized waveform, facilitated by the use of commercially available software.[24] The parameter $\phi_{obs,i}$ is the observed fraction of photon energy released as heat which, when multiplied by the molar energy of the laser photons ($E_m = N_A h\nu$), corresponds to the observed enthalpic change, $\Delta_{obs}H_i$.

For instance, considering a two step sequential reaction, the enthalpy of the first step (photochemical) and of the second (thermal) are given by eqs 1 and 2, respectively.

$$\Delta_r H_1 = \frac{E_m - \Delta_{obs}H_1}{\Phi_r} + \frac{\Delta_r V_1}{\chi} \quad (1)$$

$$\Delta_r H_2 = \frac{-\Delta_{obs}H_2}{\Phi_r} + \frac{\Delta_r V_2}{\chi} \quad (2)$$

In these equations, Φ_r represents the quantum yield of the first step. As indicated, $\Delta_{obs}H_i$ are calculated from the respective amplitude $\phi_{obs,i}$ obtained from the deconvolution. Note, however, that $\phi_{obs,i}$ consists not only of a thermal contribution, due to the enthalpy of the reaction but also of a reaction volume contribution, due to the differences between the partial molar volumes of the reactants and products.[25] The latter leads to the introduction of a correction factor when calculating the reaction enthalpies. The correction term includes the reaction volume change, $\Delta_r V_i$, and the adiabatic expansion coefficient of the solution, χ. Because the solutions used are usually very diluted, the adiabatic expansion coefficient of the solvent is used as a substitute for the solution value.

Our photoacoustic calorimeter setup and experimental procedure have been described in detail.[19,26,27] Briefly, benzene solutions of ca. 0.33 M of di-*tert*-butyl peroxide and ca. 0.1 M of 1,3-cyclopentadiene were flowed through a quartz flow cell (Hellma 174-QS) and photolyzed with pulses from a nitrogen laser (PTI PL 2300, 337.1 nm, pulse width 800 ps). The incident laser energy was varied by using neutral density filters and the induced acoustic wave was detected by a piezoelectric transducer (Panametrics V101, 0.5 MHz) in contact with the bottom of the cell. The photoacoustic signals were measured by a digital oscilloscope (Tektronix 2430A), where the signal-to-noise ratio was improved by averaging 32 acquisitions. Waveforms were collected at various laser intensities to check for multiphoton effects. The apparatus was calibrated by carrying out a photoacoustic run using an optically matched (within typically 5% absorbance units at 337.1 nm) solution of the photoacoustic calibrant ortho-hydroxybenzophenone ($\phi_{obs} = 1$)[21] in benzene (this solution does not include the peroxide but contains 1,3-cyclopentadiene, with the same concentration as in the experiment). The sample waveform was deconvoluted with the calibration waveform using the software Sound Analysis by Quantum Northwest.[24]

Theoretical Calculations. Different theoretical methods were applied to determine the gas-phase C−H BDE of 1,3-cyclopentadiene, including the complete basis-set composite schemes CBS-Q and CBS-QB3.[28−30] Further calculations were based on the ab initio coupled-cluster method with single and double excitations and perturbative treatment of triple excitations (CCSD(T)).[31−33] The Dunning's correlation consistent basis sets cc-pVxZ ($x = 2, 3$)[34−36] were used in coupled-cluster calculations. Initially, optimized geometries and frequencies were determined at the B3LYP/cc-pVTZ level. The choice of this approach was oriented by previous investigations indicating that it is adequate for a reliable prediction of both closed-shell and open-shell structures.[37] A dual (2, 3) extrapolation procedure to complete basis-set proposed by Truhlar[38] has been applied to CCSD(T) single-point energies using the B3LYP/cc-pVTZ optimized structures. Thermal corrections to 298.15 K were based on B3LYP/cc-pVTZ unscaled frequencies.

The energetics of the bond homolysis reaction 3 and isogyric reactions with methyl, ethyl, allyl, and benzyl radicals (reaction 4, where R = CH_3, CH_3CH_2, CH_2CHCH_2, and $C_6H_5CH_2$) were studied. In reaction 4, for R = allyl and benzyl, the number of

$$C_5H_6 \rightarrow C_5H_5^{\bullet} + H^{\bullet} \quad (3)$$

$$C_5H_6 + R^{\bullet} \rightarrow C_5H_5^{\bullet} + RH \quad (4)$$

electron pairs, the number of each type of chemical bond, and the number of carbon atoms in corresponding states of hybridization are all equal in both sides of the chemical equation. Moreover, the number of hydrogen atoms bonded to each carbon atom in a given hybridization is similar in reagents and products. All these factors should contribute to error cancellation. All the

SCHEME 1

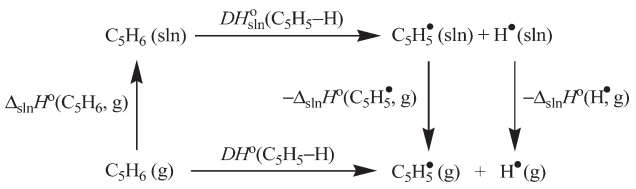

calculations were carried out with the Gaussian-03 program and thermal corrections to 298.15 K were applied.[39]

Results and Discussion

TR-PAC Bond Dissociation Enthalpies. The reactions examined by photoacoustic calorimetry are shown below. A *tert*-butoxyl radical generated from the photolysis of di-*tert*-butylperoxide (reaction 5) in benzene abstracts a hydrogen from the 1,3-cyclopentadiene substrate (C_5H_6), yielding the corresponding cyclopentadienyl radical (reaction 6).

$$t\text{-BuOOBu-}t\ (\text{sln}) \xrightarrow{h\nu} 2t\text{-BuO}^{\bullet}(\text{sln}) \qquad (5)$$

$$2C_5H_6\ (\text{sln}) + 2t\text{-BuO}^{\bullet}\ (\text{sln}) \rightarrow 2C_5H_5^{\bullet}\ (\text{sln}) + 2t\text{-BuOH}\ (\text{sln}) \qquad (6)$$

The kinetics of reaction 6 was previously studied using laser flash photolysis and electron paramagnetic resonance techniques.[40] Although the *tert*-butoxyl radical can also undergo an addition reaction to the C_5H_6 double bonds, it was found that the intensity of the EPR signal from the adduct was hardly detected at temperatures above −20 °C. This indicates that the extension of the addition reaction should be negligible at room temperature.

The enthalpy of reaction 6, $\Delta_r H_2$, can be calculated from eq 2 by assuming that the volume change $\Delta_r V_2 \approx 0$, which is sensible because the hydrogen abstraction is a metathesis reaction.[41] Using our experimental value for $\Delta_{obs}H_2 = 153.3 \pm 7.7$ kJ mol^{-1} and the quantum yield for the photolysis of di-*tert*-butylperoxide in benzene, $\Phi_r = 0.83$,[41] we obtain $\Delta_r H_2 = -184.8 \pm 9.3$ kJ mol^{-1}.

$\Delta_r H_2$ is twice the difference between the solution-phase BDEs of C_5H_5−H and *t*-BuO−H, respectively. Therefore, the C_5H_5−H BDE in solution can be calculated using eq 7. Our experimental

$$DH^{\circ}_{sln}(C_5H_5{-}H) = \frac{\Delta_r H_2}{2} + DH^{\circ}_{sln}(t\text{-BuO}{-}H) \qquad (7)$$

value for $\Delta_r H_2$ coupled with $DH^{\circ}_{sln}(t\text{-BuO}-H) = 455.2 \pm 5.2$ kJ mol^{-1} in benzene,[27] led to $DH^{\circ}_{sln}(C_5H_5-H) = 362.8 \pm 7.0$ kJ mol^{-1}. To calculate the gas-phase value for the C_5H_5−H BDE, we need to consider the solvation enthalpies in Scheme 1. Equation 8 is obtained from this scheme.

$$DH^{\circ}(C_5H_5{-}H) = DH^{\circ}_{sln}(C_5H_5{-}H) + \Delta_{sln}H^{\circ}(C_5H_6,g) - \Delta_{sln}H^{\circ}(C_5H_5^{\bullet},g) - \Delta_{sln}H^{\circ}(H^{\bullet},g) \qquad (8)$$

The difference between the solvation enthalpies of 1,3-cyclopentadiene and the 1,3-cyclopentadienyl radical, $\Delta_{sln}H^{\circ}(C_5H_6,g) - \Delta_{sln}H^{\circ}(C_5H_5^{\bullet},g)$ should be negligible.[19] The solvation of the hydrogen atom can be estimated using the hydrogen molecule as a suitable model, yielding $\Delta_{sln}H^{\circ}(H^{\bullet},g) = 5 \pm 1$ kJ mol^{-1} for organic solvents.[42−45] Hence, we obtain $DH^{\circ}(C_5H_5-H) = 357.8 \pm 7.1$ kJ mol^{-1}.

Finally, the standard enthalpy of formation for the $C_5H_5^{\bullet}$ radical in the gas phase was obtained as $\Delta_f H^{\circ}(C_5H_5^{\bullet},g) = 274.1 \pm 7.3$ kJ mol^{-1}, by using $\Delta_f H^{\circ}(C_5H_6,g) = 134.3 \pm 1.5$ kJ mol^{-1} [46] and $\Delta_f H^{\circ}(H^{\bullet},g) = 217.998 \pm 0.006$ kJ mol^{-1}.[47]

Theoretical Gas-Phase Bond Dissociation Enthalpies. Theoretical enthalpies from homolysis reactions (eq 3), which are identified with the C−H BDEs for methane, ethane, 1-propene, 1,3-cyclopentadiene, and toluene, are displayed in Table 2, together with selected experimental data.[48,49]

The analysis of Table 2 indicates that, with the exception of the results for methane and ethane, which are accurately predicted, significant deviations from experiment are observed for CBS calculations. For example, the CBS-Q result for the C−H BDE of 1,3-cyclopentadiene is −11.7 kJ mol^{-1} below the present experimental determination (357.8 ± 7.1 kJ mol^{-1}). A similar trend is observed for propene (−10.2 kJ mol^{-1}), and toluene (−15.6 kJ mol^{-1}), indicating that the discrepancies occur mainly when resonance stabilized radicals are formed in the homolysis reaction. CBS-QB3 results are in better agreement with experiment, in particular for the C−H bond homolysis of toluene, which is only 3.6 kJ mol^{-1} above experiment (375.5 ± 1.8 kJ mol^{-1}). Yet, the CBS-QB3 result for 1,3-cyclopentadiene is still −11.9 kJ mol^{-1} below our experimental result.

The above results could have led us to conclude that the C_5H_5-H BDE derived by TR-PAC might be a high upper limit. However, this is not confirmed by basis-set extrapolated CCSD(T) results. Based on these theoretical calculations, the C-H BDE of 1,3−cyclopentadiene is only 4.4 kJ mol^{-1} below the present experimental value. An interesting discussion on the reliability of CCSD(T) calculations was reported by Dunning.[50]

Also reported in Table 2 (bracketed values) are the CCSD(T)/cc-pV*x*Z//B3LYP/cc-pVTZ ($x = 2, 3$) results. Two features should be emphasized. First, even calculations with a triple-ζ quality basis-set may exhibit deviations from extrapolated results as large as −7.4 kJ mol^{-1} (see CCSD(T) results for 1,3-cyclopentadiene). The deviations are, in general, above chemical accuracy (ca. 4 kJ mol^{-1}) and illustrate the importance of carrying out extrapolation to complete basis-set. Second, in keeping with previous investigations,[51] theoretical homolytic BDEs predicted by coupled-cluster calculations using the dual (2, 3) extrapolation scheme proposed by Truhlar[38] are in very good agreement with experiment.

The results for the enthalpies of isodesmic and isogyric reactions 4 are collected in Table 3. The C_5H_5−H BDE in each case was calculated from eq 9 by using the corresponding experimental C−H BDE (see Table 2).

$$DH^{\circ}(C_5H_5{-}H) = \Delta_r H^{\circ}(4) + DH^{\circ}(R{-}H) \qquad (9)$$

The CBS results for C_5H_5−H BDE in Table 3 exhibit some dependence on the choice of R$^{\bullet}$, the largest deviations from experiment being observed for radicals that are *not* resonance stabilized. This is in keeping with the data in Table 2, where it is observed that these methods underestimate the enthalpies of homolysis reactions involving the formation of resonance stabilized radicals. Therefore, it is expected that the best estimates for C_5H_5−H BDE, obtained from reaction 4, should be the ones where R$^{\bullet}$ corresponds to the allyl and benzyl radicals. Indeed, with exception of the CBS-QB3 result for R$^{\bullet}$ = benzyl, which leads to a deviation from the present experimental value of −15.5 kJ mol^{-1}, the theoretical results for R$^{\bullet}$ = allyl or benzyl are close to chemical accuracy (ca. 4 kJ mol^{-1}). It is also observed in Table 3 that the CCSD(T) values show smaller deviations from experiment, even when R$^{\bullet}$ is the

TABLE 2: Theoretical Carbon−Hydrogen BDEs (kJ mol^{-1}) Predicted from Homolysis Reactions[a]

	DH°(C−H)			
	CBS-Q	CBS-QB3	CCSD(T)	experimental
CH_3−H	439.6 (0.5)	440.9 (1.8)	441.4[b] (2.3) [418.9; 432.9][c]	439.1 ±0.5[c]
CH_3CH_2 −H	425.5 (2.5)	425.5 (2.5)	426.8[b] (3.8) [406.6; 419.3][c]	423.0 ±1.7[e]
allyl−H	361.3 (−10.2)	364.9 (−6.6)	371.5[b] (0) [351.9; 364.7][c]	371.5 ±1.7[e]
C_5H_5−H	346.1 (−11.7)	345.9 (−11.9)	353.4[b] (−4.4) [332.4; 346.0][c]	357.8 ±7.1[f]
benzyl−H	359.9 (−15.6)	379.1 (3.6)		375.5 ±1.8[d]

[a] Values in parentheses are deviations from experimental results. [b] Complete basis-set extrapolated result using the dual (2,3) extrapolation scheme of ref 38. [c] CCSD(T)/cc-pV*x*Z//B3LYP/cc-pVTZ results for x=2 and 3, respectively. [d] Reference 49. [e] Reference 48. [f] This work.

TABLE 3: Theoretical Results for $\Delta_f H°(4)$[a] and Carbon−Hydrogen BDE for 1,3-Cyclopentadiene (Data in kJ mol^{-1})

	$\Delta_f H°(4)$			*DH*°(C_5H_5−H)[b]		
R$^\bullet$	CBS-Q	CBS-QB3	CCSD(T)	CBS-Q	CBS-QB3	CCSD(T)[c]
CH_3	−93.4	−94.9	−88.0	345.7 (−12.1)	344.2 (−13.6)	351.1 (−6.7)
CH_3CH_2	−79.4	−79.5	−73.4	343.6 (−14.2)	343.5 (−14.3)	349.6 (−8.2)
allyl	−15.1	−18.9	−18.2	356.4 (−1.4)	352.6 (−5.2)	353.3 (−4.5)
benzyl	−13.7	−33.2		361.8 (4.0)	342.3 (−15.5)	

[a] C_5H_5−H + R$^\bullet$ → $C_5H_5^\bullet$ + RH. [b] Values in parentheses are deviations from the present experimental result (357.8 ± 7.1 kJ mol^{-1}). [c] Complete basis-set extrapolated results using the dual (2, 3) scheme of ref 38.

methyl or the ethyl radical. CCSD(T) results for the C−H BDE of 1,3-cyclopentadiene estimated from reaction 3 or 4 when R$^\bullet$ = allyl, practically coincide (353 kJ mol^{-1}).

The very good agreement between complete basis-set extrapolated CCSD(T) results and the experimental C−H BDEs for the series of molecules presently investigated, strongly supports the present TR-PAC measurements. However, having in mind the experimental uncertainty and also the best theoretical data in Tables 2 and 3, we recommend a value of 355 ± 8 kJ mol^{-1} for the C_5H_5−H BDE and $\Delta_f H°(C_5H_5^\bullet,g)$ = 271 ± 8 kJ mol^{-1}. These values are in the high range of literature data (Table 1), but in keeping with the data recommended by Parker et al.[16] and Kern et al.[17]

The standard enthalpy of formation of the cyclopentadienyl radical has been previously computed as 259.4 kJ mol^{-1}, corresponding to *DH*°(C_5H_5−H) = 343.1 kJ mol^{-1}, by using the G2(B3LYP/MP2,SVP) method for an isodesmic and isogyric reaction with methane (reaction 10).[7] The 12 kJ mol^{-1} difference

$$C_5H_5^\bullet + 5CH_4 \rightarrow C_2H_5^\bullet + 2C_2H_6 + 2C_2H_4 \qquad (10)$$

between that result and our recommended value (355 ± 8 kJ mol^{-1}) is not surprising, because in reaction 10 there is no "resonance conservation".

To check that the discrepancy was not due to the different calculation methods, we have computed the enthalpy of reaction 10 with CBS-Q, CBS-QB3, and CCSD(T) methods, which led to 172.2, 170.9, and 162.0 kJ mol^{-1}, respectively. From these results and the standard enthalpies of formation of methane (−74.4 ± 0.4 kJ mol^{-1}), ethane (−83.8 ± 0.3 kJ mol^{-1}), ethylene (52.5 ± 0.3 kJ mol^{-1}), and ethyl radical (121.2 ± 1.7 kJ mol^{-1}),[46,48] $\Delta_f H°(C_5H_5^\bullet,g)$ can be estimated as 258.4 kJ mol^{-1} (CBS-Q), 259.7 kJ mol^{-1} (CBS-QB3), and 268.6 kJ mol^{-1} (CCSD(T)). The first two estimates are very close to the value derived by Wang and Brezinsky using the G2(B3LYP/MP2,SVP) method (259.4 kJ mol^{-1}).[7] The CCSD(T) result for $\Delta_f H°(C_5H_5^\bullet,g)$ derived from reaction 10 (268.6 kJ mol^{-1}) is quite similar to the one based on the homolysis reaction 3, $\Delta_f H°(C_5H_5^\bullet,g)$ = 269.6 kJ mol^{-1}. Both predictions are only ∼2 kJ mol^{-1} below our recommended value (271 ± 8 kJ mol^{-1}).

Conclusions

Time-resolved photoacoustic calorimetry (TR-PAC) experiments and ab initio calculations (CBS-Q, CBS-QB3, and CCSD(T)) were carried out for predicting the gas-phase C−H homolytic bond dissociation enthalpy of 1,3-cyclopentadiene, *DH*°(C_5H_5−H), and the enthalpy of formation of the cyclopentadienyl radical, $\Delta_f H°(C_5H_5^\bullet,g)$. Our recommended values are *DH*°(C_5H_5−H) = 355 ± 8 kJ mol^{-1} and $\Delta_f H°(C_5H_5^\bullet,g)$ = 271 ± 8 kJ mol^{-1}. The best theoretical agreement with experiment is based on complete basis-set CCSD(T) calculations and a simple dual (2,3) energy extrapolation scheme proposed by Truhlar.[38]

CCSD(T) results for the enthalpies of formation of resonance stabilized radicals are less dependent on the reactions chosen to derive those values (homolysis or isodesmic and isogyric) than the CBS-Q or CBS-QB3 approaches. The CBS methods may lead to significant discrepancies with experiment even when an isodesmic and isogyric reaction is used. To minimize these errors, it is important to "balance" the resonance stabilization of the species in both sides of the reaction.

Acknowledgment. This work was supported by Fundação para a Ciência e a Tecnologia (FCT), Portugal (POCTI/43315/QUI/2001). P.M.N. and F.A. thank FCT for a postdoctoral (SFRH/BPD/11465/2002) and a Ph.D. (SFRH/BD/22854/2005) grant, respectively.

References and Notes

(1) Cotton, F. A.; Wilkinson, G. *Advanced Inorganic Chemistry*, 5th ed.; Wiley-Interscience: New York, 1988.
(2) Crabtree, R. H. *The Organometallic Chemistry of the Transition Metals*; Wiley: New York, 1988.
(3) Collman, J. P.; Hegedus, L. S.; Norton, J. R.; Finke, R. G. *Principles and Applications of Organotransition Metal Chemistry*; University Science Books: Mill Valley, CA, 1987.
(4) Connor, J. A. *Top. Curr. Chem.* **1977**, *71*, 71−110.
(5) Tel′noi, V. I.; Rabinovich, I. B. *Russ. Chem. Rev.* **1977**, *46*, 689−705.
(6) Martinho Simões, J. A.; Beauchamp, J. L. *Chem. Rev.* **1990**, *90*, 629−688.
(7) Wang, H.; Brezinsky, K. *J. Phys. Chem. A* **1998**, *102*, 1530−1541.
(8) Roy, K.; Braun-Unkhoff, M.; Frank, P.; Just, T. *Int. J. Chem. Kinet.* **2001**, *33*, 821−833.
(9) Rabinovich, I. B.; Nistranov, V. P.; Telnoy, V. I.; Sheiman, M. S. *Thermochemical and Thermodynamic Properties of Organometallic Compounds*; Begell House: New York, 1999.
(10) McMillen, D. F.; Golden, D. M. *Annu. Rev. Phys. Chem.* **1982**, *33*, 493−532.
(11) Furuyama, S.; Golden, D. M.; Benson, S. W. *Int. J. Chem. Kinet.* **1971**, *3*, 237−248.
(12) DeFrees, D. J.; McIver Jr., R. T.; Hehre, W. J. *J. Am. Chem. Soc.* **1980**, *102*, 3334−3338.

(13) Puttemans, J. P.; Smith, G. P.; Golden, D. M. *J. Phys. Chem.* **1990**, *94*, 3226−3227.
(14) Bordwell, F. G.; Cheng, J.-P.; Harrelson, J. A., Jr. *J. Am. Chem. Soc.* **1988**, *110*, 1229−1231.
(15) Bordwell, F. G.; Cheng, J.-P.; Ji, G.-Z.; Satish, A. V.; Zhang, X. *J. Am. Chem. Soc.* **1991**, *113*, 9790−9795.
(16) Parker, V. D.; Handoo, K. L.; Roness, F.; Tilset, M. *J. Am. Chem. Soc.* **1991**, *113*, 7493−7498.
(17) Kern, R. D.; Zhang, Q.; Yao, J.; Jursic, R. S.; Tranter, R. S.; Greybill, M. A.; Kiefer, J. H. *Proc. Combust. Inst.* **1998**, *102*, 143−150.
(18) Linstrom, P. J.; Mallard, W. G. *NIST Chemistry WebBook, NIST Standard Reference Database Number 69 (http://webbook.nist.gov)*; National Institute of Standards and Technolog:y Gaithersburg, MD, 2005.
(19) Muralha, V. S.; Borges dos Santos, R. M.; Martinho Simões, J. A. *J. Phys. Chem. A* **2004**, *108*, 936−942.
(20) Diogo, H. P.; Minas da Piedade, M. E.; Martinho Simões, J. A.; Nagano, Y. *J. Chem. Thermodyn.* **1995**, *27*, 597−604.
(21) Braslavsky, S. E.; Heibel, G. E. *Chem. Rev.* **1992**, *92*, 1381−1410.
(22) Peters, K. S. *Angew. Chem., Int. Ed. Engl.* **1994**, *33*, 294−302.
(23) Small, J. R.; Libertini, L. J.; Small, E. W. *Biophys. Chem.* **1992**, *42*, 29−48.
(24) Sound Analysis, version 1.5D.; Quantum Northwest: Spokane, WA, 1999.
(25) Hung, R. R.; Grabowski, J. J. *J. Am. Chem. Soc.* **1992**, *114*, 351−353.
(26) Borges dos Santos, R. M.; Lagoa, A. L. C.; Martinho Simões, J. A. *J. Chem. Thermodyn.* **1999**, *31*, 1483−1510.
(27) Correia, C. F.; Nunes, P. M.; Borges dos Santos, R. M.; Martinho Simões, J. A. *Thermochim. Acta* **2004**, *420*, 3−11.
(28) Ochterski, J. W.; Petersson, G. A.; Montgomery, J. A. *J. Chem. Phys.* **1996**, *104*, 2598−2619.
(29) Montgomery, J. A.; Frisch, M. J.; Ochterski, J. W.; Petersson, G. A. *J. Chem. Phys.* **1999**, *110*, 2822−2827.
(30) Montgomery, J. A.; Frisch, M. J.; Ochterski, J. W.; Petersson, G. A. *J. Chem. Phys.* **2000**, *112*, 6532−6542.
(31) Cizek, J. *Adv. Chem. Phys.* **1969**, *14*, 35.
(32) Pople, J. A.; Headgordon, M.; Raghavachari, K. *J. Chem. Phys.* **1987**, *87*, 5968−5975.
(33) Krishnam, R.; Frisch, M. J.; Pople, J. A. *J. Chem. Phys.* **1980**, *72*, 4244−4245.
(34) Woon, D. E.; Dunning Jr., T. H. *J. Chem. Phys.* **1993**, 1358.
(35) Kendall, R. A.; Dunning, T. H.; Harrison, R. J. *J. Chem. Phys.* **1992**, *96*, 6796−6806.
(36) Dunning, T. H. *J. Chem. Phys.* **1989**, *90*, 1007−1023.
(37) Byrd, E. F. C.; Sherrill, C. D.; Head-Gordon, M. *J. Phys. Chem. A* **2001**, *105*, 9736−9747.
(38) Truhlar, D. G. *Chem. Phys. Lett.* **1998**, *294*, 45−48.
(39) Frisch, M. J.; Trucks, G. W.; Schlegel, H. B.; Scuseria, G. E.; Robb, M. A.; Cheeseman, J. R.; Montgomery, Jr., J. A.; Vreven, T.; Kudin, K. N.; Burant, J. C.; Millam, J. M.; Iyengar, S. S.; Tomasi, J.; Barone, V.; Mennucci, B.; Cossi, M.; Scalmani, G.; Rega, N.; Petersson, G. A.; Nakatsuji, H.; Hada, M.; Ehara, M.; Toyota, K.; Fukuda, R.; Hasegawa, J.; Ishida, M.; Nakajima, T.; Honda, Y.; Kitao, O.; Nakai, H.; Klene, M.; Li, X.; Knox, J. E.; Hratchian, H. P.; Cross, J. B.; Bakken, V.; Adamo, C.; Jaramillo, J.; Gomperts, R.; Stratmann, R. E.; Yazyev, O.; Austin, A. J.; Cammi, R.; Pomelli, C.; Ochterski, J. W.; Ayala, P. Y.; Morokuma, K.; Voth, G. A.; Salvador, P.; Dannenberg, J. J.; Zakrzewski, V. G.; Dapprich, S.; Daniels, A. D.; Strain, M. C.; Farkas, O.; Malick, D. K.; Rabuck, A. D.; Raghavachari, K.; Foresman, J. B.; Ortiz, J. V.; Cui, Q.; Baboul, A. G.; Clifford, S.; Cioslowski, J.; Stefanov, B. B.; Liu, G.; Liashenko, A.; Piskorz, P.; Komaromi, I.; Martin, R. L.; Fox, D. J.; Keith, T.; Al-Laham, M. A.; Peng, C. Y.; Nanayakkara, A.; Challacombe, M.; Gill, P. M. W.; Johnson, B.; Chen, W.; Wong, M. W.; Gonzalez, C.; Pople, J. A. *Gaussian 03*, Revision C.02; Gaussian, Inc.: Wallingford, CT, 2004.
(40) Wong, P. C.; Griller, D.; Scaiano, J. C. *J. Am. Chem. Soc.* **1982**, *104*, 5106−5108.
(41) Wayner, D. D. M.; Lusztyk, E.; Pagé, D.; Ingold, K. U.; Mulder, P.; Laarhoven, L. J. J.; Aldrich, H. S. *J. Am. Chem. Soc.* **1995**, *117*, 8737−8744.
(42) Parker, V. D. *J. Am. Chem. Soc.* **1992**, *114*, 7458−7462.
(43) Parker, V. D. *J. Am. Chem. Soc.* **1993**, *115*, 1201−1201.
(44) Borges dos Santos, R. M.; Martinho Simões, J. A. *J. Phys. Chem. Ref. Data* **1998**, *27*, 707−739.
(45) Bakalbassis, E. G.; Lithoxoidou, A. T.; Vafiadis, A. P. *J. Phys. Chem. A* **2003**, *107*, 8594−8606.
(46) Pedley, J. B. *Thermochemical Data and Structures of Organic Compounds*; Thermodynamics Research Center: College Station, TX, 1994; Vol. I.
(47) Cox, J. D.; Wagman, D. D.; Medvedev, V. A. *Codata Key Values for Thermodynamics*; Hemisphere: New York, 1989.
(48) Blanksby, S. J.; Ellison, G. B. *Acc. Chem. Res.* **2003**, *36*, 255−263.
(49) Ruscic, B.; Boggs, J. E.; Burcat, A.; Csaszar, A. G.; Demaison, J.; Janoschek, R.; Martin, J. M. L.; Morton, M. L.; Rossi, M. J.; Stanton, J. F.; Szalay, P. G.; Westmoreland, P. R.; Zabel, F.; Berces, T. *J. Phys. Chem. Ref. Data* **2005**, *34*, 573−656.
(50) Dunning, T. H. *J. Phys. Chem. A* **2000**, *104*, 9062−9080.
(51) Cabral, B. J. C.; Canuto, S. *Chem. Phys. Lett.* **2005**, *406*, 300−305.

CHAPTER 4

DFT structures and CBS extrapolation

We had seen in **P1** that Truhlar's extrapolation method for CCSD(T)[82] provided accurate estimates of thermochemical data. Since this extrapolation method relied on data calculated with only the cc-pVDZ and cc-pVTZ basis sets it was cost-effective and affordable for the larger molecules we intended to study (*cf.* Chapters 5 and 6). However, Truhlar determined the parameters of his extrapolation scheme using only the estimates for the complete basis set energies of Ne, N_2, and H_2O which had been obtained by Halkier *et al.*,[83] and concluded by noting that:

> "One could imagine various improvements on the scheme presented here. Foremost among these would be parameterizing the method against a greater number of basis-set-limit data when such data become available. Meanwhile the parameterization presented here should be useful for a variety of applications."

This lead us to believe that there was room for improvement. Moreover, the fit set above contained no open-shell species, on which we were particularly interested, so an analysis of the performance of (2,3) extrapolations for such species was needed. Since cost-effectiveness was of the utmost importance, geometry optimizations had to be performed with DFT. This was not damaging for the accuracy of structural data since it had been well demonstrated that B3LYP/cc-pVTZ yielded accurate structures and vibrational frequencies.[168,169] Nevertheless, some new functionals had emerged and we wanted to compare their performance with B3LYP, hoping to find a more accurate optimization method.

This analysis of (2,3) extrapolation methods and DFT optimized geometries was performed in ref. 170 (**P2**).* A facsimile of this article is provided in this chapter. The structures of 33 open-shell and 19 closed-shell molecules (*cf.* **P2**:tab. 1) were optimized with B3LYP, PBEPBE,[171,172] B98,[173,174] VSXC,[175] HCTH/407,[176] and TPSS[177] always using the cc-pVTZ basis set. As in previous studies[168,169] B3LYP/cc-pVTZ performed consistently well, and therefore, its optimized structures were used in the subsequent study of extrapolation methods.

CCSD(T) complete basis set correlation energies for the molecules were estimated from a two-point extrapolation of CCSD(T)/cc-pV5Z and CCSD(T)/cc-pV6Z energies with the scheme of Halkier *et al.*[83] Using this data we optimized the exponent in the Truhlar extrapolation scheme. This new method was then compared with the original method of ref. 82 and another recent (2,3) extrapolation scheme.[84] All three methods preformed well, even surpassing the accuracy of CCSD(T)/cc-pV6Z correlation energies. Even though Truhlar's method performed slightly worse, the differences between the methods are small (*cf.* **P2**:tab. 7, **P2**:tab. 8, and **P2**:fig. 7). The impact of CBS extrapolation of Hartree-Fock energies was also studied. The rapid convergence of HF energies to their CBS limits was illustrated by the fact that data calculated with HF/cc-pV6Z differ little from data calculated with *ad hoc* extrapolated HF energies using cc-pVxZ with x = D, T, Q, 5, 6.

* The author of this dissertation performed all quantum chemical calculations along with the related analysis and planning, and actively participated in the bibliographic research and in the writing of the manuscript of **P2**.

ELSEVIER

Journal of Molecular Structure: THEOCHEM 811 (2007) 361–372

THEO CHEM

www.elsevier.com/locate/theochem

A cost-effective basis-set extrapolation scheme: Application to the energetics of homolytic bond dissociation

Filipe Agapito [a,b], Benedito J. Costa Cabral [a,b,*], José A. Martinho Simões [b]

[a] *Grupo de Física Matemática da Universidade de Lisboa, Av. Professor Gama Pinto 2, 1649-003 Lisboa, Portugal*
[b] *Departamento de Química e Bioquímica, Faculdade de Ciências, Universidade de Lisboa, 1749-016 Lisboa, Portugal*

Received 29 November 2006; accepted 22 December 2006
Available online 30 January 2007

Abstract

A composite procedure based on density functional theory (DFT) geometry optimizations and coupled cluster calculations with single and double excitations and perturbative treatment of triple excitations (CCSD(T)) is proposed for the evaluation of homolytic bond dissociation enthalpies (BDEs). The performance of several functionals for predicting the structure and vibrational frequencies of a selected set of closed- and open-shell species was investigated. By using the correlation consistent cc-pVTZ basis-set, it was found that B3LYP and VSXC geometries are in good agreement with experiment. B3LYP/cc-pVTZ geometries were then selected for CCSD(T) single-point energy calculations. The Hartree-Fock (HF) contribution to the total energy was estimated at the HF/cc-pV6Z level and also by using a (x = D(2),T(3),Q(4),5,6) ad hoc extrapolation. Complete basis-set values for CCSD(T) correlation energies were evaluated through dual (x, x + 1;x = 2) extrapolation schemes relying on calculations with the cc-pVxZ basis-set. The results illustrate the importance of the extrapolation schemes and show that (2, 3) extrapolated BDEs are more accurate than those calculated with the cc-pV6Z basis-set.

PACS: 31.15.Ew; 31.15.Dv; 33.15.−e; 33.15.Fm

Keywords: Bond dissociation enthalpies; Basis-set extrapolation

1. Introduction

Bond dissociation enthalpies (BDEs) are required to understand the energetics of chemical reactions. Despite their importance, the available BDE database is still fairly small and many values need to be reevaluated [1–3]. This situation reflects the experimental difficulties of investigating the thermochemistry of short-lived species, which are not amenable to the traditional calorimetric techniques.

In recent years, it has been demonstrated that computational chemistry can be a reliable method of determining BDEs [4,5]. However, the development of model chemistries that allow an accurate computation of BDEs, along with many other properties, is still an ongoing task and an active research field. Density functional theory (DFT) [6] has been particularly useful in the study of thermochemical, electronic, and structural properties of large molecules. Ab initio methods also provide accurate prediction of such properties. However, the accuracy of the theoretical results, particularly of those based on ab initio calculations, is seriously limited by the truncation of the one-electron basis-set expansion. This is due to the fact that the rate of convergence of ab initio energies with the basis-set size is extremely slow, while the computational cost grows enormously with the basis-set size: the computational effort of ab initio calculations scales as $n^k N^4$, where n is the number of electrons, N the number of basis function per atom, and $k = 4$, 5, 6, 7, respectively for Hartree-Fock (HF) [7], Møller–Plesset second order perturbation theory (MP2) [8], coupled cluster with single and double excitations CCSD [9], and with perturbative

* Corresponding author. Tel.: +351 21 796 4296; fax: +351 21 765 4288.
E-mail address: ben@cii.fc.ul.pt (B.J. Costa Cabral).

0166-1280/$ - see front matter © 2007 Elsevier B.V. All rights reserved.
doi:10.1016/j.theochem.2006.12.050

treatment of triple excitations CCSD(T) [10]. This problem has been addressed in several investigations on basis-set dependence and CBS extrapolation schemes [11–26].

To systematically assess the convergence of the energy with the basis set size it is mandatory to adopt an hierarchical family of basis-set functions. This can be accomplished by carrying out calculations with correlation consistent polarized valence basis-sets (cc-pVxZ; x = D(2),T(3),Q(4),5,6) [27], which lead to improved results for the energy from the cardinal number x to x + 1. Extrapolation methods are usually based on the asymptotic behavior of the HF and correlation energies. Separate extrapolations for each one of these contributions to the total energy improve the accuracy of the results [16] because the convergence of the correlation part is significantly slower than that of the HF contribution. On the other hand, the selection of a given extrapolation method is very dependent on the system of interest. For atoms or small molecules, accurate methods for complete basis-set extrapolation relying on calculations with very large basis-sets (x = 5, 6) are possible [15–17,19–21]. However, for medium-size and large molecules even calculations at a high correlated method with a cc-pVQZ basis-set are not affordable. In these cases, reliable extrapolation procedures from calculations with smaller basis-sets (x = D(2),T(3)) [22,23] can be extremely important.

One of the most popular (2, 3) dual level extrapolation method was proposed by Truhlar [23]. Although the scheme was parameterized for one atom (Ne) and two molecules (HF and H_2O), it leads, usually, to extrapolated energies with a smaller root-mean-square (rms) deviation from the CBS limit than the energies from cc-pV6Z calculations. This extrapolation scheme, as well as others previously reported, is empirical [20,23]. Therefore, some criticism has been raised concerning the possibility that overfitting may compromise the accuracy of the method when species not included in the selected data set are considered [22]. Interestingly, although the economically motivated (2, 3) method of Ref. [23] relies on fitting of ab initio energies for only three species, it has been applied with success to several others systems [5,28].

In the present work, we propose a cost-effective extrapolation to complete basis-set (CBS) procedure, which is oriented for the calculation of accurate molecular properties, in particular, bond dissociation enthalpies. The extrapolation scheme is based on DFT geometries and frequencies, and CCSD(T) energies. The performance of several functionals for predicting the structure and vibrational frequencies of a selected set of closed- and open-shell molecules was analyzed. These properties have been recently investigated for the same set of molecules by ab initio methods and detailed comparisons between theoretical and experimental information have been reported [29,30]. Therefore, using the same set of molecules our DFT results can be compared with both experimental data and ab initio predictions. Moreover, since the selected set comprises a large number of small molecules, for which ab initio calculations with very large basis-sets are affordable, it is particularly suited for the study of CBS extrapolation schemes.

2. Computational details

2.1. Geometry optimization and vibrational frequencies

Accurate geometries and vibrational frequencies are crucial for the computation of thermodynamic properties. As such, this was the starting point of our study. Density functional theory is a cost-effective method to perform geometry optimizations and frequency calculations, since it has the advantage of including correlation effects, while having a computational effort similar to a Hartree-Fock calculation. Some recent investigations [30,31] pointed out that B3LYP [32,33] calculations with a cc-pVTZ basis-set can provide structures that are in very good agreement with experimental information. In the present work, we performed a comparison between the geometry optimization performances of B3LYP and some more recent functionals, namely PBEPBE [34,35], B98 (i.e., Becke's 1998 revisions to B97) [36,37], VSXC [38], HCTH/407 [39], and TPSS [40]. To perform this comparison, the geometries of 19 closed-shell molecules and 33 open-shell molecules (Table 1) were optimized, using the above mentioned functionals and Dunning's cc-pVTZ basis-set. The results were then compared with the experimental bond lengths [29,30] for the set of test molecules displayed in Tables 2 and 3. Frequency calculations were performed for all the optimized geometries, not only to ensure that these were in fact minimum energy structures, but also to determine zero-point vibrational energies (ZPVEs) and thermal corrections (at 298.15 K), which include the contribution to the internal thermal energy due to translational and rotational motions, and the contribution to internal thermal energy resulting from molecular vibrations (ZPVE included). The calculated frequencies are harmonic and were not scaled. Although for some cases, significant deviations from harmonicity can be observed, harmonic frequencies are accurate enough for estimating ZPVEs and thermal corrections of bond dissociation enthalpies (BDEs) to 298.15 K.

Additionally, the vibrational frequencies obtained with the six functionals for open-shell molecules were compared

Table 1
List of the 52 molecules used in this work

Closed-shell						
HF	H_2O	HOF	H_2O_2	HNC	NH_3	N_2H_2
C_2H_2	HNO	HCN	C_2H_4	CH_4	N_2	CH_2O
CH_2	CO	CO_2	O_3	F_2		
Open-shell						
OH	HO_2	H_2O^+	FH^+	NH_2	HNF	$C_4H_2^+$
HCC	NH^+	HCP^+	CH_3	CH_3O	O_2^+	N_2^+
CH	HCO	CO^+	NO	CN	CO_2^+	BH_2
N_3	BO	BH^+	CNC	C_2^-	CF	F_2^+
OF	CH_2CHO	C_3H_5	NCO	CH_2^-		

Table 2
Experimental bond lengths (in pm) for the closed-shell molecules

	Molecule	Bond	Exp.[a]
1	HF	F–H	91.7
2	H_2O	H–O	95.7
3	HOF	H–O	96.57
4	H_2O_2	H–O	96.7
5	HNC	H–N	99.4
6	NH_3	H–N	101.2
7	N_2H_2	H–N	102.8
8	C_2H_2	C–H	106.2
9	HNO	H–N	106.3
10	HCN	C–H	106.5
11	C_2H_4	C–H	108.1
12	CH_4	C–H	108.6
13	N_2	N–N	109.77
14	CH_2O	C–H	109.9
15	CH_2	C–H	110.7
16	CO	C–O	112.8
17	HCN	C–N	115.3
18	CO_2	C–O	116.0
19	HNC	C–N	116.9
20	C_2H_2	C–C	120.3
21	CH_2O	C–O	120.3
22	HNO	N–O	121.2
23	N_2H_2	N–N	125.2
24	O_3	O–O	127.2
25	C_2H_4	C–C	133.4
26	F_2	F–F	141.2
27	HOF	F–O	143.5
28	H_2O_2	O–O	145.56

[a] Taken from Ref. [29].

Table 3
Experimental bond lengths (in pm) for the open-shell molecules

	Molecule	Bond	Exp.[a]
1	OH	O–H	96.97
2	HO_2	O–H	97.7
3	H_2O^+	O–H	100.1
4	FH^+	F–H	100.1
5	NH_2	N–H	102.5
6	HNF	H–N	103.5
7	$C_4H_2^+$	H–C	104.6
8	HCC	H–C	104.653
9	NH^+	N–H	107
10	HCP^+	H–C	107.3
11	CH_3	H–C	107.67
12	CH_3	H–C	107.67
13	CH_3O	H–C	109.58
14	CH_3O	H–C	109.58
15	O_2^+	O–O	111.64
16	N_2^+	N–N	111.642
17	CH	H–C	111.99
18	HCO	H–C	112.5
19	CO^+	C–O	112.83
20	NO	N–O	115.08
21	CN	C–N	117.18
22	HCO	C–O	117.5
23	CO_2^+	C–O	117.682
24	CO_2^+	C–O	117.682
25	BH_2	B–H	118.1
26	N_3	N–N	118.15
27	N_3	N–N	118.15
28	BO	B–O	120.5
29	BH^+	B–H	121.5
30	HCC	C–C	121.652
31	$C_4H_2^+$	C–C	123.4
32	CNC	C–N	124.5
33	CNC	C–N	124.5
34	C_2^-	C–C	126.8
35	CF	C–F	127.2
36	F_2^+	F–F	130.5
37	HO_2	O–O	133.5
38	$C_4H_2^+$	C–C	134.6
39	OF	O–F	135.4
40	CH_3O	C–O	136.37
41	HNF	N–F	137.3
42	HCP^+	C–P	160.0

[a] Taken from Ref. [30].

with experimental data (Table 4) [30]. One of the best methods to determine both structures and frequencies was found to be B3LYP/cc-pVTZ. Therefore, the corresponding structures and frequencies were used in all subsequent calculations.

2.2. Complete basis-set extrapolation

We have carried out CCSD(T)/cc-pVxZ//B3LYP/cc-pVTZ (x = D(2),T(3),Q(4),5,6) calculations for all the molecules in Table 1, with the exception of C_3H_5, $C_4H_2^+$, CH_3O, CH_2CHO, and HCP^+ (excluded due to computational limitations). Since one of the main concerns of this work was cost-effectiveness, the inner-shells were excluded from the correlation calculations (i.e., we performed frozen-core calculations). By using correlation consistent basis-sets, the number of basis functions per atom, N, is given by

$$N = (\mathrm{x}+1)\left(\mathrm{x}+\frac{3}{2}\right)\left(\frac{\mathrm{x}+2}{3}\right). \quad (1)$$

In contrast with the extrapolation of the correlation energy, CBS limit for the HF energy can be accurately estimated even for medium or large sized molecules by using accurate ad hoc schemes and larger basis-sets. Halkier et al. [21], pointed out that two- and three-point extrapolation schemes of the Hartree-Fock energy exhibit some limitations and should be only applied when calculations with larger basis-set are not possible. In addition, these authors also provided some evidence that HF/cc-pV6Z energies are converged within 0.1 mE_h to complete basis-set limit. In the present study, the CBS limit of the HF energy contribution was estimated by using the HF/cc-pV6Z value and application of a (2–6) ad hoc extrapolation scheme.

To study the convergence of the correlation energy with the basis-set, the following ansatz was adopted

$$E_{\mathrm{x}} = E_\infty + A(\mathrm{x}+\alpha)^{-\beta}. \quad (2)$$

In this expression E_{x} is the correlation energy obtained using a cc-pVxZ basis-set and E_∞ is the complete basis-set limit. Based on a dual (x, x+1) procedure E_∞ can be easily derived from Eq. (2), and written as

Table 4
Experimental vibrational frequencies (in cm^{-1}) for open-shell molecules

		Exp.[a]
1	CNC	321
2	CNC	321
3	HCC	372
4	CH_2CHO	404
5	C_3H_5	427
6	$C_4H_2^+$	432
7	$C_4H_2^+$	432
8	N_3	457
9	N_3	457
10	CH_2CHO	500
11	CO_2^+	511
12	CO_2^+	511
13	C_3H_5	518
14	NCO	535
15	NCO	535
16	C_3H_5	549
17	CH_2CHO	557
18	CH_3	606
19	HCP^+	642
20	HCP^+	642
21	CH_3O	653
22	CH_3O	653
23	CH_2CHO	703
24	C_3H_5	802
25	CH_2CHO	957
26	C_3H_5	968
27	$C_4H_2^+$	972
28	HNF	1000
29	BH_2	1030
30	CH_3O	1047
31	OF	1053[b]
32	C_3H_5	1066
33	HCO	1081
34	HO_2	1098
35	F_2^+	1104[b]
36	CH_2CHO	1143
37	HCP^+	1147
38	C_3H_5	1182
39	CH_2^-	1230
40	CO_2^+	1244
41	C_3H_5	1245
42	NCO	1273
43	CF	1308[b]
44	N_3	1320
45	CH_3O	1362
46	CH_2CHO	1366
47	C_3H_5	1389
48	HO_2	1392
49	CH_3	1398
50	H_2O^+	1408
51	HNF	1419
52	CO_2^+	1423
53	CNC	1453
54	C_3H_5	1463
55	CH_2CHO	1486
56	CH_3O	1487
57	CH_3O	1487
58	C_3H_5	1488
59	NH_2	1497
60	CH_2CHO	1543
61	N_3	1645
62	C_2^-	1781[b]
63	HCC	1841
64	HCO	1868
65	BO	1886[b]
66	NO	1904[b]
67	O_2^+	1905[b]
68	NCO	1921
69	CN	2069[b]
70	CO^+	2170[b]
71	$C_4H_2^+$	2177
72	N_2^+	2207[b]
73	HCO	2434
74	BH^+	2435
75	CH_3O	2774
76	CH_3O	2774
77	CH_3O	2840
78	CH	2858[b]
79	NH^+	2922
80	CH_3	3005
81	C_3H_5	3016
82	C_3H_5	3048
83	FH^+	3090[b]
84	C_3H_5	3105
85	HCP^+	3125
86	$C_4H_2^+$	3137
87	CH_3	3161
88	H_2O^+	3213
89	NH_2	3219
90	H_2O^+	3259
91	NH_2	3301
92	HO_2	3437
93	OH	3738[b]

[a] Taken from Ref. [30].
[b] Experimental harmonic frequency.

$$E_\infty = \frac{(x+1+\alpha)^\beta}{(x+1+\alpha)^\beta - (x+\alpha)^\beta} E_{x+1} - \frac{(x+\alpha)^\beta}{(x+1+\alpha)^\beta - (x+\alpha)^\beta} E_x. \quad (3)$$

When $\alpha = 0$ and $\beta = 3$, Eq. (2) is the same proposed by Helgaker et al. [19], and taking $\alpha = 0$ and $\beta = 2.4$ we obtain the expression derived by Truhlar [23] for CCSD and CCSD(T). A recent study [26] revealed that the combination of $\alpha = 1/2$ and $\beta = 3$ yields good results for CCSD(T) dual (2, 3) extrapolations. These values were found by varying the parameters and studying their impact on the quality of the extrapolation scheme. However, it should be observed that the same values can be derived directly from the partial-wave expansion [24]

$$E_x = E_\infty + \sum_{m=4} A_{m-1}(L+1)^{-m+1}. \quad (4)$$

The crucial point is the relationship between x and the angular momentum, L. This relationship is a serious limitation to the application of partial-wave expansion to molecules, because the angular momentum is not a good quantum number and molecular wave functions from atomic basis-sets are usually not constructed in a systematic way, i.e., function spaces of a given (atomic) angular

momentum should be saturated before the next function space is added [18]. For Dunning's basis-sets, the use of $\alpha = 1/2$ represents a compromise between the highest angular momentum in the basis for H and He ($L = x - 1$) and for Li–Ar ($L = x$) [18]. Using the average value $L = x - 1/2$ in Eq. (4) and truncating the summation after the first term, we obtain the above extrapolation scheme with $\alpha = 1/2$ and $\beta = 3$. In Ref. [26] different optimal values of α and β were found for extrapolations with MP2 and CCSD. This does not invalidate the derivation outlined above, since one can predict that the approximations made should not be valid when E_x is very different from E_∞. In particular, we note that the summation in Eq. (4) represents the error in E_x. Therefore, when this error is large, the contribution of the terms with $m > 4$ will be nonnegligible and consequently, their truncation from the summation will not be possible.

In the present work, the accuracy of the above mentioned (2, 3) dual extrapolation schemes for CCSD(T) correlation energies will be investigated. As in previous works [23,24], the correlation energies extrapolated using the (5, 6) dual scheme proposed by Halkier et al. [20] were taken as reference values. This scheme can be derived by setting $\alpha = 0$ and $\beta = 3$ in Eq. (3).

2.3. Bond dissociation enthalpies

We have applied different CBS extrapolation schemes for predicting bond dissociation enthalpies (BDEs). The HO–OH bond dissociation enthalpy, as well as the N–H, O–H, F–H, and C–H BDEs in NH_3, ONH, H_2O_2, H_2O, HF, CH_4, and NCH were calculated. The calculation procedure has been described elsewhere [41]. In short, for a bond homolysis reaction

$$R_1 - R_2 \rightarrow R_1^{\cdot} + R_2^{\cdot} \quad (5)$$

the enthalpies of all the reactants and products were computed by adding the HF energy, the correlation energy, and thermal corrections to 298 K. Obviously, thermal corrections must be determined with the same method used to optimize the geometry of the species. The $R_1 - R_2$ BDE is then simply the enthalpy of reaction (5).

3. Results and discussion

3.1. Geometry optimization and vibrational frequencies

The errors in bond lengths (defined as the difference between the calculated and the experimental values) of the optimized geometries for all open and closed-shell molecules, and for different DFT methods, are displayed in Figs. 1–4. The average errors ($\bar{\Delta}$), average absolute errors ($|\bar{\Delta}|$), standard deviations (σ), and maximum errors (Δ_{max}) for each functional are summarized in Table 5.

The analysis of Table 5 and Figs. 1 and 2 reveals that B3LYP and VSXC yield the smallest average absolute errors, 0.52 and 0.44 pm, respectively. Both methods lead to small average errors and small standard deviations. This fact is clearly illustrated in Fig. 1. Between these two, VSXC is the one with a smaller dispersion of errors, but B3LYP has the smallest maximum (absolute) error. TPSS and PBEPBE results show the largest absolute errors.

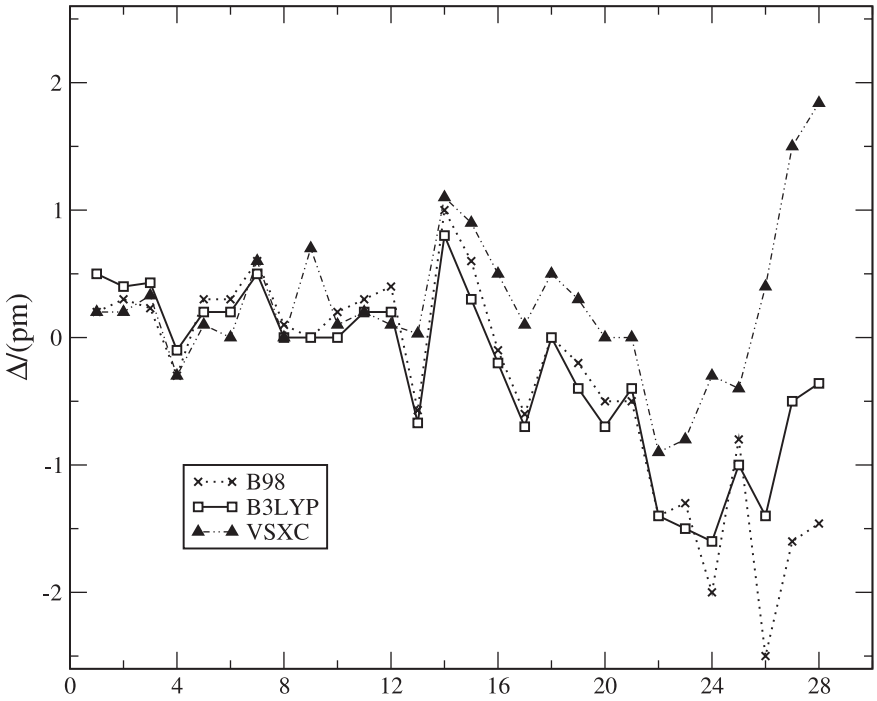

Fig. 1. Errors (in pm) in the bond lengths of closed-shell molecules optimized with B98, B3LYP, and VSXC. The bond lengths are numbered according to Table 2.

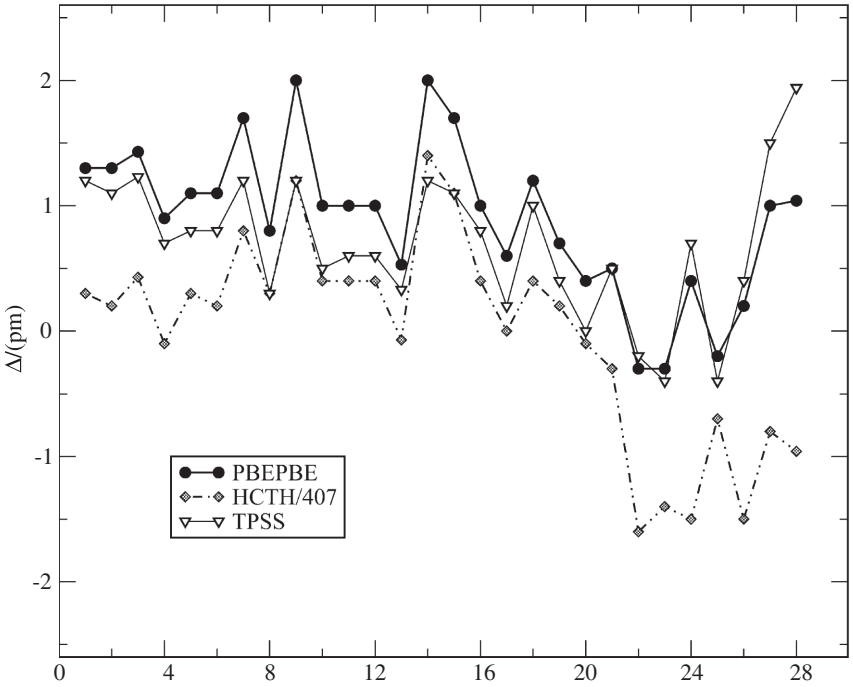

Fig. 2. Errors (in pm) in the bond lengths of closed-shell molecules optimized with PBEPBE, HCTH/407, and TPSS. The bond lengths are numbered according to Table 2.

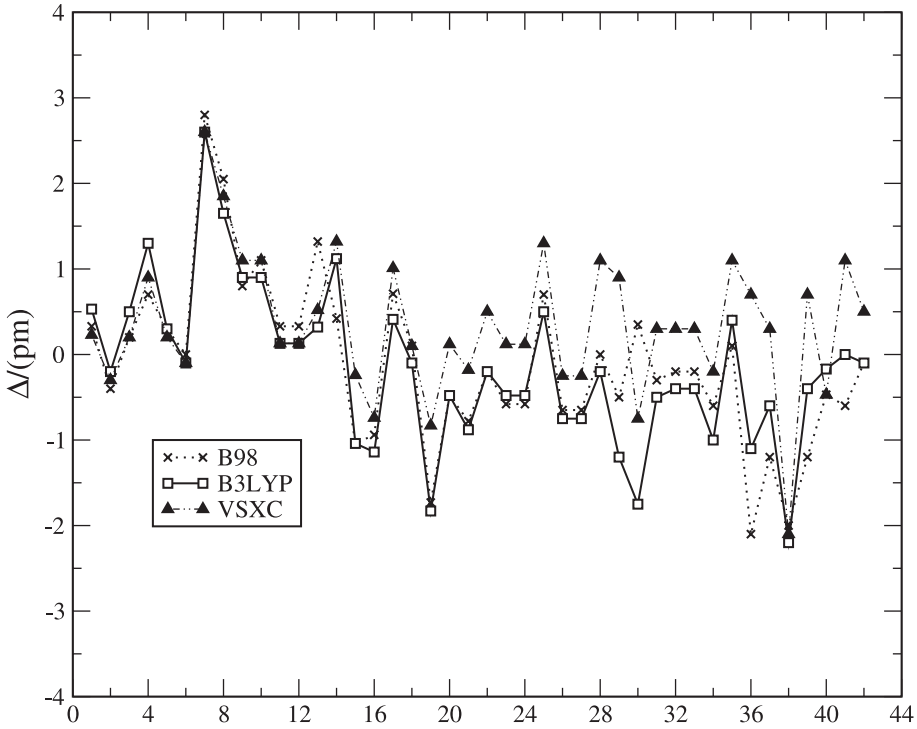

Fig. 3. Errors (in pm) in the bond lengths of open-shell molecules optimized with B98, B3LYP, and VSXC. The bond lengths are numbered according to Table 3.

With regard to the results for open-shell molecules, the analysis of Table 5 and Figs. 3 and 4 indicates that B98, B3LYP and VSXC are the most accurate functionals. In this case, the errors associated with bond lengths for these functionals are -0.12 ± 0.96, -0.16 ± 0.93, and 0.34 ± 0.80 pm, respectively. The maximum and absolute average errors are also smaller for these three functionals. B98 behaves very similarly to B3LYP, but has a slightly

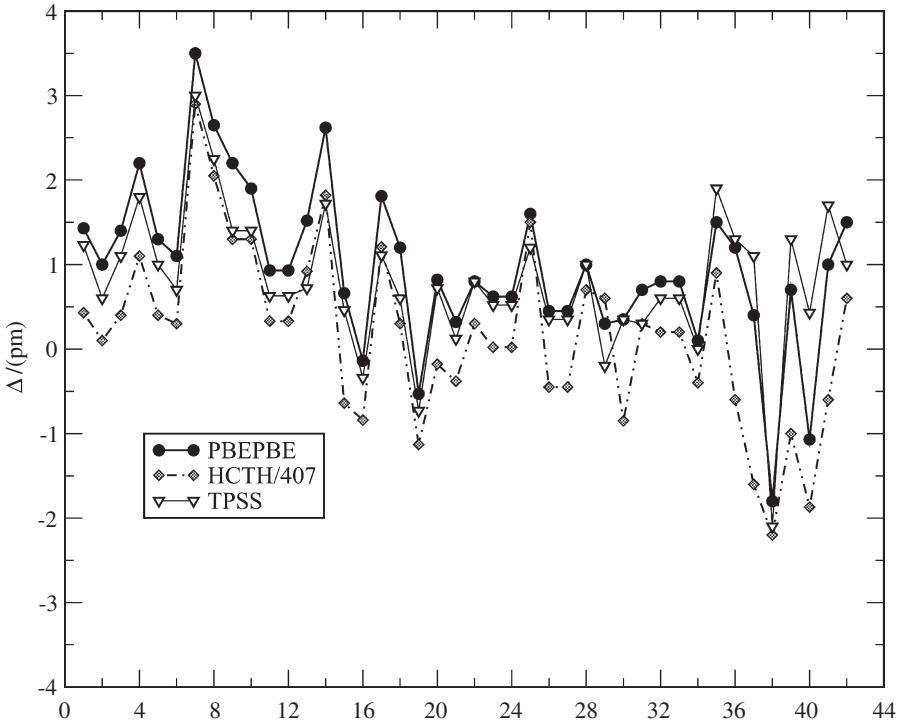

Fig. 4. Errors (in pm) in the bond lengths of open-shell molecules optimized with PBEPBE, HCTH/407, and TPSS. The bond lengths are numbered according to Table 3.

Table 5
Statistical analysis of the errors in bond lengths (in pm)

	$\bar{\Delta}$	$\lvert\bar{\Delta}\rvert$	σ	Δ_{max}
Closed-shell molecules				
PBEPBE	0.90	0.95	0.61	2.00
B98	−0.33	0.66	0.86	−2.50
B3LYP	−0.26	0.52	0.66	−1.60
VSXC	0.25	0.44	0.60	1.84
HCTH/407	−0.02	0.62	0.81	−1.60
TPSS	0.69	0.76	0.56	1.94
Open-shell molecules				
PBEPBE	0.97	1.14	0.95	3.50
B98	−0.12	0.72	0.96	2.80
B3LYP	−0.16	0.72	0.93	2.60
VSXC	0.34	0.65	0.80	2.60
HCTH/407	0.17	0.80	1.03	2.90
TPSS	0.79	0.95	0.83	3.00

higher maximum error. Again, as Table 5 and Figs. 3 and 4 clearly indicate, TPSS and PBEPBE are the functionals with the worst performance.

The data in Table 3 and Figs. 3 and 4 also allow to check the correct determination of point groups for CH_3, CH_3O, CO_2^+, N_3, and CNC. In the case of CO_2^+, N_3, and CNC, all functionals accurately predicted their point group to be $D_{\infty h}$. The correct point group of the methyl radical, D_{3h}, was also predicted by all functionals. The only exception was the methoxy radical for which all methods failed in predicting the correct C_{3v} point group, leading instead to a C_s point group of $^2A'$ symmetry. However, as noted by Byrd et al. [30], this is due to the availability of a Jahn–Teller distortion to a lower energy geometry. We add to that remark that this distortion can be pictured as the result of a hyperconjugation effect. Only one of the C–H bonds σ orbitals will have an appropriate symmetry to overlap with the partially occupied orbital in the oxygen atom. This overlap leads to an elongation of that C–H bond, and consequently, to a distortion away from the C_{3v} point group.

In Table 6 and Figs. 5 and 6 we summarize the errors in theoretical harmonic vibrational frequencies obtained with each method as well as the respective statistical treatment. Experimental frequencies are anharmonic, with the exception of diatomic molecules (see Table 2) for which experimentally derived harmonic frequencies are available. Analysis of these data reveals that in contrast with what was previously observed for geometry optimizations, TPSS and PBEPBE are the most accurate functionals for the

Table 6
Statistical analysis of the errors in vibrational frequencies (in cm^{-1}) for open-shell molecules

	$\bar{\Delta}$	$\lvert\bar{\Delta}\rvert$	σ	Δ_{max}
PBEPBE	9(−24)	50(60)	75(79)	266(−173)
B98	55(63)	76(76)	83(70)	309(171)
B3LYP	60(50)	75(78)	77(76)	307(145)
VSXC	37(14)	75(50)	98(56)	−330(104)
HCTH/407	33(16)	69(66)	88(73)	284(114)
TPSS	25(−16)	52(54)	71(66)	287(−135)

Deviations from experimental harmonic frequencies in parentheses.

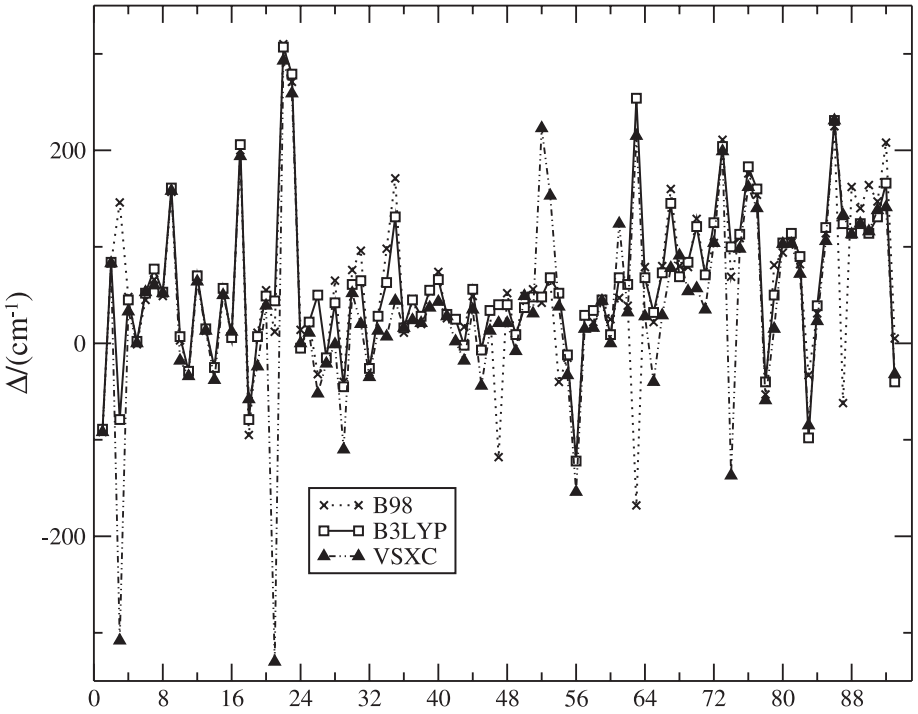

Fig. 5. Errors (in cm^{-1}) in the vibrational frequencies of open-shell molecules optimized with B98, B3LYP, and VSXC. The vibrational frequencies are numbered according to Table 4.

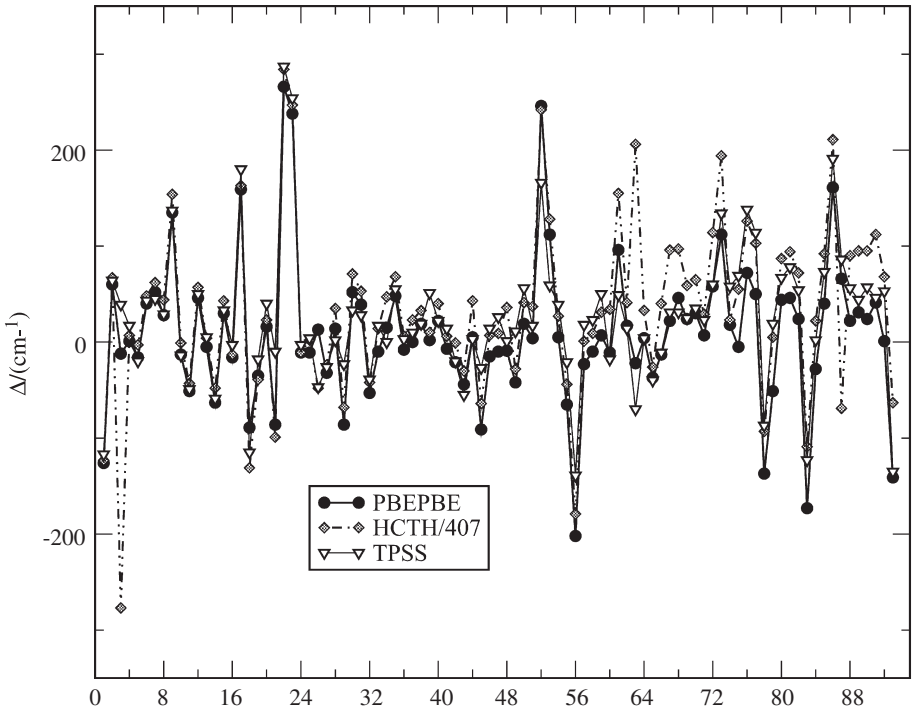

Fig. 6. Errors (in cm^{-1}) in the vibrational frequencies of open-shell molecules optimized with PBEPBE, HCTH/407, and TPSS. The vibrational frequencies are numbered according to Table 4.

determination of vibrational frequencies of open-shell molecules. In particular, the error associated with vibrational frequencies determined with PBEPBE is on average $9 \pm 75\ cm^{-1}$. Therefore, PBEPBE clearly performs better then the remaining methods. As previously discussed by Byrd et al. [30] comparison of theoretical frequencies with experiment may lead to significant deviations. In general, as illustrated in Table 6, theoretical harmonic frequencies

are significantly higher than experimental values. This is related to anharmonicity in the experimental values. Deviations from experimentally derived harmonic frequencies of diatomic molecules are also reported in Table 6 (values in parentheses). Smaller deviations from experiment are then observed for all the functionals if comparison between theoretical (harmonic) frequencies and experimental harmonic frequencies is carried out. In this case, the VSXC, TPSS and HCTH/407 functionals show the best agreement with experimental information. However, since our main objective when calculating vibrational frequencies is the determination of the thermal corrections at 298 K, and in view of the fact that these are small when compared with the electronic energy, the performance of all the methods is acceptable.

Considering the above discussion, we can conclude that among the functionals studied, B3LYP and VSXC are the overall best. However, since VSXC displayed a somewhat erroneous behavior in the determination of vibrational frequencies (Fig. 5) and mainly because previous works [30,31] also indicate that B3LYP/cc-pVTZ geometries are in good agreement with experimental data, these geometries were used in the remainder of our study. Also noteworthy is the fact that some trends are found, for both geometries and vibrational frequencies. This can be clearly observed in Figs. 1–6, where it is evident that the error plots of each property are similar with all the functionals. These trends can either indicate errors in experimental values or systematic failures of all the DFT methods considered.

3.2. Complete basis-set extrapolation

In Table 7 we summarize the errors in extrapolated correlation energies using three dual (2,3) extrapolation schemes, taking as reference the respective (5,6) extrapolation values. In this table, method I is Truhlar's extrapolation scheme for CCSD(T) [23] ($\alpha = 0$, $\beta = 2.4$) and method II is the extrapolation scheme of Ref. [26] ($\alpha = 1/2$, $\beta = 3$). Method III was obtained by optimizing α and β in Eq. (3) to minimize the root-mean-square error of the extrapolation scheme. We conducted this minimization by optimizing both α and β as well as by optimizing only one of the parameters, keeping the other fixed to its value in other extrapolation schemes. However, all attempts lead to different parameters but precisely to the same rms error (4.22 mE_h) and the same errors in extrapolated energies. Therefore, we only report the results for one of these schemes. We have also verified that a (2,3) extrapolation scheme with $\alpha = 0$ and $\beta = 3$ is not adequate and leads to significant deviations from the (5,6) reference values. We note that this behavior indicates a significant covariant relationship between α and β, which in turn implies that, for a given set of molecules and each α, there is only one β for which the rms error is minimum. Thus, in keeping with our previous argument, it is possible that there is a universally optimal (2,3) extrapolation scheme. What are the parameters of such a scheme, and how accurate would it be, are still two unanswered questions. The scheme we present here was obtained by optimizing β in Scheme I, and leads to $\beta = 2.47182$. Given that for Scheme I the rms error is 4.74 mE_h, this change in β conveys only a slight improvement in the rms error. However, since the rms error is largely dominated by the error in F_2^+, for which all (2,3) schemes perform poorly, there is a significant improvement of the extrapolated energies (Table 7 and Fig. 7). Analysis of Fig. 7 reveals that method II performs

Table 7
Errors (in mE_h) in (2,3) extrapolated correlation energies, when compared to (5,6) extrapolation values

		I[a]	II[b]	III[c]
1	BH_2	2.85	2.32	2.42
2	BH^+	0.70	0.48	0.53
3	BO	0.44	−1.60	−1.21
4	C_2^-	2.80	1.05	1.39
5	C_2H_2	6.01	4.15	4.51
6	C_2H_4	8.10	6.06	6.45
7	CF	1.03	−1.84	−1.29
8	CH_2	4.53	3.58	3.76
9	CH_2^-	1.39	0.14	0.38
10	CH_2O	4.57	1.85	2.37
11	CH_3	5.18	4.12	4.32
12	CH_4	6.34	5.10	5.34
13	CH	3.35	2.63	2.77
14	CNC	5.25	2.61	3.11
15	CN	3.31	1.46	1.81
16	CO_2	2.23	−1.96	−1.16
17	CO_2^+	2.89	−0.83	−0.12
18	CO	2.01	−0.37	0.08
19	CO^+	1.15	−0.87	−0.49
20	F_2	−0.64	−5.15	−4.28
21	F_2^+	−19.76	−23.63	−22.89
22	FH^+	1.41	−0.51	−0.14
23	H_2O_2	5.42	1.58	2.31
24	H_2O	3.67	1.60	2.00
25	H_2O^+	3.34	1.76	2.07
26	HCC	4.73	3.07	3.39
27	HCN	4.69	2.59	2.99
28	HCO	3.07	0.54	1.03
29	HF	0.50	−1.94	−1.47
30	HNC	4.91	2.81	3.21
31	HNF	2.76	−0.80	−0.12
32	HNO	3.80	0.77	1.35
33	HO_2	3.67	0.12	0.80
34	HOF	2.23	−1.96	−1.16
35	N_2	3.26	0.90	1.36
36	N_2^+	2.51	0.59	0.96
37	N_2H_2	6.13	3.44	3.95
38	N_3	4.79	1.29	1.96
39	NCO	4.83	1.17	1.87
40	NH_2	4.90	3.49	3.76
41	NH_3	5.94	4.28	4.60
42	NH^+	3.00	2.13	2.30
43	NO	2.74	−0.05	0.48
44	O_2^+	0.90	−1.91	−1.37
45	O_3	1.58	−3.47	−2.50
46	OF	1.17	−2.71	−1.96
47	OH	3.00	1.21	1.56

[a] Extrapolation method of Ref. [23].
[b] Extrapolation method of Ref. [26].
[c] Extrapolation method using fitted parameters.

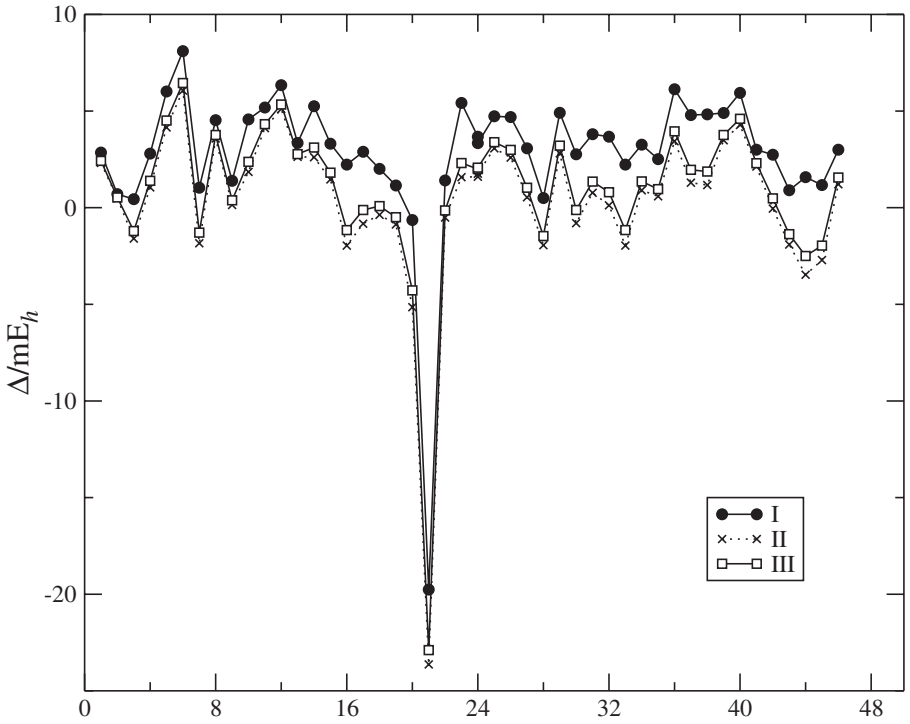

Fig. 7. Errors (in mE$_h$) in correlation energies extrapolated using the (2,3) dual schemes. The molecules are numbered according to Table 7.

very similarly to our optimized extrapolation scheme. Indeed, the rms error for Scheme II is only 4.25 mE$_h$ and therefore, very close to that of method III. This is remarkable if we bear in mind that, as outlined above, method II can almost be derived from first principles, by making some approximations, and without any need for parameter optimization. The accuracy of method II can be more deeply scrutinized in Table 7, where we can see that it often even surpasses the accuracy of method III. It is also clear from these data that both schemes II and III outperform Truhlar's scheme for CCSD(T). The results reported in Table 7 also indicate that (2,3) extrapolated energies for

Table 8
Errors (kJ mol^{-1}) in computed bond dissociation enthalpies relative to experimental values

	NH_2–H	HOO–H	HO–OH	HO–H	H–F	CH_3–H	NC–H	ON–H
				Experimental DH° (kJ mol^{-1}):				
	450.1 ± 1.1[a]	367.4 ± 2.1[b]	210.5 ± 0.5[a]	497.12 ± 0.30[a]	570.7 ± 0.8[c]	439.1 ± 0.5[a]	528.5 ± 0.8[b]	207.1 ± 2.9[b]
x				*cc-pVxZ calculations (no extrapolation)*				
D(2)	−37.10	−37.40	−31.74	−46.54	−63.19	−20.02	−26.81	−32.83
T(3)	−12.22	−11.17	−10.99	−14.94	−19.04	−6.09	−2.41	−12.73
Q(4)	−5.56	−5.23	−6.38	−5.72	−6.53	−3.00	2.27	−7.39
5	−3.35	−3.31	−4.27	−2.54	−2.35	−2.32	3.63	−5.40
6	−2.82	−2.86	−3.16	−1.57	−1.08	−1.96	4.11	−4.87
Method				*HF/cc-pV6Z energy*				
(5,6)	−2.04	−2.12	−1.27	−0.42	0.40	−1.47	4.82	−4.15
I	0.67	2.48	−2.78	1.34	0.95	1.57	8.45	−1.38
II	0.03	1.69	−3.51	0.59	0.06	1.12	7.78	−1.98
III	0.15	1.84	−3.37	0.74	0.23	1.21	7.91	−1.86
Method				ad hoc *extrapolated HF energy*				
(5,6)	−2.05	−2.21	−0.75	−0.44	0.22	−1.53	3.95	−4.20
I	0.66	2.38	−2.27	1.32	0.77	1.51	7.59	−1.43
II	0.02	1.60	−2.99	0.57	−0.12	1.05	6.91	−2.03
III	0.14	1.75	−2.85	0.71	0.05	1.14	7.04	−1.92

[a] Ref. [3].
[b] Ref. [2].
[c] Ref. [42].

open-shell species are closer to the (5,6) reference values than the corresponding energies for closed-shell species.

3.3. Bond dissociation enthalpies

The differences between the BDEs computed using the procedures described above and the selected experimental data are collected in Table 8. The analysis of this table reveals that the extrapolated values are in better agreement with experiment than the CCSD(T)/cc-pV6Z non-extrapolated results. This alone represents an outstanding achievement, in particular for the cost-effective (2,3) schemes. The only exception is the NC–H bond dissociation enthalpy. Interestingly, for this BDE the deviation from experiment increases with the basis-set size and therefore, all extrapolation schemes overestimate its value. The (5,6) values are, with the exception the NC–H BDE when using the HF/cc-pV6Z energy, always within chemical accuracy (i.e., the deviation is within ca. 4 kJ mol^{-1} of the experimental value). This coherent behavior supports their use as reference values. In general, the use of ad hoc extrapolated HF energies has a lowering effect on the BDEs, but the accuracy is similar to that of the extrapolation methods using the HF/cc-pV6Z energy. This net lowering effect can even be harmful, as seen in the case of the H–F bond dissociation enthalpy obtained by method II. Comparison between the (2,3) extrapolation schemes reveals that methods II and III are generally more accurate than method I. This is not surprising since, as we saw above, these methods also perform better in the determination of correlation energies. What is indeed surprising is the fact that BDEs obtained with schemes II and III are often more accurate than those obtained with the (5,6) scheme, which was used as reference. However, in contrast with the (5,6) extrapolated BDEs, which exhibit a systematic and predictable behavior, the (2,3) extrapolation schemes lead to deviations from experimental values that are system dependent.

4. Conclusions

The performance of several functionals for predicting the structure and vibrational frequencies of a selected data set including closed- and open-shell species was investigated. It was concluded that when the calculations are carried out with the Dunning cc-pVTZ basis-set, VSXC and B3LYP functionals yield the best agreement with experimental information. In a second step, CCSD(T)/cc-pVxZ//B3LYP/cc-pVTZ (x = D(2),T(3),Q(4),5,6) single-point energy calculations were carried out and the accuracy of different (2,3) extrapolation procedures (named I, II, and III) for the correlation energy was discussed by taking (5,6) extrapolated energies as reference values. Schemes II and III afforded the best results. Regarding Scheme II, we showed how it could be obtained from the partial-wave expansion, without any need for empirical parameter determination.

The extrapolation schemes were then applied for computing bond dissociation enthalpies and it was verified that (2,3) extrapolations lead to more accurate results than those relying on non-extrapolated CCSD(T)/cc-pV6Z data. In the calculation of these CBS extrapolated BDEs both the cc-pV6Z and the ad hoc (x = 2–6) extrapolated values were used for the Hartree-Fock energy. From these results we concluded that both approaches provide accurate results, but the use of ad hoc (x = 2–6) extrapolated HF energies leads to slightly lower values for the BDEs.

Acknowledgments

This work was supported by Fundação para a Ciência e a Tecnologia (FCT), Portugal (POCI/MAT/55977/2004). F.A. thanks FCT for a Ph.D. grant (SFRH/BD/22854/2005).

References

[1] Y.-R. Luo, Handbook of Bond Dissociation Energies in Organic Compounds, CRC Press, Boca Raton, 2003.
[2] S.J. Blanksby, G.B. Ellison, Acc. Chem. Res. 36 (2003) 255.
[3] B. Ruscic, J.E. Boggs, A. Burcat, A.G. Császár, J. Demaison, R. Janoschek, J.M.L. Martin, M.L. Morton, M.J. Rossi, J.F. Stanton, P.G. Szalay, P.R. Westmoreland, F. Zabel, T. Berces, J. Phys. Chem. Ref. Data 34 (2005) 573.
[4] E.R. Johnson, O.J. Clarkin, G.A. DiLabio, J. Phys. Chem. A 107 (2003) 9953.
[5] B.J. Costa Cabral, S. Canuto, Chem. Phys. Lett. 406 (2005) 300.
[6] R.G. Parr, W. Yang, Density-Functional Theory of Atoms and Molecules, Oxford University Press, Oxford, 1989.
[7] A. Szabo, N.S. Ostlund, Modern Quantum Chemistry, Introduction to Advanced Electronic Structure Theory, McGraw Hill, New York, 1989.
[8] C. Møller, M.S. Plesset, Phys. Rev. 46 (1934) 618.
[9] G.D. Purvis III, R.J. Bartlett, J. Chem. Phys. 76 (1982) 1910.
[10] K. Raghavachari, G.W. Trucks, J.A. Pople, M. Head-Gordon, Chem. Phys. Lett. 157 (1989) 479.
[11] D. Feller, J. Chem. Phys. 96 (1992) 6104.
[12] D. Feller, J. Chem. Phys. 98 (1993) 7059.
[13] K.A. Peterson, T.H. Dunning Jr., J. Phys. Chem. 99 (1995) 3898.
[14] J.M.L. Martin, Chem. Phys. Lett. 259 (1996) 669.
[15] J.M.L. Martin, J. Mol. Struct. (Theochem) 398 (1997) 135.
[16] J.M.L. Martin, P.R. Taylor, J. Chem. Phys. 106 (1997) 8620.
[17] J.M.L. Martin, Am. Chem. Soc. Symp. Ser. 677 (1998) 212.
[18] W. Klopper, K.L. Bak, P. Jørgensen, J. Olsen, T. Helgaker, J. Phys. B: At. Mol. Opt. Phys. 32 (1999) R103–R130.
[19] T. Helgaker, W. Klopper, H. Koch, J. Noga, J. Chem. Phys. 106 (1997) 9639.
[20] A. Halkier, T. Helgaker, P. Jørgensen, H. Koch, J. Olsen, A.K. Wilson, Chem. Phys. Lett. 286 (1998) 243.
[21] A. Halkier, T. Helgaker, P. Jørgensen, W. Klopper, J. Olsen, Chem. Phys. Lett. 302 (1999) 437.
[22] A. Halkier, T. Helgaker, W. Klopper, P. Jørgensen, A.G. Császár, Chem. Phys. Lett. 310 (1999) 385.
[23] D.G. Truhlar, Chem. Phys. Lett. 294 (1998) 45.
[24] A.J.C. Varandas, J. Chem. Phys. 113 (2000) 8880.
[25] D. Feller, J.A. Sordo, J. Chem. Phys. 112 (2000) 5604.
[26] S.B. Huh, J.S. Lee, J. Chem. Phys. 118 (2003) 3035.
[27] T.H. Dunning Jr., J. Chem. Phys. 90 (1989) 1007.
[28] P. Cabral do Couto, B.J. Costa Cabral, J.A. Martinho Simões, Chem. Phys. Lett. 421 (2006) 504.

[29] T. Helgaker, J. Gauss, P. Jørgensen, J. Olsen, J. Chem. Phys. 106 (1997) 6430.
[30] E.F.C. Byrd, C.D. Sherrill, M. Head-Gordon, J. Phys. Chem. A 105 (2001) 9736.
[31] N.X. Wang, A.K. Wilson, J. Chem. Phys. 121 (2004) 7632.
[32] A.D. Becke, J. Chem. Phys. 98 (1993) 5648.
[33] C. Lee, W. Yang, R.G. Parr, Phys. Rev. B 37 (1988) 785.
[34] J.P. Perdew, K. Burke, M. Ernzerhof, Phys. Rev. Lett. 77 (1996) 3865.
[35] J.P. Perdew, K. Burke, M. Ernzerhof, Phys. Rev. Lett. 78 (1997) 1396.
[36] A.D. Becke, J. Chem. Phys. 107 (1997) 8554.
[37] H.L. Schmider, A.D. Becke, J. Chem. Phys. 108 (1998) 9624.
[38] T. Van Voorhis, G.E. Scuseria, J. Chem. Phys. 109 (1998) 400.
[39] A.D. Boese, N.C. Handy, J. Chem. Phys. 114 (2001) 5497.
[40] J. Tao, J.P. Perdew, V.N. Staroverov, G.E. Scuseria, Phys. Rev. Lett. 91 (2003) 146401.
[41] F. Agapito, B.J. Costa Cabral, J.A. Martinho Simões, J. Mol. Struct. (Theochem) 729 (2005) 223.
[42] J.D. Cox, D.D. Wagman, V.A. Medvedev (Eds.), CODATA Key Values for Thermodynamics, Hemisphere, New York, 1989.

CHAPTER 5

The allyl group

Some terpenes (terpinolene, α-terpinene, and γ-terpinene) have antioxidant properties comparable to α-tocoferol,[178] without the pro-oxidant effects this compound displays at high concentrations.[179] This capability is linked with the abstraction of an hydrogen atom from the terpene,[179] and therefore, to the formation of a radical center near a double bond. In order to better understand this effect, a knowledge of the C—H BDEs in these terpenes is fundamental. A review of available experimental data revealed that these BDEs were not known. Even worse, we found that experimental BDEs for small molecules containing structural motifs present in these terpenes were missing, inaccurate, or imprecise.[180] It made little sense to study larger and more complex compounds without fully comprehending the energetics of the allyl moiety and its influence on the stability of radicals.

In ref. 180 (**P3**) we analyzed the available experimental data and studied the energetics of the allyl moiety using TR-PAC and computational chemistry.* A facsimile of this article is included in the present chapter.† Rooted in the knowledge gained in **P2** we used B3LYP/cc-pVTZ to optimize geometries. CCSD(T) extrapolated with Truhlar's method was selected to calculate enthalpies. While this method performed slightly worse than the other two used in **P2**, it yields the exact value for the C—H BDE in propene. Moreover, the difference between the three extrapolation schemes of **P2** is often less than 1 mE_h (*ca.* 2.6 kJ$\cdot$mol^{-1}), and thus below what is commonly designated as chemical accuracy

* The author of this dissertation performed all quantum chemical calculations along with the related analysis and planning, and actively participated in the bibliographic research and in the writing of the manuscript of **P3**.

† Unfortunately some errors found their way into the manuscript, and an errata was later published.[181] A facsimile of Ref. 181 is also included in this chapter after **P3**.

(*ca.* 4 $kJ \cdot mol^{-1}$). CBS-Q and CBS-QB3 were also used to calculate enthalpies. Based on what we knew from **P1**, isodesmic reactions with the allyl radical were used in order to obtain accurate data from these two methods.

Calculations were performed for propene, isobutene, 1-butene, (*E*)-2-butene, 3-metylbut-1-ene, (*E*)-2-pentene, (*E*)-1,3-pentadiene, 1,4-pentadiene, cyclohexene, 1,3-cyclohexadiene, and 1,4-cyclohexadiene. This allowed us to rationalize the stabilization of radicals containing the allyl moiety in terms of π-delocalization, hyperconjugation, and thermodynamic stabilities of parent compounds. Theoretical BDEs were found to be in good agreement with the TR-PAC data obtained for cyclohexene and 1,3-cyclohexadiene, but some doubt about the data for the C—H BDE in 1,4-cyclohexadiene still remained. A recent re-evaluation of this value by Gao *et al.*[182] using laser photolysis experiments coupled with ab initio quantum mechanical calculations lead to a BDE of 321.7 ± 2.9 $kJ \cdot mol^{-1}$. While this value is (excluding error bars) some 9 $kJ \cdot mol^{-1}$ higher than our TR-PAC result, 312.8 ± 6.1 $kJ \cdot mol^{-1}$, it is close to data obtained with extrapolated CCSD(T), 326.3, and in keeping with our considerations about the validity of our experimental data for this compound.

JOC*Article*

Energetics of the Allyl Group

Filipe Agapito,[†,‡] Paulo M. Nunes,[†] Benedito J. Costa Cabral,[†,‡] Rui M. Borges dos Santos,[§] and José A. Martinho Simões*[,†]

Departamento de Química e Bioquímica, Faculdade de Ciências, Universidade de Lisboa, 1749-016 Lisboa, Portugal, Grupo de Física Matemática da Universidade de Lisboa, Av. Professor Gama Pinto 2, 1649-003 Lisboa, Portugal, and Institute for Biotechnology and Bioengineering, Centro de Biomedicina Molecular e Estrutural, Universidade do Algarve, Campus de Gambelas, 8005-139 Faro, Portugal

jams@fc.ul.pt

Received June 27, 2007

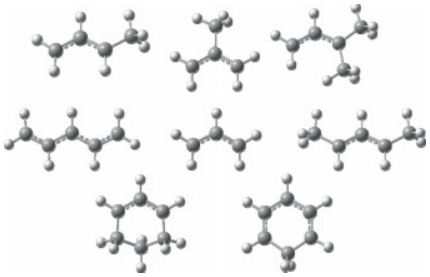

Aiming to improve our understanding of the stability of radicals containing the allylic moiety, carbon−hydrogen bond dissociation enthalpies (BDEs) in propene, isobutene, 1-butene, (*E*)-2-butene, 3-metylbut-1-ene, (*E*)-2-pentene, (*E*)-1,3-pentadiene, 1,4-pentadiene, cyclohexene, 1,3-cyclohexadiene, and 1,4-cyclohexadiene have been determined by quantum chemistry calculations. The BDEs in cyclohexene, 1,3-cyclohexadiene, and 1,4-cyclohexadiene have also been obtained by time-resolved photoacoustic calorimetry. The theoretical study involved a DFT method as well as ab initio complete basis-set approaches, including the composite CBS-Q and CBS-QB3 procedures, and basis-set extrapolated coupled-cluster calculations (CCSD(T)). By taking the $C(sp^3)-H$ BDE in propene as a reference, we have concluded that one methyl group bonded to C3 in propene (i.e., 1-butene) leads to a decrease of 12 kJ mol^{-1} and that a second methyl group bonded to C3 (3-methylbut-1-ene) further decreases the BDE by 8 kJ mol^{-1}. When the methyl group is bonded to C2 in propene (isobutene), an increase of 7 kJ mol^{-1} is observed. Finally, a methyl group bonded to C1 in propene (2-butene) has essentially no effect (−1 kJ mol^{-1}). While this trend can be rationalized in terms of stabilization of the corresponding radical (through hyperconjugation and π-delocalization), the BDE values observed for the dienes can only be understood by considering the thermodynamic stabilities of the parent compounds.

Introduction

Bond dissociation enthalpies (BDEs) are fundamental to discuss molecular structure−reactivity relationships. For instance, it has been shown that the antioxidant properties of terpinolene (**1**), α-terpinene (**2**), and γ-terpinene (**3**) are comparable to those of α-tocoferol,[1] without the pro-oxidant effects of this latter compound at higher concentrations.[2] The initial step of the proposed terpene peroxidation mechanism involves hydrogen abstraction by a hydroperoxyl radical.[2] The efficiency of this step will increase with the exothermicity of the abstraction, which in turn corresponds to a decrease of the C−H BDE in the terpene. Therefore, the knowledge of the C−H BDEs in terpenes and other structurally related compounds is of great interest to understand which structural factors influence the antioxidant properties of these compounds.

* Address correspondence to this author. Phone: 351−217500005, Fax: 351−217500088.
† Faculdade de Ciências, Universidade de Lisboa.
‡ Grupo de Física Matemática da Universidade de Lisboa.
§ Universidade do Algarve.

(1) Ruberto, G.; Baratta, M. T. *Food Chem.* **2000**, *69*, 167−174.

(2) Foti, M. C.; Ingold, K. U. *J. Agric. Food Chem.* **2003**, *51*, 2758−2765.

10.1021/jo701397r CCC: $37.00
Published on Web 10/09/2007

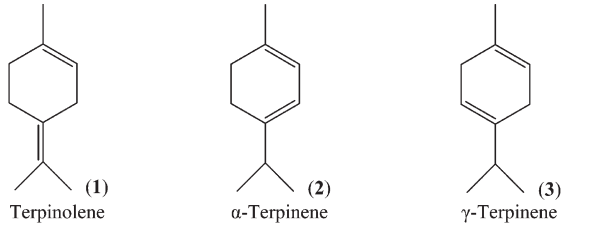

(1) Terpinolene (4-isopropylidene-1-methylcyclohexene)

(2) α-Terpinene (1-isopropyl-4-methyl-1,3-cyclohexadiene)

(3) γ-Terpinene (1-isopropyl-4-methyl-1,4-cyclohexadiene)

The C−H BDE in an organic molecule RH, $DH°$(C−H), is closely related to the thermodynamic stability of the corresponding carbon-centered radical R$^•$, as measured by its standard enthalpy of formation $\Delta_fH°$(R$^•$,g). The relation is illustrated by eq 1, the definition of BDE, which corresponds to the enthalpy of reaction 2. Note that all the molecules are in the ideal gas phase (isolated).

$$DH°(\text{C}-\text{H}) = \Delta_fH°(\text{R}^•,\text{g}) + \Delta_fH°(\text{H}^•,\text{g}) - \Delta_fH°(\text{RH},\text{g}) \quad (1)$$

$$\text{RH (g)} \rightarrow \text{R}^• \text{ (g)} + \text{H}^• \text{ (g)} \quad (2)$$

The stability of a large number of long-lived organic molecules is well established.[3,4] This standard enthalpy of formation database has been very important for the assessment of quantum chemistry methods[5] and has fostered the development of reliable empirical schemes to predict new values.[5−7] The present knowledge on the stability of organic free radicals (as measured by their standard enthalpies of formation or by the corresponding C−H BDEs in their parent molecules, eq 1) is far less satisfactory than that for stable molecules. This is due to the fact that traditional experimental techniques, such as combustion calorimetry, are not suitable to probe the thermochemistry of species whose lifetime is less than ca. 1 μs. Most of the "best" BDEs known for organic compounds have been obtained in the gas phase from kinetics studies, ion cycles, and photoionization mass spectrometry.[8,9] Although these methods may afford chemically accurate results (i.e., with an error smaller than ca. 4 kJ mol^{-1}) this accuracy has only been achieved for a relatively small number of compounds.[8,10] On the other hand, there are abundant examples of large disagreements in literature data for BDEs in many basic compounds.[9,11] For instance, the literature values of α-C−H BDEs in 1,4-cyclohexadiene and in 3-methyl-1-butene span almost 30 kJ mol^{-1}. These uncertainties hinder our understanding of structural effects on C−H BDEs and therefore affect our ability to predict new data.

In this work we report our determinations of C−H BDEs for a series of hydrocarbons containing structural features of terpene molecules. We started our study with the terpenes body, cyclohexene, 1,3-cyclohexadiene, and 1,4-cyclohexadiene, using time-resolved photoacoustic calorimetry (TR-PAC)[12] and quantum chemistry methods. PAC (and hence TR-PAC) is a very reliable method to determine BDEs.[13] However, unlike the experimental methods referred to above, it is a solution technique (i.e., all the species in reaction 2 are in solution), affording solution-phase BDEs. To derive the gas-phase BDEs, one needs to consider the solvation enthalpies of all the species in reaction 2. For some types of radicals (e.g., oxygen-centered radicals), these data are still a matter of some debate.[14,15] In the case of carbon-centered radicals, there is evidence that the solvation enthalpies of R$^•$ and RH are identical and therefore the solution- and gas-phase BDEs differ only by the solvation enthalpy of the hydrogen atom.[16] An additional advantage of TR-PAC is that it allows discrimination between competitive reactions, provided that these occur at different rates.

The TR-PAC experimental results were then complemented by quantum chemistry calculations, aiming to understand the effects of the carbon−carbon double bonds and alkyl groups on the C−H BDE. The computational study included the following molecules: propene, isobutene, 1- and (*E*)-2-butene, 3-methylbut-1-ene, (*E*)-2-pentene, (*E*)-1,3- and 1,4-pentadiene, and 1,3- and 1,4-cyclohexadiene. As remarked above, we have found that the accuracy of the literature data for such simple molecules was not sufficient to draw useful conclusions about structural effects on C−H BDEs. On the other hand, a quantitative discussion of the stabilization of the corresponding radical requires only *relative* BDEs. Computational chemistry is a particularly suitable source of these relative data. Their accuracy can in some cases be assessed by using thermochemical cycles that involve well-established enthalpies of formation of parent molecules (RH in reaction 2).

Experimental Section

Materials. Benzene (HPLC grade, 99.9+%) was used without further purification. Cyclohexene (initial purity 99%) was chromatographed in a column of activated alumina grade I under nitrogen and stored in a refrigerator under inert atmosphere. 1,3-Cyclohexadiene (initial purity 97%) was dried over $CaCl_2$, distilled from $NaBH_4$ under nitrogen, stored under inert atmosphere, and refrigerated. 1,4-Cyclohexadiene (initial purity 97%) was dried over $CaCl_2$, distilled under nitrogen, stored in an inert atmosphere, and refrigerated. All three substrates were passed through a column of activated alumina under nitrogen prior to use. Di-*tert*-butyl peroxide was purified according to a literature procedure.[17] *o*-Hydroxybenzophenone was recrystallized twice from an ethanol−water mixture.

(3) Linstrom, P. J.; Mallard, W. G. *NIST Chemistry WebBook*; NIST Standard Reference Database No. 69 (http://webbook.nist.gov); National Institute of Standards and Technology: Gaithersburg, MD, 2005.

(4) Pedley, J. B. *Thermochemical Data and Structures of Organic Compounds*; Thermodynamics Research Center: College Station, TX, 1994; Vol. I.

(5) Irikura, K. K.; Frurip, D. J., Eds. *Computational Thermochemistry. Prediction and Estimation of Molecular Thermodynamics*; ACS Symp. Ser. No. 677: Washington, DC, 1998.

(6) Cox, J. D.; Pilcher, G. *Thermochemistry of Organic and Organometallic Compounds*; Academic Press: New York, 1970.

(7) Benson, S. W. *Thermochemical Kinetics*, 2nd ed.; Wiley: New York, 1976.

(8) Blanksby, S. J.; Ellison, G. B. *Acc. Chem. Res.* **2003**, *36*, 255−263.

(9) Luo, Y.-R. *Handbook of Bond Dissociation Energies in Organic Compounds*; CRC Press: Boca Raton, FL, 2003.

(10) Ruscic, B.; Boggs, J. E.; Burcat, A.; Csaszar, A. G.; Demaison, J.; Janoschek, R.; Martin, J. M. L.; Morton, M. L.; Rossi, M. J.; Stanton, J. F.; Szalay, P. G.; Westmoreland, P. R.; Zabel, F.; Berces, T. *J. Phys. Chem. Ref. Data* **2005**, *34*, 573−656.

(11) McMillen, D. F.; Golden, D. M. *Annu. Rev. Phys. Chem.* **1982**, *33*, 493−532.

(12) Peters, K. S. *Angew. Chem., Int. Ed. Engl.* **1994**, *33*, 294−302.

(13) Laarhoven, L. J. J.; Mulder, P.; Wayner, D. D. M. *Acc. Chem. Res.* **1999**, *32*, 342−349.

(14) Wayner, D. D. M.; Lusztyk, E.; Pagé, D.; Ingold, K. U.; Mulder, P.; Laarhoven, L. J. J.; Aldrich, H. S. *J. Am. Chem. Soc.* **1995**, *117*, 8737−8744.

(15) Guedes, R. C.; Coutinho, K.; Cabral, B. J. C.; Canuto, S.; Correia, C. F.; Borges dos Santos, R. M.; Martinho Simões, J. A. *J. Phys. Chem. A* **2003**, *107*, 9197−9207.

(16) Muralha, V. S.; Borges dos Santos, R. M.; Martinho Simões, J. A. *J. Phys. Chem. A* **2004**, *108*, 936−942.

(17) Diogo, H. P.; Minas da Piedade, M. E.; Martinho Simões, J. A.; Nagano, Y. *J. Chem. Thermodyn.* **1995**, *27*, 597−604.

Photoacoustic Calorimetry. The basis of photoacoustic calorimetry,[12,18] our photoacoustic calorimeter setup,[19,20] and the experimental technique are described in detail elsewhere.[21,22] Briefly, argon-purged solutions in benzene of ca. 0.4 M di-*tert*-butyl peroxide and an adequate concentration (see Analysis of Thermochemical Data) of each organic molecule studied (cyclohexene, 1,3-cyclohexadiene, and 1,4-cyclohexadiene) were flowed through a quartz flow cell and photolyzed with pulses from a nitrogen laser (337.1 nm, pulse width 800 ps). To check for multiphoton effects, the incident laser energy was varied by using neutral density filters (ca. 5−30 μJ/pulse at the cell, flux <40 J m^{-2}). Each pulse produced photolysis of di-*tert*-butyl peroxide (*t*-BuOOBu-*t*), generating *tert*-butoxyl radicals (reaction 3), which in turn abstracted an allylic hydrogen from the organic molecule RH, reaction 4.

$$t\text{-BuOOBu-}t\ (\text{sln}) \xrightarrow{h\nu} 2\ t\text{-BuO}^{\bullet}\ (\text{sln}) \qquad (3)$$

$$2\text{RH}\ (\text{sln}) + 2\ t\text{-BuO}^{\bullet}\ (\text{sln}) \rightarrow 2\text{R}^{\bullet}\ (\text{sln}) + 2\ t\text{-BuOH}\ (\text{sln}) \qquad (4)$$

Each laser pulse induced a sudden volume change in solution, which generated an acoustic wave, detected by a piezoelectric transducer (0.5 MHz) in contact with the bottom of the cell. The signals were amplified and measured by a digital oscilloscope. The signal-to-noise ratio was improved by averaging 32 acquisitions for each data point obtained at a given laser energy. The apparatus was calibrated by carrying out a photoacoustic run with an optically matched solution of *o*-hydroxybenzophenone (in the same mixtures but without the peroxide), which dissipates all of the absorbed energy as heat.[18] For each run (experiment or calibration), four data points were collected corresponding to four different laser intensities obtained with the neutral density filters. The resulting waveforms from each data point were recorded for subsequent mathematical analysis, affording two waveforms for each point: sample and calibration. The analysis involved, for each laser energy, first the normalization of both waveforms and then their deconvolution, using the software Sound Analysis.[23] This analysis first allowed the confirmation of the reaction scheme indicated above (reactions 3 and 4) and then afforded the observed fraction of photon energy released as heat, $\phi_{\text{obs,i}}$, for each process, and the lifetime of the second, τ_2. An estimate of the rate constant can be obtained from this lifetime.[24] The enthalpy of the hydrogen abstraction reaction was derived from eq 5,

$$\Delta_r H_2 = \frac{-\Delta_{\text{obs}} H_2}{\Phi_r} \qquad (5)$$

where $\Delta_{\text{obs}}H_2$ corresponds to the observed enthalpy change and is calculated by multiplying $E_m = N_A h\nu$ (the molar photon energy) by $\phi_{\text{obs,2}}$ (the observed heat fraction associated with reaction 2). Φ_r is the reaction quantum yield for the photolysis of di-*tert*-butyl peroxide. All experiments were performed at 293 ± 0.5 K.

Theoretical Calculations. The structures of propene, isobutene, 1- and (*E*)-2-butene, 3-methylbut-1-ene, (*E*)-2-pentene, (*E*)-1,3- and 1,4-pentadiene, cyclohexene, and 1,3- and 1,4-cyclohexadiene, as well as the respective radicals resulting from homolysis of an α-C−H bond, were determined by using density functional theory (DFT).[25] In this approach the energy of a system, $E[\rho]$, is given by eq 6, where V_{NN} is the nucleus−nucleus repulsion energy, H^{core} is the one-electron kinetic and electron-nuclei potential energy contribution to the total energy, and V_{ee} is the Coulombic electron−electron repulsion energy.

$$E[\rho] = V_{NN} + H^{\text{core}} + V_{ee} + E_x[\rho] + E_c[\rho] \qquad (6)$$

The terms $E_x[\rho]$ and $E_c[\rho]$ are respectively the exchange and correlation functionals of the electronic density, ρ. The optimized geometry for a molecule is found by determining the set of nuclear coordinates that minimizes the energy given by eq 6. In this work the geometry optimizations were carried out with Becke's three-parameter hybrid method[26] with the correlation functional of Lee, Yang, and Parr (B3LYP).[27] The accuracy of the energy also depends on the completeness of the basis set in which the molecular orbitals are expanded. For these geometry optimizations Dunning's triple-ζ correlation consistent basis set (cc-pVTZ) was used.[28] Vibrational analysis was performed for all optimized geometries to ensure that they represented minima of the energy surfaces. The choice of B3LYP/cc-pVTZ geometries for the structural analysis was dictated by its cost-effectiveness and the fact that several works indicate that the molecular geometries thus obtained are in good agreement with experimental data.[29−31] Nevertheless, it is well-known that DFT methods systematically underestimate bond dissociation enthalpies.[32,33] Therefore, in addition to B3LYP, BDEs were also computed by using two composite theoretical procedures, namely CBS-Q and CBS-QB3.[34−36] These were specifically devised to allow an accurate determination of thermochemical properties for large systems, by resorting to extrapolation to the complete basis set limit. We note, however, that the geometry optimizations of CBS-Q and CBS-QB3 are performed respectively with MP2(FC)/6-31G† (frozen-core Møller−Plesset second-order perturbation theory,[37] in which the electrons from inner shells are excluded from the calculation of the correlation energy) and B3LYP/6-31G†, and therefore are slightly less accurate than B3LYP/cc-pVTZ geometries.[29,31]

Complete basis set extrapolated coupled cluster calculations with single and double excitations and perturbative inclusion of triple excitations (CCSD(T)),[38] using B3LYP/cc-pVTZ geometries, are also reported. Extrapolation of CCSD(T) energies to complete basis set was carried out through a dual (2=cc-pVDZ,3=cc-pVTZ) scheme proposed by Truhlar for both the Hartree−Fock and correlation energies.[39] This procedure has proven to be very reliable for the determination of BDEs,[40,41] although computationally more demanding than any of the aforementioned methods.

(18) Braslavsky, S. E.; Heibel, G. E. *Chem. Rev.* **1992**, *92*, 1381−1410.
(19) Borges dos Santos, R. M.; Lagoa, A. L. C.; Martinho Simões, J. A. *J. Chem. Thermodyn.* **1999**, *31*, 1483−1510.
(20) Nunes, P. M.; Correia, C. F.; Dos Santos, R. M. B.; Simoes, J. A. M. *Int. J. Chem. Kinet.* **2006**, *38*, 357−363.
(21) Correia, C. F.; Nunes, P. M.; Borges, dos Santos, R. M.; Martinho Simões, J. A. *Thermochim. Acta* **2004**, *420*, 3−11.
(22) Nunes, P. M.; Agapito, F.; Costa Cabral, B. J.; Borges dos Santos, R. M.; Martinho Simões, J. A. *J. Phys. Chem. A* **2006**, *110*, 5130−5134.
(23) *Sound Analysis*, version 1.50D; Quantum Northwest: Spokane, WA, 1999.
(24) Nunes, P. M.; Correia, C. F.; Borges dos Santos, R. M.; Martinho Simões, J. A. *Int. J. Chem. Kinet.* **2006**, *38*, 357−363.
(25) Zhou, Z.; Parr, R. G. *J. Am. Chem. Soc.* **1989**, *111*, 7371−7379.
(26) Becke, A. D. *J. Chem. Phys.* **1993**, *98*, 5648.
(27) Lucas, C. R.; Gabe, E. J.; Lee, F. L. *Can. J. Chem.* **1988**, *66*, 429−434.
(28) Dunning, T. H., Jr. *J. Chem. Phys.* **1989**, *90*, 1007.
(29) Byrd, E. F. C.; Sherrill, C. D.; Head-Gordon, M. *J. Phys. Chem. A* **2001**, *105*, 9736−9747.
(30) Agapito, F.; Cabral, B. J. C.; Martinho Simões, J. A. *THEOCHEM* **2005**, *719*, 109−114.
(31) Wang, J. T.; Feng, Y.; Liu, L.; Li, X.-S.; Guo, Q.-X. *Chin. J. Chem.* **2004**, *22*, 642−648.
(32) Cabral do Couto, P.; Guedes, R. C.; Cabral, B. J. C.; Martinho Simões, J. A. *Int. J. Quantum Chem.* **2002**, *86*, 297−304.
(33) Kern, R. D.; Zhang, Q.; Yao, J.; Jursic, R. S.; Tranter, R. S.; Greybill, M. A.; Kiefer, J. H. *Proc. Combust. Inst.* **1998**, *102*, 143−150.
(34) Ochterski, J. W.; Petersson, G. A.; Montgomery, J. A. *J. Chem. Phys.* **1996**, *104*, 2598−2619.
(35) Montgomery, J. A.; Frisch, M. J.; Ochterski, J. W.; Petersson, G. A. *J. Chem. Phys.* **1999**, *110*, 2822−2827.
(36) Montgomery, J. A.; Frisch, M. J.; Ochterski, J. W.; Petersson, G. A. *J. Chem. Phys.* **2000**, *112*, 6532−6542.
(37) Møller, C.; Plesset, M. S. *Phys. Rev.* **1934**, *46*, 618.
(38) Raghavachari, K.; Trucks, G. W.; Pople, J. A.; Headgordon, M. *Chem. Phys. Lett.* **1989**, *157*, 479−483.
(39) Truhlar, D. G. *Chem. Phys. Lett.* **1998**, *294*, 45−48.

TABLE 1. C−H Bond Dissociation Enthalpies (in kJ mol^{-1}) from the Literature and Determined by Using Theoretical Methods, at 298.15 K

molecule	radical	lit.[a]	CBS-Q[b]	CBS-QB3[b]	B3LYP[b,c]	CCSD(T)[d]
propene	allyl	371.5 ± 1.7[e]	361.3[f]	364.9[f]	352.2	371.5[f]
isobutene	2-methylallyl	360.7 ± 4.2; 372.8	366.9 [377.1]	371.3 [377.9]	359.2 [378.6]	378.2
1-butene	1-methylallyl	341.0 ± 6.3; 350.6	347.8 [358.1]	351.9 [358.5]	334.9 [354.2]	359.6
(*E*)-2-butene	1-methylallyl		360.4 [370.7]	363.1 [369.7]	349.4 [368.7]	370.8
3-methylbut-1-ene	3-methyl-1-buten-3-yl	322.1 ± 6.3;[g] 347.7	340.1 [350.3]	343.8 [350.4]	322.8 [342.1]	351.7
(*E*)-2-pentene	2-penten-4-yl		344.9 [355.2]	351.7 [358.3]	334.0 [353.3]	360.0
(*E*)-1,3-pentadiene	pentadienyl	333.5 ± 4.2; 347.3 ± 12.6	333.5 [343.7]	338.3 [344.9]	326.9 [346.2]	352.5
1,4-pentadiene	pentadienyl	319.7; 332.6 ± 7.1	301.9 [312.1]	310.5 [317.2]	291.9 [311.2]	325.0
cyclohexene	cyclohexen-3-yl	343 ± 10[h]	347.2 [357.5]	349.5 [356.1]	333.8 [353.2]	357.9
1,3-cyclohexadiene	cyclohexadienyl		305.8 [316.1]	311.3 [317.9]	296.4 [315.7]	325.3
1,4-cyclohexadiene	cyclohexadienyl	292.9; 322.2	307.8 [318.0]	311.0 [317.6]	297.0 [316.4]	326.3

[a] Interval of available experimental values quoted from ref 9 (see text), unless noted otherwise. The TR-PAC values determined in the present work are given in the text. [b] Results from the direct homolysis (reaction 2) and from the isodesmic and isogyric reaction (reaction 9 with R′ = allyl and using the experimental C(sp^3)−H BDE in propene, 371.5 kJ mol^{-1}). The later values are bracketed. [c] Calculations performed with Dunning's cc-pVTZ basis set. [d] Complete basis set extrapolated results based on the dual (2,3) scheme proposed by Truhlar (see text). In this case there is no need to derive the BDEs from reaction 9 since the computed C(sp^3)−H BDE in propene matches the experimental result. [e] Selected experimental value, from ref 8. [f] From ref 41. [g] From ref 48. [h] The uncertainty was estimated.

The ground state enthalpies of each parent molecule and radical were calculated from eq 7,

$$H = U + k_BT = E_{elec} + E_{thermal} + k_BT \quad (7)$$

where U is the internal energy, E_{elec} is the computed electronic energy, $E_{thermal}$ is the thermal correction to the internal energy at T = 298.15 K (which is calculated from the partition function for each species and includes the zero-point energy correction), and k_B is the Boltzmann constant. For a C−H bond homolysis reaction (eq 2) the reaction enthalpy $\Delta_rH°$, identified with the R−H bond dissociation enthalpy, was computed from eq 8.

$$\Delta_rH° = H(R^\bullet) + H(H^\bullet) - H(RH) \quad (8)$$

The B3LYP/cc-pVTZ calculations were also used to determine the Mulliken atomic spin densities[42−45] for the radical species under study. It is well-known that this population analysis can prove to be unreliable and is, by definition, basis set-dependent. Nonetheless, B3LYP/6-311G** Mulliken spin densities have been successfully used in the study of heterosubstituded allyl radicals.[46] Another factor that led to the choice of this population analysis is the fact that, due to its formal simplicity, it is widely used.

All calculations were carried out with the Gaussian-03 program.[47]

(40) Cabral, B. J. C.; Canuto, S. *Chem. Phys. Lett.* **2005**, *406*, 300−305.
(41) Nunes, P. M.; Agapito, F.; Cabral, B. J. C.; dos Santos, R. M. B.; Simoes, J. A. M. *J. Phys. Chem. A* **2006**, *110*, 5130−5134.
(42) Mulliken, R. S. *J. Chem. Phys.* **1955**, *23*, 2338−2342.
(43) Mulliken, R. S. *J. Chem. Phys.* **1955**, *23*, 2343−2346.
(44) Mulliken, R. S. *J. Chem. Phys.* **1955**, *23*, 1833−1840.
(45) Mulliken, R. S. *J. Chem. Phys.* **1955**, *23*, 1841−1846.
(46) Wiberg, K. B.; Cheeseman, J. R.; Ochterski, J. W.; Frisch, M. J. *J. Am. Chem. Soc.* **1995**, *117*, 6535−6543.
(47) Frisch, M. J.; Trucks, G. W.; Schlegel, H. B.; Scuseria, G. E.; Robb, M. A.; Cheeseman, J. R.; Montgomery, J. A., Jr.; Vreven, T.; Kudin, K. N.; Burant, J. C.; Millam, J. M.; Iyengar, S. S.; Tomasi, J.; Barone, V.; Mennucci, B.; Cossi, M.; Scalmani, G.; Rega, N.; Petersson, G. A.; Nakatsuji, H.; Hada, M.; Ehara, M.; Toyota, K.; Fukuda, R.; Hasegawa, J.; Ishida, M.; Nakajima, T.; Honda, Y.; Kitao, O.; Nakai, H.; Klene, M.; Li, X.; Knox, J. E.; Hratchian, H. P.; Cross, J. B.; Bakken, V.; Adamo, C.; Jaramillo, J.; Gomperts, R.; Stratmann, R. E.; Yazyev, O.; Austin, A. J.; Cammi, R.; Pomelli, C.; Ochterski, J. W.; Ayala, P. Y.; Morokuma, K.; Voth, G. A.; Salvador, P.; Dannenberg, J. J.; Zakrzewski, V. G.; Dapprich, S.; Daniels, A. D.; Strain, M. C.; Farkas, O.; Malick, D. K.; Rabuck, A. D.; Raghavachari, K.; Foresman, J. B.; Ortiz, J. V.; Cui, Q.; Baboul, A. G.; Clifford, S.; Cioslowski, J.; Stefanov, B. B.; Liu, G.; Liashenko, A.; Piskorz, P.; Komaromi, I.; Martin, R. L.; Fox, D. J.; Keith, T.; Al-Laham, M. A.; Peng, C. Y.; Nanayakkara, A.; Challacombe, M.; Gill, P. M. W.; Johnson, B.; Chen, W.; Wong, M. W.; Gonzalez, C.; Pople, J. A. *Gaussian-03*; Gaussian, Inc.: Wallingford, CT, 2004.

Analysis of Thermochemical Data

We have not attempted to make a comprehensive critical analysis of carbon−hydrogen bond dissociation enthalpies for the molecules investigated in the present study. Instead we have relied mainly on the compilation by Luo,[9] although we have examined in some detail the data collected by this author. This option is enough to provide a clear picture of the available experimental BDE data and to assess their quality.

Table 1 collects literature C−H BDEs for the molecules studied (displayed in Figure 1) and summarizes the values obtained in this work by theoretical methods. Relative BDEs, which provide a clearer picture of BDE trends and are particularly important in discussing the computational data, are presented in Table 2.

Accuracy of Computational Results. As noted in the case of the allyl radical (Table 1), the α-C−H BDEs calculated from eq 8, which relies on reaction 2, are usually low limits of the true values. This problem can be avoided by using isodesmic and isogyric reactions such as

$$RH + R'^\bullet \rightarrow R^\bullet + R'H \quad (9)$$

In these reactions the number and type of chemical bonds, the number of carbon atoms in a given state of hybridization, and the number of electron pairs are equal on both sides of the reaction, and therefore advantage is taken from error cancellation.[5] It is also important to ensure that the number of hydrogen atoms bonded to each carbon atom in a given state of hybridization is conserved.[22] If these criteria are met, the differences $DH°$(R−H) − $DH°$(R′−H), which are equal to the enthalpy of reaction 9, are largely method-independent and usually more accurate than the BDEs obtained from eq 8. Moreover, these differences can then be used to derive absolute BDE values by using a highly reliable value for the anchor, $DH°$(R′−H).

The bracketed values in Table 1 were obtained from reaction 9 with R′ = allyl and using the experimental C(sp^3)−H BDE for propene, 371.5 kJ mol^{-1}. In the case of the 2-methylallyl radical, it is noted that while the BDEs computed from reaction 2 range from 359 to 371 kJ mol^{-1}, the results from reaction 9 agree within 2 kJ mol^{-1}. A similar pattern is observed for the remaining theoretical results in Table 1: the BDEs derived from reaction 9 are much less dependent on the theoretical method than those obtained from the direct homolysis. Analysis of the

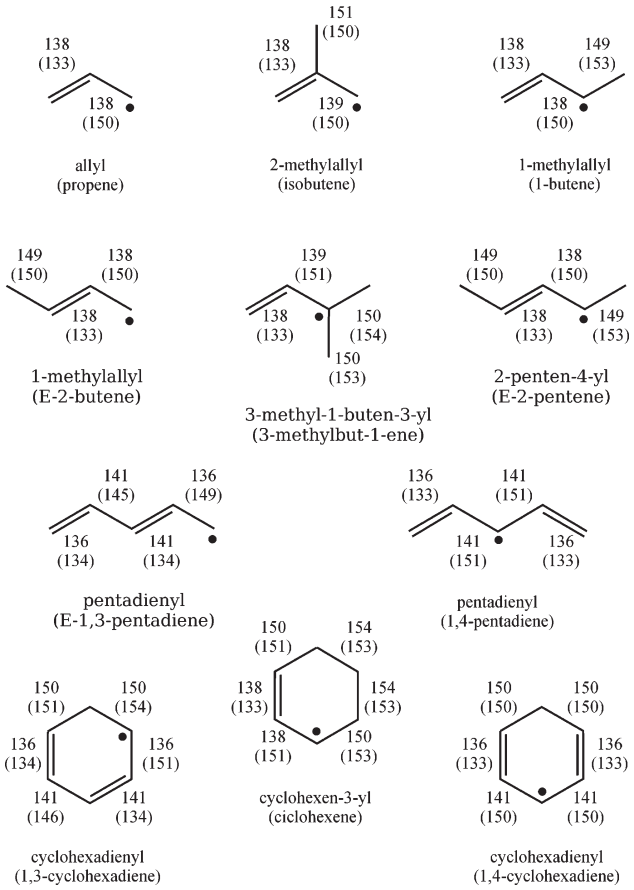

FIGURE 1. Bond lengths (pm) for the radicals and their parent molecules (in parentheses), calculated with B3LYP/cc-pVTZ.

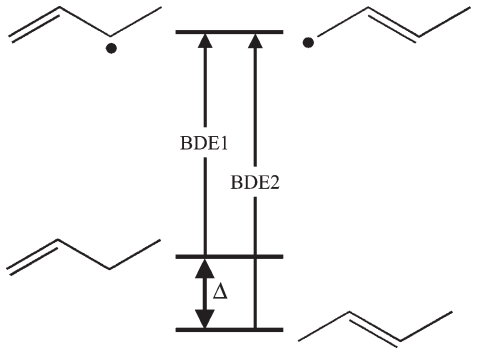

FIGURE 2. Thermochemical cycle relating the C−H bond dissociation enthalpies of 1- and (*E*)-2-butene with their gas-phase standard enthalpies of formation.

DFT and CBS data in Table 1 reveals that the discrepancies between the BDEs obtained from reactions 2 and 9 are smaller for CBS-QB3, which is a strong indication that this is the most accurate of those methods for the systems under study, closely followed by CBS-Q. It is also noted that, apart from CCSD(T) calculations, CBS-QB3 is the one that yields the best value for the C(sp^3)−H BDE in propene.

The CBS-QB3 bracketed values and the data derived from CCSD(T) calculations are in excellent agreement, with the exception of the BDEs for (*E*)-1,3- and 1,4-pentadiene, and 1,3- and 1,4-cyclohexadiene (Table 1). However, even in these cases the discrepancy is smaller than 8 kJ mol^{-1}. In the following discussion we will use the results from these two methods.

(a) Allyl. The enthalpy of formation of the allyl radical seems well established as 173.5 ± 1.8 kJ mol^{-1}, which corresponds to 371.5 ± 1.7 kJ mol^{-1} for the C(sp^3)−H BDE in propene.[8] The CBS-Q and CBS-QB3 results derived from the direct homolysis of the same C−H bond are 361.3 and 364.9 kJ mol^{-1}, respectively. The B3LYP result is even lower, 352.2 kJ mol^{-1}. A CCSD(T) calculation (371.5 kJ mol^{-1}) is in excellent agreement with experiment.[41]

(b) 2-Methylallyl. There are three experimental results for the C(sp^3)−H BDE in isobutene quoted in Luo's compilation,[9] viz. 361 ± 4,[49] 363 ± 3,[50] and 373 kJ mol^{-1}.[51] The first was derived from a pyrolysis study of 2-methyl-1-butene and was in close agreement with the result from a previous shock tube study.[52] Yet, the latter value was recently re-evaluated by its author as 373 kJ mol^{-1}.[51] The second result quoted above (363 ± 3 kJ mol^{-1}) was obtained from a gas-phase kinetic study,[50] which also reported the enthalpy of formation of the allyl radical as 167 ± 3 kJ mol^{-1}, i.e., some 7 kJ mol^{-1} lower than the presently accepted value (see above). This suggests that the best experimental value must be the one recommended by Tsang, 373 kJ mol^{-1}, rather than the one selected by Luo (363 kJ mol^{-1}).[9] Indeed, Tsang's value is closer to the bracketed data in Table 1 and to the result derived from CCSD(T), 378.2 kJ mol^{-1}.

(c) 1-Methylallyl. There are several experimental values for the α-C−H BDE in 1-butene quoted in Luo's compillation,[9] ranging from 341 ± 6 to 351 kJ mol^{-1}. The CBS-QB3 result is 358.5 kJ mol^{-1} (Table 1), in excellent agreement with the one obtained from CCSD(T) (359.6 kJ mol^{-1}), suggesting that the experimental values are low limits.

The C(sp^3)−H BDE in (*E*)-2-butene also leads to the enthalpy of formation of the 1-methylallyl radical. Unfortunately, no experimental values are available. The BDEs derived from CBS-QB3 and CCSD(T) are 369.7 and 370.8 kJ mol^{-1}, respectively (Table 1).

It is very important to note that the computed BDEs for 1- and (*E*)-2-butene are thermodynamically consistent. This can be demonstrated by taking the enthalpies of formation of the respective parent molecules, as shown in Figure 2. The quantity Δ can be calculated as 11.2 kJ mol^{-1} (CBS-QB3 and CCSD(T)) from the difference BDE2 − BDE1. This is in remarkable agreement with 11.3 kJ mol^{-1}, the result obtained from the difference between the experimental enthalpies of formation of 1-butene (−0.1 ± 0.9 kJ mol^{-1}) and (*E*)-2-butene (−11.4 ± 1.0 kJ mol^{-1}).[4]

(d) 3-Methyl-1-buten-3-yl. The available experimental values for the α-C−H BDE in 3-methylbut-1-ene range from 322 to 348 kJ mol^{-1}.[9,48,53,54] The CBS-QB3 and CCSD(T) results are

(48) Trenwith, A. B. *Trans. Faraday Soc.* **1970**, *66*, 2805−2811.
(49) Trenwith, A. B.; Wrigley, S. P. *J. Chem. Soc., Faraday Trans. I* **1977**, *73*, 817−822.
(50) Roth, W. R.; Bauer, F.; Beitat, A.; Ebbrecht, T.; Wüstefeld, M. *Chem. Ber.* **1991**, *124*, 1453−1460.
(51) Tsang, W. In *Shock Waves in Chemistry*; Lifshitz, A., Ed.; Marcel Dekker: New York, 1981; pp 59−129.
(52) Tsang, W. *Int. J. Chem. Kinet.* **1973**, *5*, 929−946.
(53) Trenwith, A. B. *J. Chem. Soc., Faraday Trans. I* **1982**, *78*, 3131−3136.
(54) Luo incorrectly quotes a lower value of 319.7 kJ mol^{-1}, which in fact corresponds to the C(sp^3)−H BDE in 1,4-pentadiene determined by Trenwith (ref 53). The value for 3-methylbut-1-ene was determined in a previous work by the same author (ref 48).

TABLE 2. Computed α-C−H Bond Dissociation Enthalpies (in kJ mol^{-1}) *Relative* to the C(sp^3)−H BDE in Propene Using the Data Corresponding to the Direct Homolysis Reaction from Table 1

molecule	radical	CBS-Q	CBS-QB3	B3LYP	CCSD(T)
propene	allyl	0.0	0.0	0.0	0.0
isobutene	2-methylallyl	5.6	6.4	7.0	6.7
1-butene	1-methylallyl	−13.5	−13.0	−17.3	−11.9
(*E*)-2-butene	1-methylallyl	−0.9	−1.8	−2.8	−0.7
3-methylbut-1-ene	3-methyl-1-buten-3-yl	−21.2	−21.1	−29.4	−19.8
(*E*)-2-pentene	2-penten-4-yl	−16.3	−13.2	−18.2	−11.5
(*E*)-1,3-pentadiene	pentadienyl	−27.8	−26.6	−25.3	−19.0
1,4-pentadiene	pentadienyl	−59.4	−54.4	−60.3	−46.5
cyclohexene	cyclohexen-3-yl	−14.0	−15.4	−18.4	−13.6
1,3-cyclohexadiene	cyclohexadienyl	−55.5	−53.6	−55.8	−46.2
1,4-cyclohexadiene	cyclohexadienyl	−53.5	−53.9	−55.2	−45.2

350.4 and 351.7 kJ mol^{-1}, respectively (Table 1), i.e., some 18 kJ mol^{-1} higher than the selection by Luo.[9] However, they are close to the value recommended by Brocks et al., 348 kJ mol^{-1}.[55]

(e) 2-Penten-4-yl. The α-C−H BDE in (*E*)-2-pentene, obtained by CBS-QB3, is 358.3 kJ mol^{-1}. To our knowledge there are no experimental values for this BDE.

(f) Pentadienyl. The C(sp^3)−H BDE in (*E*)-1,3-pentadiene ranges from 334 to 347 kJ mol^{-1}.[9] The upper limit, selected by Luo, was recommended in McMillen and Golden's review,[11] and is in good agreement with the CBS-QB3 result, 344.9 kJ mol^{-1}. However, in this case the result derived from CCSD(T) (352.5 kJ mol^{-1}) is some 8 kJ mol^{-1} higher than the CBS-QB3 value (Table 1).

The same radical is also produced by cleaving the C(sp^3)−H bond in 1,4-pentadiene. The corresponding BDE ranges from 320 to 333 kJ mol^{-1}.[9,56] Luo's selection, 321 kJ mol^{-1}, is close to the CBS-QB3 value, 317.2 kJ mol^{-1}. As for the 1,3 isomer, the result derived from CCSD(T) (325.0 kJ mol^{-1}) is 8 kJ mol^{-1} higher than the CBS-QB3 value (Table 1).[57]

As in the case of 1-methylallyl, the thermodynamic consistency of the BDEs for (*E*)-1,3- and 1,4-pentadiene can be assessed by using the experimental enthalpies of formation of the respective parent molecules (Figure 3). The quantity Δ can be calculated as 27.7 (CBS-QB3) or 27.5 kJ mol^{-1} (CCSD(T)) from the difference BDE2 − BDE1. This is in good agreement with the Δ value of 29.6 kJ mol^{-1}computed from the difference between the enthalpies of formation of 1,4-pentadiene (105.7 ± 1.1 kJ mol^{-1}) and (*E*)-1,3-pentadiene (76.1 ± 0.8 kJ mol^{-1}).[4]

(g) Cyclohexen-3-yl. The only experimental result for α-C−H BDE available in the literature and quoted by Luo is 343 kJ mol^{-1}. This value was determined through an electrochemical cycle by Bordwell and co-workers and its uncertainty is no less than 10 kJ mol^{-1}.[58]

TR-PAC experiments in our laboratory led to 349.8 ± 5.6 kJ mol^{-1} for the same BDE. These experiments were performed with cyclohexene concentrations ranging from 0.25 to 0.56 M. From the lifetime obtained for reaction 4, τ_2, we derived 5 × 10^6 M^{-1} s^{-1} for the rate constant of hydrogen abstraction from cyclohexene (k_2), which is in good agreement with a reported laser flash photolysis value, 5.8 × 10^6 M^{-1} s^{-1}.[59]

Both the TR-PAC result and the BDE computed from CBS-QB3 (356.1 kJ mol^{-1}) are higher than the electrochemical value but in keeping with the complete basis set extrapolated CCSD-(T) result, 357.9 kJ mol^{-1}.

(h) Cyclohexadienyl. The literature values for C(sp^3)−H BDE in 1,3-cyclohexadiene vary in a narrow range, viz., 305 to 311 kJ mol^{-1}.[9] However, contrary to the information provided by Luo, none of these is a direct experimental result.

It is noted that the CBS-QB3 result (317.9 kJ mol^{-1}) differs by 7 kJ mol^{-1} from the CCSD(T) result (325.3 kJ mol^{-1}). However, the latter is quite close to our TR-PAC value (329.3 ± 5.5 kJ mol^{-1}). In the photoacoustic experiments we used 1,3-cyclohexadiene concentrations ranging from 0.030 to 0.043 M. The lifetime obtained for reaction 4, τ_2, led to a rate constant for the hydrogen abstraction from 1,3-cyclohexadiene of k_2 = 4 × 10^7 M^{-1} s^{-1}. This value is in agreement with a reported laser flash photolysis result, 4.2 × 10^7 M^{-1} s^{-1}.[60]

The cyclohexadienyl radical can also be obtained from 1,4-cyclohexadiene. The literature values for C(sp^3)−H BDE range from 293 to 322 kJ mol^{-1}.[9,61−63] Luo's selection, 318 ± 5 kJ mol^{-1}, relies on a gas-phase kinetic study by Tsang[64] and is in excellent agreement with the CBS-QB3 result, 317.6 kJ mol^{-1}. A BDE value of 312.8 ± 6.1 kJ mol^{-1} was obtained in our laboratory from TR-PAC experiments, which were carried out with 1,4-cyclohexadiene concentrations ranging from 0.032 to 0.036 M. The lifetime calculated for reaction 4, τ_2, led to k_2 = 5 × 10^7 M^{-1} s^{-1} for the rate constant of hydrogen abstraction from 1,4-cyclohexadiene, in agreement with a reported laser flash photolysis value, 5.4 × 10^7 M^{-1} s^{-1}.[60]

In this case, Truhlar's extrapolation of CCSD(T) energies led to 326.3 kJ mol^{-1}, 13 kJ mol^{-1} higher than the experimental TR-PAC value and some 9 kJ mol^{-1} higher than the CBS-QB3 result.

(55) Brocks, J. J.; Beckhaus, H.-D.; Beckwith, A. L. J.; Rüchardt, C. *J. Org. Chem.* **1998**, *63*, 1935−1943.

(56) Clark, K. B.; Culshaw, P. N.; Griller, D.; Lossing, F. P.; Martinho Simões, J. A.; Walton, J. C. *J. Org. Chem.* **1991**, *56*, 5535−5539.

(57) It should be noted that Luo's selection is based on an early PAC result (ref 56) that depended on wrong assumptions and was latter reappraised by Laarhoven et al. (ref 13) as 343.0 kJ mol^{-1}. Although the older value was similar to those obtained through other techniques (namely from appearance energy measurements reported in the same work), Laarhoven et al. considered that the PAC experiment cannot be used to determine this BDE since it is beset by errors resulting from competing reactions.

(58) Bordwell, F. G.; Cheng, J.-P.; Harrelson, J. A., Jr. *J. Am. Chem. Soc.* **1988**, *110*, 1229−1231.

(59) Encinas, M. V.; Scaiano, J. C. *J. Am. Chem. Soc.* **1981**, *103*, 6393−6397.

(60) Effio, A.; Griller, D.; Ingold, K. U.; Scaiano, J. C.; Sheng, S. J. *J. Am. Chem. Soc.* **1980**, *102*, 6063−6068.

(61) Griller, D.; Wayner, D. D. M. *Pure Appl. Chem.* **1989**, *61*, 717−724.

(62) Ciriano, M. V.; Korth, H. G.; van Scheppingen, W. B.; Mulder, P. *J. Am. Chem. Soc.* **1999**, *121*, 6375−6381.

(63) It should be pointed out that, as in the case of 1,4-pentadiene (see ref 57), the older PAC result (ref 61) quoted by Luo was latter reappraised by Laarhoven et al. (ref 13) and coincides with the most recent PAC value reported in the literature, 322.2 kJ mol^{-1} (ref 62).

(64) Tsang, W. *J. Phys. Chem.* **1986**, *90*, 1152−1155.

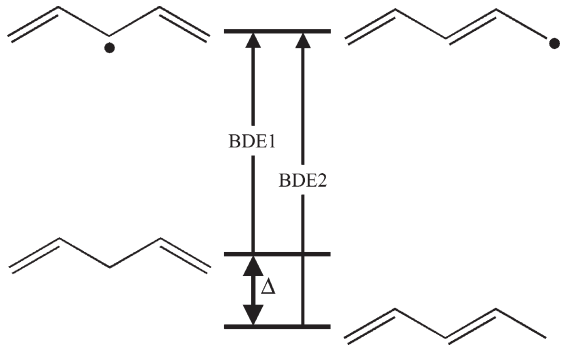

FIGURE 3. Thermochemical cycle relating the C−H bond dissociation enthalpies of (*E*)-1,3- and 1,4-pentadiene with their gas-phase standard enthalpies of formation.

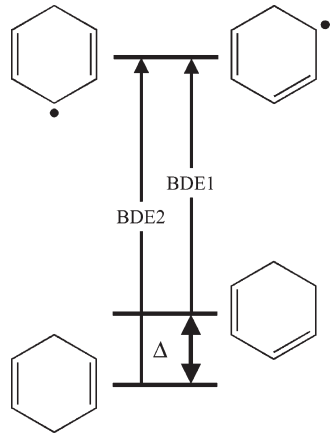

FIGURE 4. Thermochemical cycle relating the C−H bond dissociation enthalpies of 1,3- and 1,4-cyclohexadiene with their gas-phase standard enthalpies of formation.

As discussed for 1-methylallyl and pentadienyl radicals, it is possible to assess the above BDEs through the enthalpies of formation of 1,3- and 1,4-cyclohexadiene (Figure 4). However, this exercise is not as simple as in the previous two cases because there are several discrepant literature values for those enthalpies of formation. Pedley's compillation recommends 106.3 ± 0.9 and 100.4 ± 3.1 kJ mol^{-1} for 1,3- and 1,4-cyclohexadiene, respectively.[4] However, more recent experiments by Steele et al. led to 104.6 ± 0.6 and 104.8 ± 0.6 kJ mol^{-1}.[65] These two pairs of experimental data lead to Δ = 5.9 ± 3.2 and −0.2 ± 0.8 kJ mol^{-1}, respectively. The TR-PAC results lead to Δ = BDE2 − BDE1 = −16.5 ± 4.4 kJ mol^{-1}, whereas the theoretical methods imply Δ = −0.3 (CBS-QB3) and 1.0 kJ mol^{-1} (CCSD(T)).

The enthalpies of formation derived by Steele et al. are probably more accurate than the values listed by Pedley. These values imply that 1,3- and 1,4-cyclohexadiene have similar stabilities, which is consistent with both the results from CBS-QB3 and complete basis set extrapolated CCSD(T). We feel therefore inclined to consider that the TR-PAC value is a lower limit. Nevertheless, a reasonable doubt remains: a simple exercise using the extended Laidler terms tabulated by Leal to predict the enthalpies of formation of the isomers[66] leads to Δ = −16.4 kJ mol^{-1}, matching the TR-PAC result.

(65) Afeefy, H. Y.; Liebman, J. F.; Stein, S. E. In *NIST Chemistry WebBook*; NIST Standard Reference Database No. 69 (http://webbook.nist.gov); Linstrom, P. J., Mallard, W. G., Eds.; National Institute of Standards and Technology: Gaithersburg, MD, 2005.

Hyperconjugation and Resonance Effects

The previous data analysis led to the set of recommended values collected in Table 3. They are all based on the values derived from complete basis set extrapolated CCSD(T) calculations, which in most cases are similar to the CBS-QB3 results. Those values will now be used to discuss the stability of the carbon-centered radicals.

Table 4 displays selected C−H BDEs in methane, ethane, propane, and 2-methylpropane. The BDE trend can be rationalized by using different models. One of these models centers the discussion on the stability of the parent molecules (RH), rather than on the stability of the radicals (R•), and claims that the trend is due to a variation of 1,3-repulsive steric interactions (geminal repulsion).[67] This model is able to predict the trend in Table 4 by using an additive scheme and a set of empirical parameters calculated from the enthalpies of formation of the alkanes. Another way to predict the trend in Table 4 is using the electronegativity concept. For instance, Zavitsas' group demonstrated that, in the absence of steric effects, Pauling's equation relating electronegativity to bond dissociation enthalpies yields accurate BDE values.[68] A third model that is often used to explain the trend in Table 4 is focused on the stability of the alkyl radicals, discussed in terms of hyperconjugation.

Hyperconjugation can be described as the radical stabilization due to the overlap between the single-occupied orbital at the carbon atom where the bond dissociation occurred and a neighbor C−H bond σ-orbital. This effect leads to an increase of the electronic density between the two carbon atoms and therefore to a shorter C−C bond.[30] For instance, in the case of the ethyl radical the C−C bond is 4 pm shorter than the corresponding bond in ethane.[30] In the case of the isopropyl radical, our calculations revealed that both C−C bonds are also 4 pm shorter than the C−C bonds in propane, indicating that the radical is stabilized by "double" hyperconjugation.

To discuss the BDE trend in Table 3, we begin by noting that the resonance stabilization of the allyl radical is evaluated as 68 kJ mol^{-1} by comparing the C(sp^3)−H BDE in propene, 371.5 kJ mol^{-1}, with the C−H BDE in methane (Table 4).[69] This resonance effect is reflected by a decrease of the spin density in the carbon atom where the bond dissociation occurred (see below).

The BDE in the allyl radical has been used as the reference for all the remaining BDEs included in Table 3. Therefore, negative values of relative BDEs mean that the corresponding BDE is smaller than the C(sp^3)−H BDE in propene and vice versa. As will be shown below, most of the trends can be understood on the basis of hyperconjugation and resonance. For this purpose, Figure 1 and Table 5 will be used. Figure 1 contains C−C bond lengths in the radicals and their parent molecules, and Table 5 shows Mulliken spin densities in the allylic moiety of each radical. We note that the atomic spin densities for the allyl radical are in good agreement with the experimental and theoretical data reported by Wiberg et al.[46]

(a) 2-Methylallyl. Interestingly, the C(sp^3)−H BDE in isobutene is 7 kJ mol^{-1} higher than the C(sp^3)−H BDE in

(66) Leal, J. P. *J. Phys. Chem. Ref. Data* **2006**, *35*, 55−76.
(67) Gronert, S. *J. Org. Chem.* **2006**, *71*, 1209−1219.
(68) Matsunaga, N.; Rogers, D. W.; Zavitsas, A. A. *J. Org. Chem.* **2003**, *68*, 3158−3172.
(69) The comparison should not be made with the C−H BDE in ethane, because the ethyl radical is stabilized by hyperconjugation.

TABLE 3. Selected Values for the Relative, Δ*DH*°(C−H), and Absolute, *DH*°(C−H), α-C−H BDEs (in kJ mol^{-1}), and Recommended Enthalpies of Formation for the Corresponding Radicals[a]

molecule	radical	Δ*DH*°(C−H)	*DH*°(C−H)	$\Delta_f H°(R^{\bullet},g)$[b]
propene	allyl	0.0	371.5	173.5
isobutene	2-methylallyl	7	378	143
1-butene	1-methylallyl	−12	360	142
(*E*)-2-butene	1-methylallyl	−1	371	141
3-methylbut-1-ene	3-methyl-1-buten-3-yl	−20	352	106
(*E*)-2-pentene	2-penten-4-yl	−12	360	110
(*E*)-1,3-pentadiene	pentadienyl	−19	353	211
1,4-pentadiene	pentadienyl	−47	325	213
cyclohexene	cyclohexen-3-yl	−14	358	135
1,3-cyclohexadiene	cyclohexadienyl	−46	325	212[c]
1,4-cyclohexadiene	cyclohexadienyl	−45	326	213[c]

[a] Estimated uncertainty of ca. ±4 kJ mol^{-1}. [b] Calculated by using $\Delta_f H°(H^{\bullet},g) = 217.998 \pm 0.006$ kJ mol^{-1} (Cox, J. D.; Wagman, D. D.; Medvedev, V. A. *Codata Key Values for Thermodynamics*; Hemisphere: New York, 1989) and $\Delta_f H°$(RH,g) from ref 4, unless noted otherwise. [c] $\Delta_f H°$(RH,g) from ref 65.

TABLE 4. Absolute, *DH*°(C−H), and Relative, Δ*DH*°(C−H), BDEs (in kJ mol^{-1}) in Selected Alkanes

molecule	radical	*DH*°(C−H)[a]	Δ*DH*°(C−H)
methane	methyl	439.1 ± 0.5	0.0
ethane	ethyl	423.0 ± 1.7	−16.1
propane	isopropyl	412.5 ± 1.7	−26.6
2-methylpropane	*tert*-butyl	403.8 ± 1.7	−35.3

[a] Data from ref 8, except for methane, which is from ref 10.

TABLE 5. Spin Densities at the Carbon Atoms That Define the Allyl Backbone in the Radicals[a]

molecule	radical	C1	C2	C3
propene	allyl	0.643	−0.210	0.643
isobutene	2-methylallyl	0.669	−0.201	0.617
1-butene	1-methylallyl	0.597	−0.202	0.637
(*E*)-2-butene	1-methylallyl	0.637	−0.202	0.597
3-methylbut-1-ene	3-methyl-1-buten-3-yl	0.575	−0.203	0.624
(*E*)-2-pentene	2-penten-4-yl	0.593	−0.195	0.593
(*E*)-1,3-pentadiene	pentadienyl	0.466	−0.177	0.487
1,4-pentadiene	pentadienyl	0.487	−0.177	0.466
cyclohexene	cyclohexen-3-yl	0.605	−0.197	0.605
1,3-cyclohexadiene	cyclohexadienyl	0.392	−0.160	0.520
1,4-cyclohexadiene	cyclohexadienyl	0.520	−0.160	0.392

[a] C1 is the carbon atom where the bond was cleaved. See Figure 1.

propene. This is in keeping with the data in Table 5: the spin density in the carbon atom where dissociation occurred (C1) is higher than in the case of allyl, indicating a lower electron delocalization. This is probably related to an anisotropy in the electronic distribution induced by the methyl group, which impairs delocalization. Evidence of the anisotropy is provided by the fact that the allylic C−C bond lengths are not equal (Figure 1). It is also suggested by the observation that the shorter allylic C−C bond is coplanar with a C−H bond of the methyl group.

(b) 1-Methylallyl. The α-C−H BDE in 1-butene is 12 kJ mol^{-1} lower than the C(sp^3)−H BDE in propene. Indeed, Table 5 shows that the spin density in C1 is lower than that in allyl, indicating a higher electron delocalization. In addition, it is noted in Figure 1 that the C1−Me bond length in 1-methylallyl is 4 pm shorter than the corresponding bond in 1-butene, suggesting that hyperconjugation is involved.

The 1-methylallyl radical is also formed by cleaving the C(sp^3)−H bond in (*E*)-2-butene. However, as shown in Table 3, the enthalpy of this process is only 1 kJ mol^{-1} lower than the C(sp^3)−H BDE in propene. In other words, producing the 1-methylallyl radical from 1-butene costs 11 kJ mol^{-1} less than producing it from (*E*)-2-butene. The difference, discussed above, stems from the fact that (*E*)-2-butene is 11 kJ mol^{-1} more stable than 1-butene (see Figure 2) and can be rationalized by using the Laidler scheme.[6] Consider the two types of C−C single bonds in 1- and (*E*)-2-butene, by decreasing order of strength (as indicated by bond length data in Figure 1): two C(sp^2)−C(sp^3) bonds in (*E*)-2-butene and one in 1-butene; and one C(sp^3)−C(sp^3) bond in 1-butene. The higher stability of (*E*)-2-butene essentially reflects the difference between the C(sp^2)−C(sp^3) and the C(sp^3)−C(sp^3) bond strengths.

There is an alternative way to explain the 11 kJ mol^{-1} difference between the C−H BDEs in 1-butene and (*E*)-2-butene (see Figure 1). By cleaving a secondary C−H bond in 1-butene the resulting (unrelaxed) fragment is then stabilized by both hyperconjugation and resonance, whereas the fragment formed from (*E*)-2-butene (by cleaving a primary C−H bond) is only stabilized by resonance. In other words, when the C−H bonds in 1-butene and (*E*)-2-butene are cleaved the resulting fragments relax to the ground state of the 1-methylallyl radical, but this relaxation is more exothermic for the fragment formed from 1-butene than that from (*E*)-2-butene.

(c) 3-Methyl-1-buten-3-yl. The α-C−H BDE in 3-methylbut-1-ene is 20 kJ mol^{-1} lower than the C(sp^3)−H BDE in propene. Table 5 indicates a higher degree of delocalization than in the case of allyl. On the other hand, Figure 1 shows that the C1−Me and C1−Me′ in the radical are 3−4 pm shorter than the corresponding bonds in the parent molecule, suggesting "double" hyperconjugation.

(d) 2-Penten-4-yl. The α-C−H BDE in (*E*)-2-pentene is 12 kJ mol^{-1} lower than the C(sp^3)−H BDE in propene. The data in Figure 1 show a shortening of 4 pm in the C1−Me bond (relative to the corresponding bond in the parent molecule), indicating hyperconjugation. Yet, no significant shortening is observed in the C1−C2 bond in (*E*)-2-pentene.

It is interesting to note that the relative C−H BDEs in 1-butene and (*E*)-2-pentene are similar (−12 kJ mol^{-1}). In both cases we have used hyperconjugation to explain this variation. Recall that hyperconjugation was also invoked to justify the C−H BDE in ethane (−16 kJ mol^{-1}), relative to the C−H BDE in methane.

A second comparison is provided by the "double" hyperconjugated 3-methyl-1-buten-3-yl and isopropyl radicals. The relative C−H BDE in 3-methylbut-1-ene (−20 kJ mol^{-1}) can be regarded as the combination of two hyperconjugations, the

first of which contributes with −12 kJ mol^{-1} and the second with −8 kJ mol^{-1}. In the case of propane, the relative C−H BDE in propene is −27 kJ mol^{-1} and the individual contributions are −16 and −11 kJ mol^{-1}.

In summary, the hyperconjugation contributions to the stability of alkyl and allyl derivatives are similar. However, they are not equal. The hyperconjugation effect is more important for alkyl radicals than for allyl radicals because in the latter the electron is delocalized and therefore less available to hyperconjugate.

(e) Pentadienyl. The C(sp^3)−H BDE in (*E*)-1,3-pentadiene is 19 kJ mol^{-1} lower than the BDE for the corresponding bond in propene. In both cases the radicals are resonance-stabilized but, as expected, the stabilization is higher in the five-carbon-atom system. This is in keeping with the data in Table 5: the spin density in the carbon atom where dissociation occurred (C1) is lower than that in the case of allyl, indicating a higher electron delocalization.

The pentadienyl radical can also be produced by cleaving the C(sp^3)−H BDE in 1,4-pentadiene, which costs 28 kJ mol^{-1} less than when using the 1,3 isomer as the starting point. As noted in Figure 3, the difference results from the relative stabilities of the isomers, i.e., (*E*)-1,3-pentadiene is about 30 kJ mol^{-1} more stable than 1,4-pentadiene. The existence of conjugated double bonds in the 1,3 isomer, involving a C(sp^2)−C(sp^2) bond, may be responsible for its relative stability, as suggested by the application of a recent set of extended Laidler (bond enthalpy) terms that includes a term for conjugated double bonds.[66] This is consistent with the fact that the conjugated C2−C3 bond in (*E*)-1,3-pentadiene is 6 pm shorter than the C2−C3 or C3−C4 bonds of 1,4-pentadiene (see Figure 1).

(f) Cyclohexen-3-yl. The α-C−H BDE in cyclohexene is 14 kJ mol^{-1} lower than the C(sp^3)−H BDE in propene. This value is similar to the results computed for 1-butene and (*E*)-2-pentene, suggesting that the cyclohexen-3-yl radical is stabilized by hyperconjugation and resonance. The bond length variations in Figure 1 and the spin densities in Table 5, which are comparable to those observed for the 2-penten-4-yl radical, support this conclusion.

(g) Cyclohexadienyl. The α-C−H BDEs in 1,3- and 1,4-cyclohexadiene are about 46 kJ mol^{-1} lower than the C(sp^3)−H BDE in propene. This value could be expected having in mind that the stabilization of pentadienyl and cyclohexadienyl radicals should be similar. The only difference is that (*E*)-1,3-pentadiene is 30 kJ mol^{-1} more stable than the 1,4 isomer, whereas the enthalpies of formation of 1,3- and 1,4-cyclohexadiene are identical.

Understanding the different stabilities of the cyclohexadiene isomers is slightly more complex than in the case of the pentadienes. Consider the three types of C−C single bonds in 1,3- and 1,4-cyclohexadiene, by decreasing order of strength (as indicated by bond length data in Figure 1): one conjugated C(sp^2)−C(sp^2) bond in 1,3-cyclohexadiene; two C(sp^2)−C(sp^3) bonds in 1,3-cyclohexadiene and four in 1,4-cyclohexadiene; and one C(sp^3)−C(sp^3) bond in 1,3-cyclohexadiene. Therefore, the stabilizing effect of the conjugated C(sp^2)−C(sp^2) bond in the 1,3 isomer is apparently offset by a much weaker C(sp^3)−C(sp^3) bond.

Correlation between BDEs and Spin Densities. By plotting the BDEs in Table 3 against the Mulliken atomic spin density at C1 of each radical, a linear correlation is observed (Figure 5). This supports the view that the BDEs are mainly determined by the radical stabilization through electron delocalization. Similar correlations have been reported, for instance, by Brocks et al.,[55] and involved plots of either radical stabilization energies or BDEs against esr-derived hyperfine coupling constants (which can be related to the spin density at the radical center, provided that the radical is planar). An advantage of the correlation in Figure 5 is that spin densities can be directly computed for any radical, regardless of its geometry.

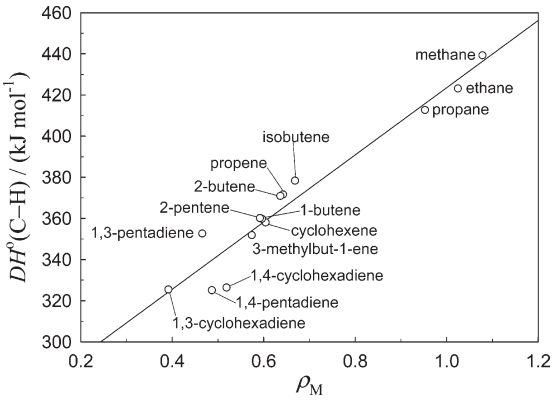

FIGURE 5. C−H bond dissociation enthalpies, ($DH°$(C−H)) vs Mulliken atomic spin densities (ρ_M) at the radical center for selected radicals: $DH°(C-H) = 163.4\rho_M + 206.3$ ($r = 0.967$).

The plot in Figure 5 (correlation coefficient of 0.967) includes the BDE data in Tables 3 and 4. The correlation fits quite well the values for the alkyl and allyl radicals but not the values for the dienes.

Conclusions

By using quantum chemistry calculations and time-resolved photoacoustic calorimetry, we have attempted to determine carbon−hydrogen bond dissociation enthalpies of selected alkenes within chemical accuracy (ca. 4 kJ mol^{-1}), aiming to improve our understanding of the stability of allylic radicals. By taking the C(sp^3)−H BDE in propene as a reference, we have concluded that one methyl group bonded to C3 in propene (i.e., 1-butene) leads to a decrease of 12 kJ mol^{-1} and that a second methyl group bonded to C3 (3-methylbut-1-ene) further decreases the BDE by 8 kJ mol^{-1}. Interestingly, however, when the methyl group is bonded to C2 in propene (isobutene), an increase of 7 kJ mol^{-1} is observed. Finally, a methyl group bonded to C1 in propene (2-butene) has essentially no effect (−1 kJ mol^{-1}).

The previous conclusions were used to rationalize other relative C−H BDEs. For instance, the α-C−H BDEs in (*E*)-2-pentene and cyclohexene (one alkyl group bonded to C1 and one to C3 in both cases) can be estimated as −13 kJ mol^{-1}, in keeping with the computed results, −12 and −14 kJ mol^{-1}, respectively.

The above values can be rationalized by assuming that the BDE changes are solely due to the stabilization of the corresponding radicals (relative to the stabilization of the allyl radical). In other words, to explain those BDEs (and therefore to predict new data), one does not need to consider the thermodynamic stabilities of the parent compounds. Indeed the relative stabilization of the simple alkenes involved in the present study correlates well with the spin density distribution,

indicating that hyperconjugation and π-delocatization can be invoked to understand the BDE trend.

For the dienes, however, the radical-based justification of the BDE trends does not hold, in keeping with the fact that these data do not correlate with the spin density at the radical center (with the probably fortuitous exception of 1,3-cyclohexadiene). The BDE values can only be understood by considering the thermodynamic stabilities of the parent compounds.

Acknowledgment. P.M.N. and F.A. thank Fundação para a Ciência e a Tecnologia, Portugal, for a postdoctoral (SFRH/BPD/26677/2005) and a Ph.D. (SFRH/BD/22854/2005) grant, respectively.

Supporting Information Available: Tables containing computed optimized geometries and total energies for radicals and parent compounds. This material is available free of charge via the Internet at http://pubs.acs.org.

JO701397R

JOC *Additions and Corrections*

Vol. 72, 2007

Bor-Cherng Hong,* Ming-Fun Wu, Hsing-Chang Tseng, Guo-Fong Huang, Cheng-Feng Su, and Ju-Hsiou Liao. Organocatalytic Asymmetric Robinson Annulation of α,β-Unsaturated Aldehydes: Applications to the Total Synthesis of (+)-Palitantin.

Pages 8459, 8463, 8465, 8466. The structures of **3g**, **3h**, **9**, and **10** in the Abstract, Table 3, and Schemes 3 and 4 are incorrect. The correct structures are shown below:

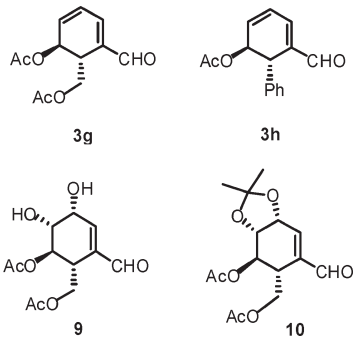

JO800081F

10.1021/jo800081f
Published on Web 02/06/2008

Filipe Agapito, Paulo M. Nunes, Benedito J. Costa Cabral, Rui M. Borges dos Santos, and José A. Martinho Simões*. Energetics of the Allyl Group.

Page 8772. Due to an error in the reference management software used, several important references are incorrect. Reference 24 is a duplicate of ref 20. Reference 25 should be: Parr, R. G.; Yang, W. *Density-Functional Theory of Atoms and Molecules*; Oxford University Press: New York, 1989. In ref 26, the ending page number is missing. The correct full reference is: Becke, A. D. *J. Chem. Phys.* **1993**, *98*, 5648−5652. Reference 27 should be: Lee, C.; Yang, W.; Parr, R. G. *Phys. Rev. B* **1988**, *37*, 785−789. A reference was omitted and should be included in ref 30: Agapito, F.; Cabral, B. J. C.; Martinho Simões, J. A. *THEOCHEM* **2007**, *811*, 361−372. Reference 31 should be: Wang, N. X.; Wilson, A. K. *J. Chem. Phys.* **2004**, *121*, 7632−7646. Reference 33 should be: Yao, X.-Q.; Hou, X.-J.; Jiao, H.; Xiang, H.-W.; Li, Y.-W. *J. Phys. Chem. A* **2003**, *107*, 9991−9996. In ref 38, an author name is incorrect. The correct full reference is: Raghavachari, K.; Trucks, G. W.; Pople, J. A.; Head-Gordon, M. *Chem. Phys. Lett.* **1989**, *157*, 479−483.

JO800097Z

10.1021/jo800097z
Published on Web 02/12/2008

CHAPTER 6

Five- and six-membered ring hydrocarbons

Striving to understand the energetics of terpenes (*cf.* Chapter 5), our next obstacle was the effect of ring strain on C—H BDEs. Indeed, all terpenes of interest contain either a cyclohexene or a cyclohexadiene ring. Ring strain may be present in parent and/or radical compounds. This has a profound effect on the thermodynamic stability of compounds and, consequently, influences BDEs. In addition, comparison of strain for six- and five-membered ring hydrocarbons provides a valuable insight into its effect on the stability of the corresponding radicals.

In ref. 183 (**P4**) we compared the ring strains of cyclohexane, cyclohexene, 1,3-cyclohexadiene, 1,4-cyclohexadiene, cyclopentane, cyclopentene, and 1,3-cyclopentadiene using enthalpies and geometries calculated with the theoretical methods that had proven useful in **P3**.* New TR-PAC data for the C—H BDEs in cyclohexane, cyclohexene, and cyclopentane were also given. A facsimile of this article is included in this chapter.

Ring strains were determined from theoretical data using the *s*-homodesmotic model[184] and compared with the operational definition of strain. Great care was given to the selection of appropriate *s*-homodesmotic models for each case.† We then proceeded to discuss the structural features responsible for ring-

* The author of this dissertation performed all quantum chemical calculations along with the related analysis and planning, and actively participated in the bibliographic research and in the writing of the manuscript of **P4**.

† Detailed description of the rules for selecting *s*-homodesmotic models was given in the supporting information of **P4**. A facsimile of the most pertinent section of this supporting information is included in this chapter after **P4**.

strain in these species. This provided a deeper understanding of differences in BDEs for five- and six-membered ring hydrocarbons. An illustration of the global importance of this information is provided by a recent work by Nett *et al.*,[185] where it aided in the study of the biological activity of β-lactone proteasome inhibitors in *salinispora tropica*. As the authors noted, these are promising drug candidates for the treatment of multiple myeloma and mantle cell lymphoma.

JOC Article

Energetic Differences between the Five- and Six-Membered Ring Hydrocarbons: Strain Energies in the Parent and Radical Molecules

Filipe Agapito,[†,‡] Paulo M. Nunes,[†] Benedito J. Costa Cabral,[‡] Rui M. Borges dos Santos,*[,†,§,||] and José A. Martinho Simões[†,§]

Centro de Química e Bioquímica, Faculdade de Ciências, Universidade de Lisboa, 1749-016 Lisboa, Portugal, Grupo de Física Matemática da Universidade de Lisboa, Av. Professor Gama Pinto 2, 1649-003 Lisboa, Portugal, Instituto de Tecnologia Química e Biológica, Universidade Nova de Lisboa, Av. da República, 2780-157 Oeiras, Portugal, and Institute for Biotechnology and Bioengineering Centro de Biomedicina Molecular e Estrutural, Universidade do Algarve, Campus de Gambelas, 8005-139 Faro, Portugal

rmsantos@fc.ul.pt

Received March 27, 2008

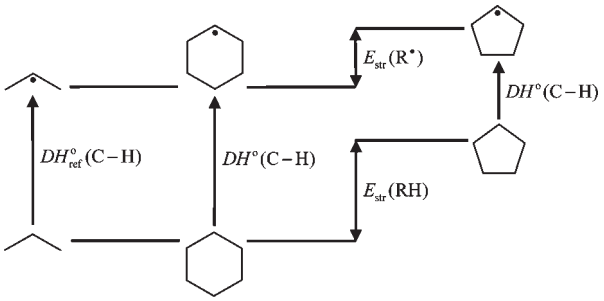

The C−H bond dissociation enthalpies (BDEs) for the five- and six-membered ring alkanes, alkenes, and dienes were investigated and discussed in terms of conventional strain energies (SEs). New determinations are reported for cyclopentane and cyclohexane by time-resolved photoacoustic calorimetry and quantum chemistry methods. The C−H BDEs for the alkenes yielding the alkyl radicals cyclopenten-4-yl and cyclohexen-4-yl and the α-C−H BDE in cyclopentene were also calculated. The *s*-homodesmotic model was used to determine SEs for both the parent molecules and the radicals. When the appropriate *s*-homodesmotic model is chosen, the obtained SEs are in good agreement with the ones derived from group additivity schemes. The different BDEs in the title molecules are explained by the calculated SEs in the parent molecules and their radicals: (1) BDEs leading to alkyl radicals are ca. 10 kJ mol^{-1} lower in cyclopentane and cyclopentene than in cyclohexane and cyclohexene, due to a smaller eclipsing strain in the five-membered radicals relative to the parent molecules (six-membered hydrocarbons and their radicals are essentially strain free). (2) C−H BDEs in cyclopentene and cyclohexene leading to the allyl radicals are similar because cyclopenten-3-yl has almost as much strain as its parent molecule, due to a synperiplanar configuration. (3) The C−H BDE in 1,3-cyclopentadiene is 27 kJ mol^{-1} higher than in 1,4-cyclohexadiene due to the stabilizing effect of the conjugated double bond in 1,3-cyclopentadiene and not to a destabilization of the cyclopentadienyl radical. The chemical insight afforded by group additivity methods in choosing the correct model for SE estimation is highlighted.

Introduction

Some terpenes exhibit antioxidant properties comparable to those of α-tocoferol,[1] without the pro-oxidant effects of this latter compound at higher concentrations.[2] Because this property is linked with the C−H BDE in the terpene, knowledge of the C−H BDEs in terpenes and other structurally related molecules is of great interest to understand which structural factors influence the antioxidant properties of these compounds.

The C−H BDE in an organic molecule RH, $DH°$(C−H), corresponds to the enthalpy of reaction 1, where all of the

[†] Faculdade de Ciências, Universidade de Lisboa.
[‡] Grupo de Física Matemática da Universidade de Lisboa.
[§] Universidade Nova de Lisboa.
[||] Universidade do Algarve.

10.1021/jo800690m CCC: $40.75
Published on Web 07/24/2008

molecules are in the ideal gas phase (isolated). It is related to the thermodynamic stability of the corresponding carbon-centered radical R•, as measured by its standard enthalpy of formation $\Delta_f H°(R^•,g)$, through eq 2.

$$RH(g) \rightarrow R^•(g) + H^•(g) \quad (1)$$

$$DH^°(C-H) = \Delta_f H^°(R^•,g) + \Delta_f H^°(H^•,g) - \Delta_f H^°(RH, g) \quad (2)$$

Most well-known BDEs for organic compounds have been obtained in the gas phase from kinetics studies, ion cycles, and photoionization mass spectrometry, but chemical accuracy (i.e., values with errors smaller than ca. 4 kJ mol^{-1}) was achieved for only relatively few data.[3–5] As the literature values for the C−H BDEs in many small hydrocarbons have uncertainties well above chemical accuracy, we investigated a number of those molecules using a combined approach of theoretical chemistry methods and time-resolved photoacoustic calorimetry (TR-PAC).[6,7]

In a previous study we determined the C−H BDEs in a series of open-chain hydrocarbons containing the allyl group.[8]We then used the results to select the "best" values for the C−H BDEs in these molecules, which allowed a quantitative discussion of the factors that determine the stability of the corresponding radicals, namely, hyperconjugation and resonance. Having dealt with all relevant molecules from the simplest propene to cyclohexadiene (viz., propane, propene, isobutene, 1-butene, 2-butene, 3-methyl-1-butene, 2-pentene, 1,3- and 1,4-pentadiene, cyclohexene, and 1,3- and 1,4-cyclohexadiene), we now turned our attention to the effect of ring strain on the C−H BDEs. To this end we need to compare the five-membered rings cyclopentane, cyclopentene, and 1,3-cyclopentadiene, with the six-membered ones, cyclohexane, cyclohexene, and 1,4-cyclohexadiene, respectively. In this work we report the TR-PAC determinations of C−H BDEs in cyclopentane and cyclohexane. The TR-PAC experimental results were complemented by quantum chemistry calculations for the same molecules and the corresponding radicals (cyclopentyl and cyclohexyl), plus cyclopentene, cyclopenten-3-yl, cyclopenten-4-yl, cyclohexen-4-yl, propane, and isopropyl. These and the previous results for the remaining cyclic hydrocarbons, together with the simpler molecules propene, 1-butene, (*E*)-2-pentene, 1,3- and 1,4-pentadiene,[8] were then used to systematically investigate the structure−energetics relationship in the five- and six-membered ring hydrocarbons (see Supporting Information for the complete list of molecules investigated).

Strain is the central concept in this discussion, used in the conventional sense of Cox and Pilcher,[9] i.e., including all the stabilizing and destabilizing effects in relation to a strain-free reference molecule, regardless of the cause. To relate BDEs to strain we need to consider it both in the parent molecule and in its radical. However, evaluating strain in the radicals is considerably more complex that in the parent molecules. An important part of this work was therefore the selection of a method that allows quantifying the strain in the radicals studied.

Results

The strategy used to obtain BDEs from photoacoustic calorimetry was based on the photochemical process below: di-*tert*-butylperoxide (*t*-BuOOBu-*t*) is photolyzed, generating *tert*-butoxyl radicals (reaction 3), each abstracting an hydrogen atom from the organic molecule RH, reaction 4.

$$t\text{-BuOOBu-}t(sln) \xrightarrow{h\nu} 2t\text{-BuO}^•(sln) \quad (3)$$

$$2RH(sln) + 2t\text{-BuO}^•(sln) \rightarrow 2R^•(sln) + 2t\text{-BuOH}(sln) \quad (4)$$

Deconvolution of the resulting waveform (see Experimental Section) first made it possible to confirm the reaction scheme (reactions 3 and 4) and then afforded the observed fraction of photon energy released as heat, $\phi_{obs,i}$, for each process, and the lifetime of the second, τ_2. An estimate of the rate constant can be obtained from this lifetime.[10] The enthalpy of the hydrogen abstraction reaction was derived from eq 5, where $\Delta_{obs}H_2$ corresponds to the observed enthalpy change and is calculated by multiplying $\phi_{obs,2}$ (the observed heat fraction associated with reaction 2) by $E_m = N_A h\nu$ (the molar photon energy). Φ_r is the reaction quantum yield for the photolysis of di-*tert*-butylperoxide.[11]

$$\Delta_r H_2 = \frac{-\Delta_{obs}H_2}{\Phi_r} \quad (5)$$

As the enthalpy of reaction 4 is simply twice the difference between the solution BDEs of the hydrocarbon C−H and *tert*-butyl alcohol O−H, $DH^°_{sln}(C-H)$ can be derived from eq 6, where the subscript "sln" indicates that both BDEs are solution values.

$$DH^°_{sln}(C-H) = \frac{\Delta_r H_2}{2} + DH^°_{sln}(t\text{-BuO}-H) \quad (6)$$

In a previous work we determined $DH^°_{sln}(t\text{-BuO}-H) = 455.2 \pm 5.2$ kJ mol^{-1} in benzene.[12] To derive the gas-phase value $DH°(C-H)$, the solvation terms illustrated in eq 7 must be considered.[13]

$$DH^°(C-H) = DH^°_{sln}(C-H) + \Delta_{sln}H^°(RH,g) - \Delta_{sln}H^°(R^•,g) - \Delta_{sln}H^°(H^•,g) \quad (7)$$

The solvation of the hydrogen atom was estimated as $\Delta_{sln}H°(H^•,g) = 5 \pm 1$ kJ mol^{-1} for organic solvents.[13] On the other hand, for carbon-centered radicals $\Delta_{sln}H°(RH,g) \approx \Delta_{sln}H°(R^•,g)$,[12] so the difference between solution and gas-phase

(1) Ruberto, G.; Baratta, M. T. *Food Chem.* **2000**, *69*, 167–174.
(2) Foti, M. C.; Ingold, K. U. *J. Agric. Food Chem.* **2003**, *51*, 2758–2765.
(3) Blanksby, S. J.; Ellison, G. B. *Acc. Chem. Res.* **2003**, *36*, 255–263.
(4) Ruscic, B.; Boggs, J. E.; Burcat, A.; Császár, A. G.; Demaison, J.; Janoschek, R.; Martin, J. M. L.; Morton, M. L.; Rossi, M. J.; Stanton, J. F.; Szalay, P. G.; Westmoreland, P. R.; Zabel, F.; Bérces, T. *J. Phys. Chem. Ref. Data* **2005**, *34*, 573–656.
(5) Luo, Y.-R. *Handbook of Bond Dissociation Energies in Organic Compounds*; CRC Press: Boca Raton, 2003.
(6) Peters, K. S. *Angew. Chem., Int. Ed. Engl.* **1994**, *33*, 294–302.
(7) Laarhoven, L. J. J.; Mulder, P.; Wayner, D. D. M. *Acc. Chem. Res.* **1999**, *32*, 342–349.
(8) Agapito, F.; Nunes, P. M.; Costa Cabral, B. J.; Borges dos Santos, R. M.; Martinho Simões, J. A. *J. Org. Chem.* **2007**, *72*, 8770–8779.
(9) Cox, J. D.; Pilcher, G. *Thermochemistry of Organic and Organometallic Compounds*; Academic Press: London, New York, 1970.
(10) Nunes, P. M.; Correia, C. F.; Borges dos Santos, R. M.; Martinho Simões, J. A. *Int. J. Chem. Kinet.* **2006**, *38*, 357–363.
(11) Wayner, D. D. M.; Lusztyk, E.; Pagé, D.; Ingold, K. U.; Mulder, P.; Laarhoven, L. J. J.; Aldrich, H. S. *J. Am. Chem. Soc.* **1995**, *117*, 8737–8744.
(12) Muralha, V. S. F.; Borges dos Santos, R. M.; Martinho Simões, J. A. *J. Phys. Chem. A* **2004**, *108*, 936–942.
(13) Borges dos Santos, R. M.; Costa Cabral, B. J.; Martinho Simões, J. A. *Pure Appl. Chem.* **2007**, *79*, 1369–1382.

TABLE 1. Theoretical and Experimental C−H Bond Dissociation Enthalpies (in kJ mol^{-1}) at 298.15 K

molecule	radical	B3LYP-TZ[a]	CBS-Q[a]	CBS-QB3[a]	CCSD(T)[a]	exptl[b]
propene[c]	allyl	352.2	361.3	364.9	371.5	371.5 ± 1.7[d]
propane	isopropyl	397.5	410.9	413.9	416.3	412.5 ± 1.7[e]
cyclopentane	cyclopentyl	388.4 [403.3][f]	404.1 [405.7][f]	403.7 [402.3][f]	406.8 [403.0][f]	401.8 ± 5.8
cyclopentene	cyclopenten-4-yl	390.5 [405.5][f]	406.6 [408.2][f]	406.1 [404.7][f]	408.7 [404.8][f]	
	cyclopenten-3-yl	335.5 [354.9][g]	347.3 [357.5][g]	350.5 [357.1][g]	358.7[h]	344.3 ± 4.2 [i]
1,3-cyclopentadiene[j]	cyclopentadienyl	333.4 [352.7][g]	346.1 [356.4][g]	345.9 [352.5][g]	353.4[h]	357.8 ± 7.1 [j]
cyclohexane	cyclohexyl	399.4 [414.3][f]	417.8 [419.4][f]	416.1 [414.7][f]	418.5 [414.6][f]	419.8 ± 6.0
cyclohexene	cyclohexen-4-yl	398.1 [413.1][f]	418.3 [419.9][f]	415.1 [413.7][f]	417.7 [413.9][f]	
	cyclohexen-3-yl[f]	333.8 [353.2][g]	347.2 [357.5][g]	349.5 [356.1][g]	357.9[h]	350.0 ± 5.6
1,4-cyclohexadiene [c]	cyclohexadienyl	297.0 [316.4][g]	307.8 [318.0][g]	311.0 [317.6][g]	326.3[h]	312.8 ± 6.1 [c]

[a] Results from the direct homolysis reaction 1 and, in brackets, from the isodesmic and isogyric reaction 9. This work unless noted otherwise. [b] TR-PAC results from this work, unless noted otherwise. The error is twice the standard deviation of the mean for 5−6 independent experiments. [c] From ref 8. [d] From ref 3. [e] From ref 4. [f] Using the literature value for the C2−H BDE in propane as the anchor (412.5 ± 1.7 kJ mol^{-1}). [g] Using the literature value for the C(sp^3)−H BDE in propene as the anchor (371.5 ± 1.7 kJ mol^{-1}). [h] In this case there is no need to derive the BDEs from reaction 9 since the computed C(sp^3)−H BDE in propene matches the experimental result. [i] From ref 16. [j] From ref 17.

C−H BDEs is equal to the solvation enthalpy of the hydrogen atom indicated above.[14]

Regarding the theoretical results, bond dissociation enthalpies were computed from eq 8, equivalent to eq 2 but with the standard enthalpies of formation replaced by the theoretically obtained entalpies *H*.

$$DH^{\circ}(\mathrm{C-H}) = H(\mathrm{R^{\bullet}}) + H(\mathrm{H^{\bullet}}) - H(\mathrm{RH}) \qquad (8)$$

The C−H BDEs for the molecules investigated in this work are presented in Table 1. The touchstone for discussing the energetics of the allyl radicals is the C(sp^3)−H BDE in propene, which is well established as 371.5 ± 1.7 kJ mol^{-1}.[3] Similarly, the basis for discussing the energetics of the alkyl radicals in this work is the also well-known C2−H BDE in propane that corresponds to the formation of the isopropyl radical (412.5 ± 1.7 kJ mol^{-1}).[4] These BDEs were used as the anchors to derive more accurate computational results in Table 1. Indeed, C−H BDEs calculated from eq 8, which relies on reaction 1, are usually low limits of the exact values. This problem can be avoided by using a particular type of reaction, eq 9, in which the structural features of reactants and products (such as the number of electron pairs, the number of carbon atoms in a given state of hybridization, etc.) are matched to some degree (for a more complete description see Calculating the Strain Energy).

$$\mathrm{RH} + \mathrm{R'^{\bullet}} \rightarrow \mathrm{R^{\bullet}} + \mathrm{R'H} \qquad (9)$$

The differences $DH°$(R−H) − $DH°$(R′−H), which are equal to the enthalpies of reaction 9, are largely method-independent and usually more accurate than the BDEs obtained from eq 8, because reaction 9 takes advantage of error cancelation.[15] Moreover, these differences may yield absolute BDE values by using a reliable value for the anchor, $DH°$(R′−H). The bracketed values in Table 1 were obtained from reaction 9 with R′ = isopropyl and using the experimental C2−H BDE for propane, 412.5 kJ mol^{-1}, whenever alkyl radicals are formed, and with R′ = allyl and using the experimental C(sp^3)−H BDE for propene, 371.5 kJ mol^{-1}, when allylic radicals are involved. Note that the accurately known C−H BDE in methane could in principle be used instead of the C2−H BDE in propane, but then the structural features in reaction 9 would be matched to a lesser extent, since R′$^{\bullet}$ would be a primary radical, whereas the product is a secondary radical. When the C2−H BDE in propane is used, both radicals are secondary.

As expected, Table 1 shows that the BDEs computed from reaction 1 have larger discrepancies than the bracketed values obtained with reaction 9. A closer analysis reveals that when alkyl radicals are involved, this difference is only important for the DFT calculations, but when allylic radicals are formed, the discrepancy is also noticeable for the complete basis set methods. These results also follow our previous observation[8] that the discrepancies are smaller for CBS-QB3 than for CBS-Q, indicating that the former is the most accurate of these two methods for the systems under study. We will however favor the results of the CCSD(T) calculations, which are expected to be the most reliable. It is also observed that the CBS-QB3 and CCSD(T) results are in excellent agreement, with the previously noted exception of the BDE for 1,4-cyclohexadiene (and the remaining dienes, (*E*)-1,3- and 1,4-pentadiene, and 1,3-cyclohexadiene), but even then the discrepancy is smaller than 8 kJ mol^{-1}.[8]

The BDEs corresponding to the C−H bond cleavages yielding the cyclopentadienyl, cyclohexen-3-yl, and cyclohexadienyl radicals (Table 1) were also the subject of previous studies by our group and the corresponding selected values were 355,[17] 357.9, and 326.3 kJ mol^{-1},[8] respectively. The first value corresponds to a rounded average of the CCSD(T) calculation with the TR-PAC result, while the remaining values are simply the CCSD(T) results (which are in good agreement with the experimental TR-PAC values). For the sake of consistency, in the present study we will also use the CCSD(T) result for the C−H BDE in cyclopentadienyl, 353.4 kJ mol^{-1}. To compare the new results with the literature data we followed our previous strategy and relied mainly on the compilation by Luo,[5] complemented with a brief analysis of the data collected by this author.

The experimental results for the C−H BDE in cyclopentane vary in a narrow range, 397 ± 4 to 400 ± 4 kJ mol^{-1}.[5] The latter value, selected by Luo, is based on the EPR determination of the equilibrium constant for the exchange reaction between methyl radical and cyclopentyl iodide.[18] It should be revised

(14) The final uncertainty of the TR-PAC determination of $DH°$(C−H) (eq 7) is equal to the uncertainty of $DH°_{sln}$(C−H) (eq 6), since the error in $\Delta_{sln}H°$(H$^{\bullet}$,g) cancels out and the error in $\Delta_{sln}H°$(RH,g)−$\Delta_{sln}H°$(R$^{\bullet}$,g) is negligible, see e.g., ref 12.

(15) *Computational Thermochemistry. Prediction and Estimation of Molecular Thermodynamics*; Irikura, K. K., Frurip, D. J., Eds.; ACS Symposium Series No. 677; American Chemical Society: Washington, DC, 1998.

(16) Furuyama, S.; Golden, D. M.; Benson, S. W. *Int. J. Chem. Kinet.* **1970**, *2*, 93–99.

(17) Nunes, P. M.; Agapito, F.; Costa Cabral, B. J.; Borges dos Santos, R. M.; Martinho Simões, J. A. *J. Phys. Chem. A* **2006**, *110*, 5130–5134.

(18) Castelhano, A. L.; Griller, D. *J. Am. Chem. Soc.* **1982**, *104*, 3655–3659.

taking into account the most recently auxiliary data, namely, the enthalpy of formation of the methyl radical (146.7 ± 0.3 kJ mol^{-1}).[4] The revision is however small, yielding 402.9 kJ mol^{-1}. Both our calculated and experimental values are in conformity with this result, and we selected 403.0 kJ mol^{-1} (CCSD(T)), in excellent agreement with our TR-PAC result of 401.8 ± 5.8 kJ mol^{-1}. The TR-PAC experiments were performed with cyclopentane concentrations of 4.0 and 10.1 M (this latter concentration referring to neat cyclopentane plus the peroxide). From the lifetime obtained for reaction 4, τ_2, we estimate 7×10^5 M^{-1} s^{-1} for the rate constant of hydrogen abstraction from cyclopentane (k_2), in good agreement with the reported laser flash photolysis values, e.g., 8.51×10^5 M^{-1} s^{-1}.[19] The value of the C−H BDE in cyclopentane is very close to the calculated β-C−H BDE in cyclopentene yielding the alkyl radical cyclopenten-4-yl, 404.8 kJ mol^{-1} (CCSD(T)).

For the α-C−H BDE in cyclopentene, which leads to the allylic radical cyclopenten-3-yl, the results reported by Luo are again very close, 344 ± 4 and 343 ± 8 kJ mol^{-1}.[5] However, all of our calculations point to a higher BDE, varying in a narrow range, viz., 355 (B3LYP-TZ) to 359 kJ mol^{-1} (CCSD(T)), in keeping with previous high-level calculations of 352.3 (G3),[20,21] 353.1 (G3B3),[22] and 355.6 kJ mol^{-1} (W1).[21] We select the result of the CCSD(T) method for this BDE, 359 kJ mol^{-1}.

The reported values for the C−H BDE in cyclohexane range from 403 to 416 kJ mol^{-1}, the latter selected by Luo.[5] The data presented by this author includes a non-time-resolved PAC result of 410 kJ mol^{-1}.[23] Since reaction 4 is too slow for PAC without deconvolution analysis, the experiment involved two competing reactions, namely, reaction 4 with cyclohexane and with 1,4-cyclohexadiene. Using this strategy, the derivation of the desired BDE for cyclohexane depends on the knowledge of both rate constants and the C−H BDE in the latter compound. TR-PAC directly affords the BDE in cyclohexane and also the rate constant for reaction 4. Our experiments led to 419.8 ± 6.0 kJ mol^{-1}, in good agreement with Luo's selection, and were performed with cyclohexane concentrations ranging from 2.2 to 9.0 M (neat cyclohexane plus the peroxide). From the lifetime obtained for reaction 4, τ_2, we derived 8×10^5 M^{-1} s^{-1} for the rate constant of hydrogen abstraction from cyclohexane (k_2), which matches a recent laser flash photolysis result (8.13×10^5 M^{-1} s^{-1})[19] and is in fair agreement with the value used in the PAC study indicated above (5.5×10^5 M^{-1} s^{-1}).[23] Our calculations are also in good agreement with Luo's recommendation, and we selected 414.6 kJ mol^{-1} (CCSD(T)). The value of this BDE is very close to the calculated β−C-H BDE in cyclohexene that leads to the alkyl radical cyclohexen-4-yl, 413.9 kJ mol^{-1} (CCSD(T)).

TABLE 2. Selected Values for the Relative [$\Delta DH°$(C−H)] and Absolute [$DH°$(C−H)] C−H BDEs (in kJ mol^{-1}), and Recommended Enthalpies of Formation for the Corresponding Radicals[a]

molecule	radical	$\Delta DH°$ (C−H)	$DH°$ (C−H)	$\Delta_f H°$ (R•,g)[b]
propane	isopropyl	0.0	412.5	89.8
cyclopentane	cyclopentyl	−9.5	403.0	108.6
cyclopentene	cyclopenten-4-yl	−7.7	404.8	220.8
cyclohexane	cyclohexyl	2.1	414.6	73.3
cyclohexene	cyclohexen-4-yl	1.4	413.9	191.0
propene	allyl	0.0	371.5	173.5
1-butene[c]	1-methylallyl	−11.9	359.6	141.7
(*E*)-2-pentene[c]	2-penten-4-yl	−11.5	360.0	110.1
(*E*)-1,3-pentadiene[c]	pentadienyl	−19.0	352.5	210.6
1,4-pentadiene[c]	pentadienyl	−46.5	325.0	212.7
cyclopentene	cyclopenten-3-yl	−12.8	358.7	174.7
cyclohexene[c]	cyclohexen-3-yl	−13.6	357.9	135.0
1,3-cyclopentadiene[d]	cyclopentadienyl	−18.1	353.4	269.7
1,4-cyclohexadiene[c]	cyclohexadienyl	−45.2	326.3	213.1[e]

[a] Estimated uncertainty of ca. ± 4 kJ mol^{-1} [b] Calculated using $\Delta_f H°$(H•,g) = 217.998 ± 0.006 kJ mol^{-1} (ref 24) and $\Delta_f H°$(RH,g) from ref 25. [c] From ref 8. [d] From ref 17. [e] $\Delta_f H°$(RH,g) from ref 26.

Discussion

The above data analysis led to the set of recommended values collected in Table 2. They are all based on the values derived from CCSD(T), with exception of the anchor molecules propane and propene, for which the recommended literature values are given. The top part of the table lists the alkyl radicals. The allyl radicals presented next include mostly earlier results[8,17] that are relevant for the present discussion.

In our previous work dealing with simple (and unstrained) alkanes, alkenes, and dienes, we explained the differences in C−H BDEs using the concepts of hyperconjugation and resonance. These effects are reflected by the structural changes that accompany radical formation. For instance, hyperconjugation can be measured by the shortening of the C−C bond(s) adjacent to the radical center; resonance in an allyl group is characterized by two carbon−carbon bonds of identical length, which were a single and a double bond in the parent molecule. Both factors are accompanied by a decrease in spin density at the carbon atom where abstraction occurs, which correlates rather well with the C−H BDEs in the alkanes and alkenes studied. This supports the view that those BDEs are mainly determined by alkyl and allyl radical stabilization through spin delocalization. In the case of the dienes we have also to consider the thermodynamic stabilities of the parent compounds, namely, the possibility of a strongly stabilizing conjugated double bond.[8]

In the present study, deviations from the above behavior will be attributed to strain and assessed by comparing the title molecules with a suitable reference. This reference should obviously be a strain-free compound but having stabilization effects that are identical to those in the molecule under study. Suitable references that will be used throughout this discussion are displayed in Figure 1.

To rationalize the effect of strain on the BDEs, we will start by inspecting the geometries of the parent molecules and radicals for "anomalous" (with regard to the references) C−C bond lengths (Figure 2) and C−C−C angles (Figure 3).

Cyclohexane versus Cyclopentane. The C−H BDE in propane leading to isopropyl (412.5 kJ mol^{-1}) is similar to the C−H BDE in cyclohexane (414.6 kJ mol^{-1}). This is consistent with the known fact that cyclohexane and its radical have little or no strain. However, the C−H BDE in cyclopentane is some

(19) Finn, M.; Friedline, R.; Suleman, N. K.; Wohl, C. J.; Tanko, J. M. *J. Am. Chem. Soc.* **2004**, *126*, 7578–7584.
(20) Bach, R. D.; Dmitrenko, O. *J. Am. Chem. Soc.* **2004**, *126*, 4444–4452.
(21) Tian, Z.; Fattahi, A.; Lis, L.; Kass, S. R. *J. Am. Chem. Soc.* **2006**, *128*, 17087–17092.
(22) Feng, Y.; Liu, L.; Wang, J.-T.; Zhao, S.-W.; Guo, Q.-X. *J. Org. Chem.* **2004**, *69*, 3129–3138.
(23) Ciriano, M. V.; Korth, H.-G.; van Scheppingen, W. B.; Mulder, P. *J. Am. Chem. Soc.* **1999**, *121*, 6375–6381.
(24) Cox, J. D.; Wagman, D. D.; Medvedev, V. A. *Codata Key Values for Thermodynamics*; Hemisphere: New York, 1989.
(25) Pedley, J. B. *Thermochemical Data and Structures of Organic Compounds*; Thermodynamics Research Center: College Station, TX, 1994; Vol. 1.
(26) Afeefy, H. Y.; Liebman, J. F.; Stein, S. E. In *NIST Chemistry WebBook*; Linstrom, P. J., Mallard, W. G., Eds.: NIST Standard Reference Database Number 69 http://webbook.nist.gov; National Institute of Standards and Technology: Gaithersburg, MD, 2005.

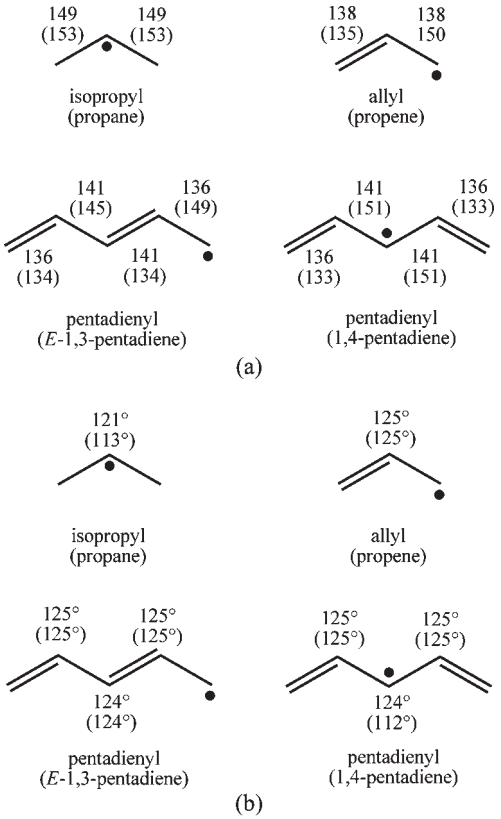

FIGURE 1. (a) Bond lengths (pm) and (b) bond angles for the radicals and their parent molecules (in parentheses) to be used as the strain-free reference molecules, calculated with B3LYP/cc-pVTZ.

11 kJ mol^{-1} lower than in the above compounds: The enthalpy of reaction 10, obtained from CCSD(T) calculations, is −11.6 kJ mol^{-1}.

(10)

The lower C−H BDE in cyclopentane can be qualitatively understood with the help of Figure 4, which relates the BDEs in cyclohexane and cyclopentane with the strain destabilizations of the parent molecule and its radical (for a quantitative description of strain energy, SE, see Calculating the Strain Energy). It is clear from Figure 4 that the lower C−H BDE in cyclopentane should result from a higher strain destabilization of cyclopentane (relative to cyclohexane) as compared with the strain destabilization of cyclopentyl (relative to cyclohexyl).

C−C bond lengths in cyclopentane (155 pm) are slightly larger than in cyclohexane (153 pm), which are equal to the ones in propane. C−C−C bond angles in cyclopentane and cyclohexane are also different, and whereas in the latter they are close to the one in propane (112° vs 113°, respectively), in the former they are smaller (ca. 106°). Both facts are consistent with a destabilization of cyclopentane due to strain.

Concerning the radicals, bond lengths in cyclopentyl and cyclohexyl are equal, and the ones adjacent to the radical center are equal to isopropyl. However, the angle corresponding to this latter structure (C−C1−C) is narrower in cyclopentyl (112°) than in a typical sp^2 hybridization, such as in cyclohexyl (119°) or isopropyl (121°). Furthermore, the spin density at the radical center is higher in cyclopentyl (0.970) than in cyclohexyl (0.955), which is quite close to isopropyl (0.953), indicating

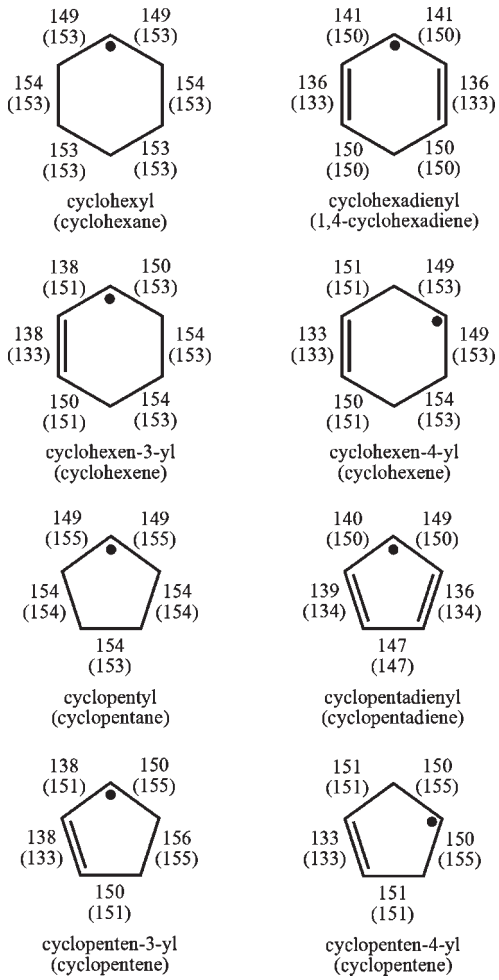

FIGURE 2. Bond lengths (pm) for the radicals and their parent molecules (in parentheses), calculated with B3LYP/cc-pVTZ.

less delocalization in cyclopentyl. All of these facts point to a destabilization of cyclopentyl due to strain.

Cyclohexene versus Cyclopentene. The BDEs leading to the alkyl radicals cyclohexen-4-yl and cyclopenten-4-yl are very close to the BDEs of the corresponding alkanes discussed above. Again, the C−H BDE in cyclohexene (413.9 kJ mol^{-1}) is equal to the C−H BDE in propane (412.5 kJ mol^{-1}) and the C−H BDE in cyclopentene is lower (404.8 kJ mol^{-1}), as illustrated by the enthalpy of reaction 11, −9.1 kJ mol^{-1} (CCSD(T)).

(11)

Repeating the previous analysis of the structural features of these molecules leads to similar observations. Regarding the parent compounds, the bonds adjacent to the radical center (C4) are longer in cyclopentene (155 pm) than in cyclohexene (153 pm), which are equal to the ones in propane. The bond angle between the same bonds in cyclohexene is close to the one in propane (111° vs 113°, respectively), while in cyclopentene it is smaller (ca. 106°). Additionally, the angles defined by the double bond and the adjacent carbon atoms in cyclopentene are narrower (112°) than in cyclohexene (124°). These three facts point to a strain destabilization of cyclopentene, while cyclohexene should have little or no strain. Concerning the radicals, bond lengths adjacent to the radical center are equal in

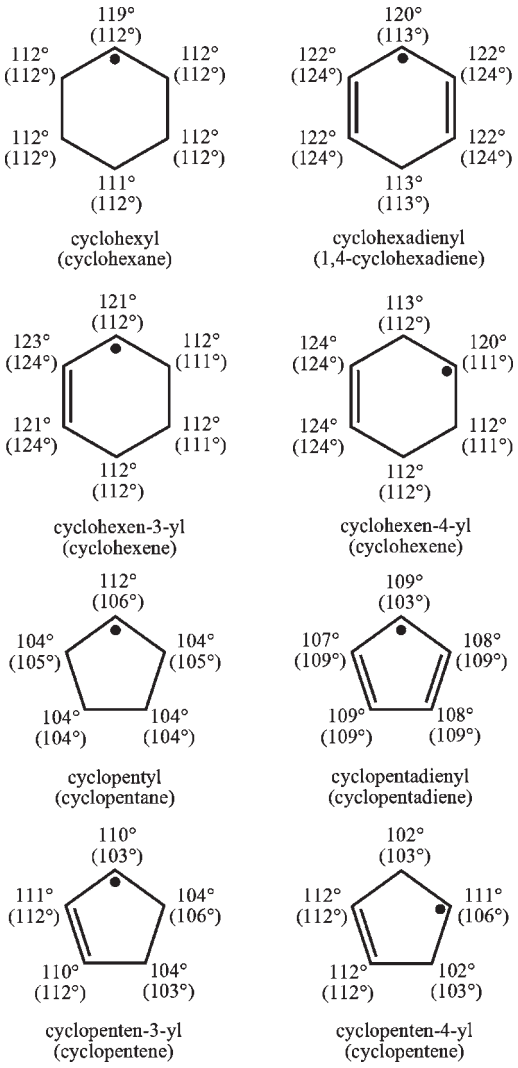

FIGURE 3. Bond angles for the radicals and their parent molecules (in parentheses), calculated with B3LYP/cc-pVTZ.

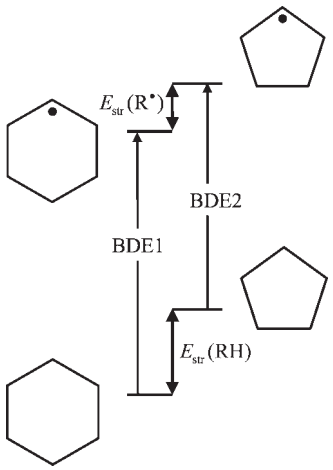

FIGURE 4. Relation between the BDEs in cyclohexane and cyclopentane, considering the destabilization of the parent molecule and its radical due to strain (E_{str}).

cyclohexen-4-yl and isopropyl (149 pm) and only slightly longer in cyclopentene-4-yl (150 pm). The radical centered angle is narrower in cyclopenten-4-yl (111°) than in cyclohexen-4-yl (120°) or isopropyl (121°). The spin density at the radical center is higher in cyclopenten-4-yl (0.970) than in cyclohexen-4-yl (0.960) and isopropyl (0.953), indicating less delocalization in cyclopenten-4-yl. The remaining structural features of the radicals are unchanged from the parent molecule. Therefore, the difference in C−H BDEs between cyclopentene and cyclohexene may be explained as before: the strain destabilization of cyclopentene is larger than the strain destabilization of the cyclopentene-4-yl radical.

Regarding the formation of the allylic radicals, the C−H BDEs of cyclohexene (357.9 kJ mol^{-1}) and cyclopentene (358.7 kJ mol^{-1}) are rather close and similar to the C−H BDEs in 1-butene (359.6 kJ mol^{-1}) and 2-pentene (360.0 kJ mol^{-1}). The BDEs in the unstrained compounds 1-butene and 2-pentene can be explained solely by spin delocalization on the radical through hyperconjugation and resonance.[8] This means that either cyclopentene, cyclohexene, and their allylic radicals are unstrained or the strain energies for each parent-radical pair are identical. However, the above discussion demonstrated that cyclopentene is strain-destabilized, whereas cyclohexene is not. Therefore, cyclopenten-3-yl radical and cyclopentene must have similar strain energies. Recall that cyclopenten-4-yl radical has less strain than cyclopentene. Hence, cyclopenten-3-yl radical has more strain than cyclopenten-4-yl radical.

By comparing the structures of cyclopenten-3-yl and cyclohexen-3-yl radicals, it is easy to accept that the former should be more strained. Indeed, the angles in cyclopenten-3-yl are around 111° in the allyl system and 104° in the sp^3 carbons, whereas in cyclohexen-3-yl they are much closer to regular values (around 122° in the allyl system and 112° in the sp^3 carbons). However, it is more difficult to demonstrate, on the basis of structural features, that the cyclopenten-3-yl radical is more strained than cyclopentyl or cyclopenten-4-yl. To make progress we need to quantify strain, which we will do in the next section before returning to this question.

Calculating the Strain Energy. As described by Feng et al.,[22] strain can be quantified in a number of ways, the most popular being the "bent bond" model introduced by Coulson[27] and developed by Bader and co-workers[28,29] in the "bond path" theory. Feng et al. also proposed a new and perhaps more chemically intuitive way to measure the effect of ring strain on BDEs, by calculating the hybridization in the parent molecule and in the radical using natural bond orbital (NBO) analysis.[30,31] Hybridization in the parent molecule is evaluated by calculating the *p*% character associated with the C−H bond orbital where abstraction will occur. Deviation from 0.75 (sp^3 hybridization) points to a destabilization of the molecule due to strain. Likewise, hybridization in the radical is assessed by calculating the *p*% of the odd electron, and *p*% < 1.00 indicates strain. The authors then proposed a three-parameter structure-energetics equation to predict C−H BDEs in strained hydrocarbons. It includes the two parameters above to quantify strain in addition to the spin density that accounts for hyperconjugation and resonance, but while the model can predict the BDEs for a variety of saturated and unsaturated strained hydrocarbons rather well, it does not explain the finer issues, like the questions raised in the previous section. Indeed, the *p*% of the odd electron is

(27) Coulson, C. A.; Goodwin, T. H. *J. Chem. Soc.* **1962**, 2851–2854.
(28) Wiberg, K. B.; Bader, R. F. W.; Lau, C. D. H. *J. Am. Chem. Soc.* **1987**, *109*, 985–1001.
(29) Wiberg, K. B.; Bader, R. F. W.; Lau, C. D. H. *J. Am. Chem. Soc.* **1987**, *109*, 1001–1012.
(30) Foster, J. P.; Weinhold, F. *J. Am. Chem. Soc.* **1980**, *102*, 7211–7218.
(31) Reed, A. E.; Curtiss, L. A.; Weinhold, F. *Chem. Rev.* **1988**, *88*, 899–926.

TABLE 3. Strain Energies (E_{str}, in kJ mol^{-1}) Derived from Experimental Data

molecule	$\Delta_f H°$(RH,g)[a]	$\Delta_f H°$(RH*,g)[b]	E_{str}(RH)	RSC[c]
cyclopentane	−76.4	−103.6	27.2	30.9
cyclopentene	34.0	11.1	22.9	23.8
cyclohexane	−123.3	−124.3	1.0	3.2
cyclohexene	−4.9	−9.6	4.7	5.3
1,3-cyclopentadiene	134.3	109.3	25.0	21.0
1,4-cyclohexadiene	104.8[d]	105	−0.2	−0.7

[a] From ref 25 except when noted otherwise. [b] For the hypothetical strain-free compound RH*, using the extended Laidler terms from ref 32. The corrective terms that account for strain were obviously *not* used. [c] Ring strain corrections (RSC ≡ E_{str}) of Benson group additivity method from ref 34. [d] From ref 26.

calculated as 1.00 in the five-membered radicals cyclopentyl, cyclopenten-3-yl, and cyclopenten-4-yl, meaning that it is completely in the p orbital and therefore strain had no effect in any of these radicals. Consequently, the structure-energetics equation applied to cyclopentane, cyclopentene, and cyclohexane (yielding the alkyl radicals) leads to similar BDEs, around 418 kJ mol^{-1}, missing the trends discussed above.

A different and, to our purpose, a better approach, would be to directly calculate the strain energy (E_{str}). Conventionally, this is defined as the difference between the enthalpies of formation of the compound of interest RH and a strain-free reference compound RH*, usually obtained through a bond additivity scheme, eq 12.[9]

$$E_{str}(\mathrm{RH}) = \Delta_f H^{\circ}(\mathrm{RH,g}) - \Delta_f H^{\circ}(\mathrm{RH^*,g}) \qquad (12)$$

Table 3 presents the calculated E_{str} for the title molecules, using the extended Laidler terms tabulated by Leal[32] to estimate the enthalpies of formation of the corresponding unstrained compounds. Our calculated E_{str} are in excellent agreement with the ring strain corrections (RSC, which are equivalent to E_{str}) obtained from the popular Benson group additivity method.[33,34] The results in Table 3 confirm the previous conclusions regarding the strain in the parent molecules: cyclopentane and cyclopentene are considerably strained while cyclohexane and cyclohexene are not. Although this agreement is reassuring, we still need to quantify the strain in the radicals.

A set of RSCs for hydrocarbon radicals, based on a consistent database of enthalpies of formation of radicals determined using ab initio calculations, was recently reported by Sabbe et al.[34] Unfortunately, this set of RSCs does not include all of the radicals investigated in the present study. However, computational chemistry also provides an alternative basis for evaluating SEs, as proposed by George et al.[35] These authors designed reactions that compare each carbon atom in the strained ring to a similar environment in an unstrained analogue and thus provide an estimate of SE. The construction of these reactions was systematized by Zhao and Gimarc in the *s*-homodesmotic model,[36] illustrated in eqs 13–15 for cyclopentane:[37]

$$s = 0 \qquad 5\ \mathrm{C_2H_6} \rightarrow \mathrm{cyclopentane} + 5\ \mathrm{CH_4} \qquad (13)$$

$$s = 1 \qquad 5\ \mathrm{C_3H_8} \rightarrow \mathrm{cyclopentane} + 5\ \mathrm{C_2H_6} \qquad (14)$$

$$s = 2 \qquad 5\ \mathrm{C_4H_{10}} \rightarrow \mathrm{cyclopentane} + 5\ \mathrm{C_3H_8} \qquad (15)$$

In the above reactions, each reactant molecule taken from the ring system has a length of $s + 2$ carbon atoms, and n reactant molecules are needed for an n-membered ring. An easy mnemonic to build these reactions is to go around the ring n times and take fragments of $s + 2$ carbon atoms for the reactants and $s + 1$ carbon atoms for the products. For instance, the $s = 1$ model for cyclopentene corresponds to reaction 16.

$$3\ \mathrm{C_3H_8} + 2\ \mathrm{CH_3CH{=}CH_2} \rightarrow \mathrm{cyclopentene} + 4\ \mathrm{C_2H_6} + \mathrm{C_2H_4} \qquad (16)$$

As detailed in Supporting Information, for $s = 0$ the reaction conserves both the number and formal types of bonds and is called isodesmic; when $s = 1$, the reaction also conserves the valence around each atom and is called homodesmotic; for $s = 2$, the valence environment around neighboring atoms is preserved as well and the reaction is said to be hyperhomodesmotic; and so on. In principle, computation of the enthalpy of any of reactions 13–15 yields an estimate of E_{str} in cyclopentane. However, the matching of structural elements increases as we consider larger fragments, and so should the accuracy of the calculated value. Indeed, Magers and co-workers have shown that the greater chemical similarity implicit in homodesmotic as compared to isodesmic reactions is essential for correct estimates, while results obtained with the homodesmotic and hyperhomodesmotic models were essentially identical. However, they also alerted to the possibility that an $s = 2$ and even an $s = 3$ *s*-homodesmotic model might be necessary in some cases,[37] as indeed we found out.

TABLE 4. Theoretical Strain Energies (E_{str}, in kJ mol^{-1}) Calculated by Using 1-Homodesmotic Reactions (See Text) for the Parent Molecules

molecule	B3LYP-TZ	CBS-Q	CBS-QB3	CCSD(T)
cyclopentane	22.9	27.4	28.3	28.2
cyclopentene	22.1	24.9	25.0	26.4
cyclohexane	2.1	−1.9	1.4	3.0
cyclohexene	6.6	4.3	5.9	8.4

Table 4 compiles the results of the calculated E_{str} using the homodesmotic model ($s = 1$) for the molecules discussed so far (the more complicated dienes will be analyzed separately), with the enthalpies of each species computed at various theory levels. There is a general good agreement not only between the results at the various theory levels in Table 4 but, most importantly, between the theoretical SEs and the corresponding data in Table 3. We thus feel confident to take the final step and use the same strategy to calculate the SEs of the radicals.

Construction of the homodesmotic reactions for the radicals follows the same rules as before.[38] Reaction 17 exemplifies this exercise for the cyclopentyl radical ($s = 1$).

$$\mathrm{isopropyl} + 2\ \mathrm{propyl} + 2\ \mathrm{propane} \rightarrow \mathrm{cyclopentyl} + 2\ \mathrm{ethyl} + 3\ \mathrm{ethane} \qquad (17)$$

Table 5 presents the results of these calculations for the radicals discussed so far. Again the results from the various theory levels are in good agreement and close to the available RSCs, with DFT displaying a slight tendency to underestimate the strain energies.

(32) Leal, J. P. *J. Phys. Chem. Ref. Data* **2006**, *35*, 55–76.
(33) Cohen, N. *J. Phys. Chem. Ref. Data* **1996**, *25*, 1411–1481.
(34) Sabbe, M. K.; Saeys, M.; Reyniers, M.-F.; Marin, G. B.; Van Speybroeck, V.; Waroquier, M. *J. Phys. Chem. A* **2005**, *109*, 7466–7480.
(35) George, P.; Trachtman, M.; Bock, C. W.; Brett, A. M. *J. Chem. Soc., Perkin Trans. 2* **1976**, 1222–1227.
(36) Zhao, M.; Gimarc, B. M. *J. Phys. Chem.* **1993**, *97*, 4023–4030.
(37) Lewis, L. L.; Turner, L. L.; Salter, E. A.; Magers, D. H. *THEOCHEM* **2002**, *592*, 161–171.
(38) To apply the *s*-homodesmotic model to the radicals, some new molecules are needed whose enthalpy was not previously calculated, such as the ethyl and the propyl radicals. The values for these molecules, which are not relevant for the discussion except in this regard, are given in Supporting Information.

TABLE 5. Theoretical Strain Energies (E_{str}, in kJ mol^{-1}) Calculated by Using 1-Homodesmotic Reactions (See Text) for the Radicals

molecule	B3LYP-TZ	CBS-Q	CBS-QB3	CCSD (T)	RSC[a]	exptl[b]
cyclopentyl	7.8	15.1	12.2	12.6	19.7	17.7
cyclopenten-4-yl	9.2	15.1	11.2	12.7		15.2
cyclohexyl	−2.0	−0.4	−2.4	−0.9	3.9	3.1
cyclohexen-4-yl	1.3	6.2	1.2	3.7		6.1
cyclopenten-3-yl	18.3	22.8	19.2	20.5	23.8	22.0
cyclohexen-3-yl	1.2	2.1	−0.9	1.7	3.5	3.0

[a] Ring strain corrections (RSC ≡ E_{str}) of Benson group additivity method from ref 34. [b] "Experimental" E_{str} values for the radicals calculated using eq 18 and the values in Tables 2 and 3.

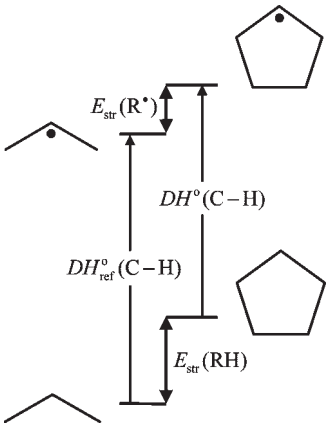

FIGURE 5. Relation between the strain energies (E_{str}) of the parent molecule and its radical, and the *relative* BDE, $\Delta DH°(C-H) = DH°(C-H) - DH^{\circ}_{ref}(C-H)$, for cyclopentane.

Table 5 also displays "experimental" E_{str} values for radicals. These data are based in Figure 5, which is a more precise depiction of the relation between strain energies and BDEs than Figure 4.

It is assumed in Figure 5 that the BDEs difference between propane and cyclopentane is due only to the strain of cyclopentane and its radical. The C2−H BDE in propane is the correct anchor to assess that difference: (1) isopropyl and cyclopentyl can both be stabilized to the same extent by hyperconjugation (the same being true for all the alkyl radicals in Table 5); (2) propane and isopropyl radical are suitable strain-free references for evaluating the strain energies of alkanes and the corresponding alkyl radicals, which are "destabilized" in relation to the references only by SE.[39] From Figure 5, eq 18, relating the BDEs and strain energies differences, is obtained.

$$\Delta DH^{\circ}(C-H) = DH^{\circ}(C-H) - DH^{\circ}_{ref}(C-H) = E_{str}(R^{\bullet}) - E_{str}(RH) \quad (18)$$

The values for the alkyl radicals in the last column of Table 5 were obtained by solving eq 18 for $E_{str}(R^{\bullet})$, with $E_{str}(RH)$ from Table 3 and $\Delta DH°(C-H)$ from Table 2. For the alkenes, a different reference has to be used when calculating $\Delta DH°(C-H)$. However, it cannot be the BDE in propene yielding the allyl radical, since this is only stabilized by resonance, whereas the cyclic allyl radicals in Table 5 are stabilized both by resonance and hyperconjugation. A suitable reference would then have to be either 1-butene or (*E*)-2-pentene, both yielding radicals stabilized in that same way (and therefore having equal BDEs). This is equivalent to adding the effect of one hyperconjugation, 11.9 kJ mol^{-1}, to the values of $\Delta DH°(C-H)$ in Table 2 before calculating $E_{str}(R^{\bullet})$ from eq 18 for the cycloalkenes. It is reassuring to find that the results from this procedure are in agreement with the theoretical SEs.[40]

Table 5 presents the final piece of the puzzle. It confirms the hypothesis that the strain is negligible for the six-membered radicals but significant in the five-membered ones, although smaller than in the corresponding parent molecules. Furthermore, it shows that the cyclopenten-3-yl radical is indeed more strained than the other two five-membered ring radicals and that, as predicted above, its strain energy is similar to the one in cyclopentene. Therefore, the fact that the BDEs in cyclopentene and in cyclohexene (yielding the allyl radicals) are equal is due to the high strain of the cyclopenten-3-yl radical.

We are now well equipped to search for the structural features that are responsible for the strain in the molecules listed in Tables 4 and 5. In our first approach, we were essentially attributing strain to deviations from normal bond angles. Yet, this angle (or Bayer) strain is just one of molecular strain types. Indeed, cyclopentane is not planar[41] due to eclipsing effects, responsible for torsional (or Pitzer) strain.[42] To minimize these repulsions, cyclopentane adopts a puckered conformation, where three C−C bonds can rest on a smaller energy gauche configuration. There is, however, a price to pay, since the two remaining bonds cannot escape from a higher energy, almost synperiplanar, configuration. The situation is similar in cyclopentene, where two C−C bonds (involving the three carbon atoms opposite the double bond) also adopt an almost synperiplanar configuration. Yet, when the corresponding alkyl radicals (cyclopentyl and cyclopenten-4-yl) are formed, the removal of the hydrogen atom decreases the repulsions with *both* the adjacent CH_2 groups, stabilizing the radical. This stabilization and the fact that the remaining interactions are identical in the parent molecules, explain the significantly smaller SEs in the alkyl radicals in relation to the parent molecules. On the other hand, in cyclopenten-3-yl the allyl moiety forces the radical to become planar, so that the C−C bond opposite to the allyl moiety cannot escape from a full synperiplanar configuration. It is this repulsive interaction that is responsible for the high SE of cyclopenten-3-yl as compared with the other two five-membered ring radicals.

1,4-Cyclohexadiene versus 1,3-Cyclopentadiene. The C−H BDE in 1,4-cyclohexadiene (326.3 kJ mol^{-1}) is essentially equal to the C−H BDE in 1,4-pentadiene (325.0 kJ mol^{-1}), which is a suitable strain-free reference because both radicals, pentadienyl and cyclohexadienyl, can be stabilized by delocalization through a five-carbon-atom system. This suggests that cyclohexadiene and its radical should also be devoid of strain. Indeed, Table 3 shows that E_{str} for 1,4-cyclohexadiene is negligible, and since its BDE is very close to the BDE in the reference strain-free

(39) Stability is a precise thermodynamic concept, measured for instance by the enthalpy of formation of a molecule, as in the definition of E_{str} in eq 12. As such, it is meaningless in comparing molecules with a different number of atoms. We are not discussing the stability of, for instance, propane versus cyclopentane. The words "stabilization" and "destabilization" refer to the effect of strain in each individual molecule, which is defined in relation to the hypothetical unstrained molecule, modeled in this case by propane or its radical.

(40) Note that the $E_{str}(R^{\bullet})$ values calculated with eq 18 used experimentally defined $E_{str}(RH)$ values from Table 3 and $\Delta DH°(C-H)$ results from Table 2 (selected from computational and experimental results). In this sense, they can be called "experimental" strain energies.

(41) Cyclopentane planarity would correspond to C−C−C angles of 108°, close to the 109° of a sp^3 hybridization.

(42) Smith, M. B.; March, J. *March's Advanced Organic Chemistry: Reactions, Mechanisms, and Structure*, 5th ed.; Wiley: New York, 2001.

TABLE 6. . Theoretical Strain Energies (E_{str}, in kJ mol^{-1}) Calculated by Using *s*-Homodesmotic Reactions ($s = 1-3$, from Top to Bottom) for the More Complicated Molecules

molecule	B3LYP-TZ	CBS-Q	CBS-QB3	CCSD (T)	RSC[a]	exptl[b]
1,4-cyclohexadiene	4.2	0.9	4.1	7.0		
	−7.6	4.1	−1.7	−2.9		
	−8.3	14.2	−0.8	−2.1	−0.7	−0.2
1,4-cyclohexadienyl	26.2	26.3	22.4	26.6		
	41.7	46.1	37.6	36.2		
	−2.1	23.7	−0.5	1.7	−0.3	1.1
1,3-cyclopentadiene	10.0	10.5	9.5	13.5		
	17.2	27.5	19.2	18.7		
	21.8	42.5	23.3	23.5	21.0	25.0

[a] Ring strain corrections (RSC ≡ E_{str}) of Benson group additivity method from ref.[34] [b] "Experimental" E_{str} values for the radicals calculated using eq 18 and the values in Tables 2 and 3.

molecule, the same can be predicted for E_{str} of cyclohexadienyl (cf. eq 18). Calculating E_{str} for 1,4-cyclohexadiene and its radical is considerably more demanding than in the previous examples but allows confirming this assertion. The summary of this exercise is displayed in Table 6, where it is shown that only a 3-homodesmotic model can provide a correct estimate of E_{str} for both 1,4-cyclohexadiene and its radical. The justification is based on the same simple chemical intuition that guided us to select the correct strain-free reference molecules for Figure 5 and eq 18. The reference for the 1,4-cyclohexadienyl radical is 1,4-pentadienyl. Therefore, an *s*-homodesmotic reaction whose enthalpy reflects only strain must include this reference, which is a fragment with $s + 2 = 5$ carbon atoms. Smaller reactants (e.g., reactions analogous to 16 and 17) cannot reproduce the bis-allylic stabilization in 1,4-cyclohexadienyl, and the resulting enthalpy would be in error by that difference. The same argument applies to the calculation of E_{str} for the parent molecule because 1,4-pentadiene must be included to balance all the relevant structural features. This can be confirmed by an analysis of the Benson groups or Laidler terms in both sides of the corresponding equation. A more detailed discussion on the application of *s*-homodesmotic reactions to evaluate SEs can be found in the Supporting Information.

Table 6 also shows that best estimates are obtained with CBS-QB3 and CCSD(T), which produce similar results. Surprisingly, DFT performs satisfactorily (having, nevertheless, a tendency to underestimate E_{str}) while CBS-Q largely overestimates E_{str}.

Regarding 1,3-cyclopentadiene, its C−H BDE is equal to the one in (*E*)-1,3-pentadiene. It is easy to understand that in this case 1,4-pentadiene would not be a suitable reference, because it does not possess the conjugated double bond that further stabilizes 1,3-pentadiene and 1,3-cyclopentadiene in relation to their 1,4- isomers. However, contrasting with the situation for 1,4-cyclohexadiene, Tables 3 and 6 indicate considerable strain in 1,3-cyclopentadiene. This fact is easily justified by angle strain alone. As shown in Figures 1 and 3, bond angles in 1,4-cyclohexadiene are close to standard values (124° for sp^2 and 113° for sp^3 carbons, identical to the corresponding angles in 1,4-pentadiene), whereas in 1,3-cyclopentadiene they are much narrower (109° for sp^2 and 103° for sp^3 carbons). Since its BDE is equal to the one in the strain-free reference, according to eq 18 cyclopentadienyl radical and 1,3-cyclopentadiene should have similar SEs. This is in keeping with the close geometric features of the two planar molecules. Hence, the strain, essentially angular, should affect both by a comparable amount.

A close inspection of cyclopentadienyl structure reveals additional interesting features. The normal bond lengths of a bis-allyl radical correspond to the ones in pentadienyl, which are equal to the ones in cyclohexadienyl radical (Figures 1 and 2). In relation to the parent molecule, they reflect a lengthening of the double bond (from 133 to 136 pm) and a shortening of the single (from 151 to 141 pm), symmetrically in relation to the radical center, indicative of delocalization through the five carbon atoms. However, the "bis-allyl" system in cyclopentadienyl (Figure 2) is not symmetrical. While bond lengths of one of the "allyl" groups change significantly, almost matching each other (139 and 140 pm), and are close to the bond lengths in the allyl radical (both 138 pm; see Figure 1), smaller changes are observed in the other allyl moiety.

The reason for the "asymmetry" in cyclopentadienyl radical is well studied and understood.[43] The more symmetrical D_{5h} geometry of this radical corresponds to a doubly degenerate state and therefore is subject to the Jahn−Teller effect: to lift the degeneracy, it will distort to a lower symmetry. A simple molecular orbital analysis shows that this can lead to either a compressed dienyl structure with a localized radical ($^2B_1$ state) or to an elongated structure comprised of an allyl radical plus a localized double bond ($^2A_2$ state), both with C_{2v} symmetry.[43] Recent calculations indicate that these two structures are very close in energy and ca. 19.3 kJ mol^{-1} more stable than the D_{5h} geometry.[44] The ground state of cyclopentadienyl was described as a Mexican hat case: the system pseudorotates around the D_{5h} geometry with little or no barrier, by alternately passing through the five equivalent geometries $^2A_2$ and the five $^2B_1$.[45] This dynamic effect was demonstrated by EPR studies, which gave indication of Jahn−Teller distortion below 70 K, while at high temperature the odd electron appears with equal probability on all five carbon atoms, consistent with the rapid pseudorotation.[46] Rotationally resolved spectroscopy of asymmetrically deuterated cyclopentadienyl radicals made it possible to assign the distortions to the two geometries $^2A_2$ and $^2B_1$.[47] Our computed ground-state geometry is compatible with the $^2A_2$ state and is in very good agreement with previous ones.[43–45,48,49] This state is therefore a correct thermodynamic description of the ground-state cyclopentadienyl radical, further confirmed by the agreement between the calculated and experimental C−H BDE of 1,3-cyclopentadiene.[17]

Unfortunately, it is not possible to estimate the SE for cyclopentadienyl with the *s*-homodesmotic model. Even the corresponding 3-homodesmotic reaction is unbalanced because it results in three bis-allylic radicals versus one cyclopentadienyl, eq 19, a situation that does not happen with the cyclohexadienyl radical, eq 20.[50] Attempting to define a reaction with $s = 4$ is

(43) See, e.g., Applegate, B. E.; Miller, T. A.; Barckholtz, T. A. *J. Chem. Phys.* **2001**, *114*, 4855–4868, and references therein.
(44) Cunha, C.; Canuto, S. *THEOCHEM* **1999**, *464*, 73–77.
(45) Zilberg, S.; Haas, Y. *J. Am. Chem. Soc.* **2002**, *124*, 10683–10691.
(46) Liebling, G. R.; McConnel, H. M. *J. Chem. Phys.* **1965**, *42*, 3931–3934.
(47) Yu, L.; Cullin, D. W.; Williamson, J. M.; Miller, T. A. *J. Chem. Phys.* **1993**, *98*, 2682–2698.
(48) Zhou, X.; Hrovat, D. A.; Borden, W. T. *J. Am. Chem. Soc.* **2007**, *129*, 10785–10794.
(49) At our theory level for structure optimization (B3LYP/cc-pVTZ), vibrational frequency analysis shows that the dienyl-like structure ($^2B_1$) is not a minimum on the potential energy surface but is essentially isoenergetic with the allylic structure (the energy difference is only ca. 3 J mol^{-1}), in agreement with the previous computations.
(50) When designing these equations, note that apparently different structures are in fact the same radical, such as 1,3-pentadien-5-yl, 1,4-pentadien-3-yl or simply pentadienyl, and 1-methylallyl or 2-buten-1-yl.

of course impossible for cyclopentadienyl for it would require fragments with $s + 2 = 6$ carbon atoms.

3 pentadienyl + 2 2-penten-4-yl → cyclopentadienyl + 4 1-metylallyl + butadiene (19)

pentadienyl + 2 2-penten-4-yl + 2 penten-1-yl + 1,4-pentadiene → cyclohexadienyl + 4 1-metylallyl + 2 1-butene (20)

Despite the shortcomings of the *s*-homodesmotic model in predicting the SE of cyclopentadienyl radical, it was possible to conclude that the SEs in cyclopentadienyl and 1,3-cyclopentadiene must be comparable (see above). Therefore, the higher BDE in 1,3-cyclopentadiene in relation to the BDE in 1,4-cyclohexadiene is essentially due to a ground-state or parent effect (identical to the relation between 1,3- and 1,4-pentadiene):[8] It is a stabilization of 1,3-cyclopentadiene due to the conjugated double bond rather than a destabilization of the radical due to impaired delocalization, that is responsible for the higher BDE.

Conclusions

The carbon−hydrogen BDEs in the five- and six-membered ring hydrocarbons differ noticeably, and the difference is attributed to strain, a concept that we use in the conventional way of Cox and Pilcher,[9] i.e., including all the stabilizing and destabilizing effects relative to strain-free reference molecules. The relation between BDEs and strain energy (SE) is given by Figure 5 or eq 18. Since strain can affect parent molecules and radicals differently, a comprehensive discussion must discriminate between these two. Although the evaluation of SE in radicals is more complex than in parent molecules, both cases can be addressed through quantum chemistry calculations by using the *s*-homodesmotic model. This methodology is a rather convenient way to design chemical reactions whose enthalpies can be identified with the SE of a given molecule. The results can then be assessed by comparison with experimental data through eq 18.

The systematization of the structural features provided by group additivity methods helps selecting the adequate *s*-homodesmotic model for a given molecule. Furthermore, the calculation of SEs with the same *s*-homodesmotic model should afford good estimates (due to error cancelation), and failure to verify eq 18 alerts to faults in the chosen model (see Supporting Information). The sources of error can then be easily identified by checking the balance of group additivity terms. It was also noted that CBS-QB3 yields SE results very similar to the much more expensive CCSD(T) method. DFT performance is poorer but acceptable in most cases, while CBS-Q shows a somewhat erratic behavior.

We concluded that a correct estimate of SE is obtained for alkanes, alkenes, and alkyl radicals with the 1-homodesmotic model, whereas allyl radicals are best described with 2-homodesmotic reactions (although a good approximation is obtained with the 1-homodesmotic). For unconjugated dienes like 1,4-cyclohexadiene, the 2-homodesmotic model must be used, while for conjugated dienes like 1,3-cyclopentadiene the requirement increases to 3-homodesmotic. For the corresponding bis-allyl radicals, the SE of cyclohexadienyl is only satisfactorily described by the 3-homodesmotic model, which however cannot be applied to cyclopentadienyl.

Our results justified the trends in BDEs by determining that the five-membered hydrocarbons all have considerable and similar strain, in the order 1,3-cyclopentadiene < cyclopentene < cyclopentane. Analysis of the corresponding structures indicates that the strain in 1,3-cyclopentadiene is essentially angular. This, together with torsional strain, should also affect cyclopentene, with torsional strain being stronger in cyclopentane. The six-membered hydrocarbons are nearly strain-free, in the order 1,4-cyclohexadiene < cyclohexane < cyclohexene. The small strain in cyclohexene relative to cyclohexane might be due to its increased rigidity, which prevents the carbon atoms from adopting fully staggered configurations, leading to an increase of torsional strain. Six-membered radicals are also almost devoid of strain, while their five-membered counterparts display considerable strain. However, the alkyl radicals cyclopentyl and cyclopenten-4-yl have SEs that are ca. 10−15 kJ mol^{-1} less than those of the corresponding parent molecules. The corresponding BDEs are, therefore, smaller than the equivalent BDEs in the six-membered hydrocarbons by a similar amount. The SE in the rigid cyclopenten-3-yl is closer to the SE in the parent molecule, leading to a BDE similar to those in the unstrained molecules cyclohexene and cyclohexen-3-yl. Finally, the BDE in 1,3-cyclopentadiene is considerable higher than in the unstrained 1,4-cyclohexadiene. However, we estimate that the conventional strain is similar in 1,3-cyclopentadiene and in its radical. Therefore, the higher BDE in 1,3-cyclopentadiene is attributed not to a destabilizing strain effect in the radical but to a stabilizing effect in the parent molecule due to the conjugated double bond, thus mimicking the relation between the BDEs in the 1,3- and 1,4-pentadienes.

Finally, we would like to refer to the recent statement[51] that, even in these days of increasingly accurate quantum chemistry methods, empirical schemes still have an important role to play, thanks to the chemical insight that they afford. We feel the present study to be a good example of this.

Experimental Section

Materials. Benzene (HPLC grade, 99.9+ %), was used without further purification. Cyclopentane (purity >99%) was used as received. Cyclohexane (HPLC grade, 99.9+%) was used as received. Di-*tert*-butylperoxide was purified according to a literature procedure.[52] *o*-Hydroxybenzophenone was recrystallized twice from an ethanol−water mixture.

Photoacoustic Calorimetry. The basis of photoacoustic calorimetry,[6,53] our photoacoustic calorimeter setup,[17,54] and the experimental technique are described in detail elsewhere.[17,55] Briefly, argon-purged solutions in benzene of ca. 0.4 M di-*tert*-butylperoxide and an adequate concentration (see Results) of each organic molecule studied (cyclopentane and cyclohexane) were flowed through a quartz flow cell (Hellma 174-QS) and photolyzed with pulses from a nitrogen laser (337.1 nm, pulse width 800 ps). The incident laser energy was varied by using neutral density filters (ca. 5−30 μJ/pulse at the cell, flux <40 J m^{-2}). Each laser pulse triggered a photochemical process (see below) that induced a sudden volume change in solution, which generated an acoustic wave, detected by a piezoelectric transducer (0.5 MHz) in contact with the bottom of the cell. The signals were amplified and measured by a digital oscilloscope. The signal-to-noise ratio was improved by averaging 32 acquisitions for each data point obtained at a given

(51) Walsh, R. *Chem. Soc. Rev.* **2008**, *37*, 686–698.
(52) Diogo, H. P.; Minas da Piedade, M. E.; Martinho Simões, J. A.; Nagano, Y. *J. Chem. Thermodyn.* **1995**, *27*, 597–604.
(53) Braslavsky, S. E.; Heibel, G. E. *Chem. Rev.* **1992**, *92*, 1381–1410.
(54) Borges dos Santos, R. M.; Lagoa, A. L. C.; Martinho Simões, J. A. *J. Chem. Thermodyn.* **1999**, *31*, 1483–1510.
(55) Correia, C. F.; Nunes, P. M.; Borges dos Santos, R. M.; Martinho Simões, J. A. *Thermochim. Acta* **2004**, *420*, 3–11.

laser energy. The apparatus was calibrated by carrying out a photoacoustic run using an optically matched solution of *o*-hydroxybenzophenone (in the same mixtures but without the peroxide), which dissipates all of the absorbed energy as heat.[53] All experiments were performed at 293 ± 1 K. For each run (experiment or calibration), four data points were collected corresponding to four different laser intensities obtained using the neutral density filters. The resulting waveforms from each data point were recorded for subsequent mathematical analysis, affording two waveforms for each point: sample and calibration. The analysis involved, for each laser energy, first the normalization of both waveforms and then the deconvolution of the sample waveform with the calibration waveform[56] using the software Sound Analysis.[57]

Theoretical Calculations. The theoretical procedures used in the present work were essentially the same outlined in our foregoing study.[8] Briefly, all geometries were optimized by density functional theory (DFT), using the B3LYP hybrid functional[58] together with the cc-pVTZ basis set.[59] The selection of this method was dictated by its known accuracy and cost-effectiveness.[60,61] In fact, it is known to outperform highly correlated (and thus, computationally demanding) wave-function-based methods such as MP2[62] or CCSD(T)[63] in this particular domain.[64] Vibrational frequencies were computed for all optimized geometries, allowing further confirmation that these were minima of the respective potential energy surfaces. Additionally, this analysis afforded the thermal correction to the energy at 298.15 K as well as the zero-point energy correction for each species. The corresponding enthalpies were then computed by adding these corrections to the energies of the respective optimized geometries. Enthalpies were also computed using two composite procedures, namely, CBS-Q and CBS-QB3,[65–67] as well as with a dual (D,T) scheme to complete basis set extrapolation of CCSD(T) energies relying on cc-pVDZ and cc-pVTZ calculations proposed by Truhlar.[68] This was necessary since previous works have shown that DFT behaves erratically in the determination of bond dissociation enthalpies.[69,70] The CBS methods, particularly CBS-QB3, as well as the (D,T) extrapolation, have shown to be adequate tools for the study of BDEs.[8] The B3LYP/cc-pVTZ calculations were also used to determine Mulliken atomic spin densities[71–74] for the radical species under study. Although this population analysis can prove to be unreliable and is, by definition, basis-set-dependent, it has been successfully used, for example, in the study of heterosubstituted allyl radicals[75] and in our previous study on the allylic moiety.[8] All calculations were carried out using the Gaussian-03[76] or the PSI3[77] programs.

Acknowledgment. P.M.N. and F.A. thank Fundação para a Ciência e a Tecnologia, Portugal, for a postdoctoral (SFRH/BPD/26677/2006) and a Ph.D. (SFRH/BD/22854/2005) grant, respectively.

Supporting Information Available: Detailed description of the rules for selecting the *s*-homodesmotic model. Tables containing computed optimized geometries and total energies for radicals and parent compounds. Complete list of reactions used to estimate strain energies with the *s*-homodesmotic model. This material is available free of charge via the Internet at http://pubs.acs.org.

JO800690M

(56) Rudzki, J. E.; Goodman, J. L.; Peters, K. S. *J. Am. Chem. Soc.* **1985**, *107*, 7849–7854.
(57) *Sound Analysis*, version 1.50D; Quantum Northwest: Spokane, WA, 1999.
(58) Becke, A. D. *J. Chem. Phys.* **1993**, *98*, 5648–5652.
(59) Dunning, T. H., Jr. *J. Chem. Phys.* **1989**, *90*, 1007–1023.
(60) Agapito, F.; Costa Cabral, B. J.; Martinho Simões, J. A. *THEOCHEM* **2007**, *811*, 361–372.
(61) Wang, N. X.; Wilson, A. K. *J. Chem. Phys.* **2004**, *121*, 7632–7646.
(62) Møller, C.; Plesset, M. S. *Phys. Rev.* **1934**, *46*, 618–622.
(63) Raghavachari, K.; Trucks, G. W.; Pople, J. A.; Head-Gordon, M. *Chem. Phys. Lett.* **1989**, *157*, 479–483.
(64) Byrd, E. F. C.; Sherrill, C. D.; Head-Gordon, M. *J. Phys. Chem. A* **2001**, *105*, 9736–9747.
(65) Ochterski, J. W.; Petersson, G. A.; Montgomery, J. A. *J. Chem. Phys.* **1996**, *104*, 2598–2619.
(66) Montgomery, J. A.; Frisch, M. J.; Ochterski, J. W.; Petersson, G. A. *J. Chem. Phys.* **1999**, *110*, 2822–2827.
(67) Montgomery, J. A.; Frisch, M. J.; Ochterski, J. W.; Petersson, G. A. *J. Chem. Phys.* **2000**, *112*, 6532–6542.
(68) Truhlar, D. G. *Chem. Phys. Lett.* **1998**, *294*, 45–48.
(69) Cabral do Couto, P.; Guedes, R. C.; Costa Cabral, B. J.; Martinho Simões, J. A. *Int. J. Quantum Chem.* **2002**, *86*, 297–304.
(70) Agapito, F.; Costa Cabral, B. J.; Martinho Simões, J. A. *THEOCHEM* **2005**, *729*, 223–227.
(71) Mulliken, R. S. *J. Chem. Phys.* **1955**, *23*, 1833–1840.
(72) Mulliken, R. S. *J. Chem. Phys.* **1955**, *23*, 1841–1846.
(73) Mulliken, R. S. *J. Chem. Phys.* **1955**, *23*, 2338–2342.
(74) Mulliken, R. S. *J. Chem. Phys.* **1955**, *23*, 2343–2346.
(75) Wiberg, K. B.; Cheeseman, J. R.; Ochterski, J. W.; Frisch, M. J. *J. Am. Chem. Soc.* **1995**, *117*, 6535–6543.
(76) Frisch, M. J.; Trucks, G. W.; Schlegel, H. B.; Scuseria, G. E.; Robb, M. A.; Cheeseman, J. R.; Jr.; Vreven, T.; Kudin, K. N.; Burant, J. C.; Millam, J. M.; Iyengar, S. S.; Tomasi, J.; Barone, V.; Mennucci, B.; Cossi, M.; Scalmani, G.; Rega, N.; Petersson, G. A.; Nakatsuji, H.; Hada, M.; Ehara, M.; Toyota, K.; Fukuda, R.; Hasegawa, J.; Ishida, M.; Nakajima, T.; Honda, Y.; Kitao, O.; Nakai, H.; Klene, M.; Li, X.; Knox, J. E.; Hratchian, H. P.; Cross, J. B.; Bakken, V.; Adamo, C.; Jaramillo, J.; Gomperts, R.; Stratmann, R. E.; Yazyev, O.; Austin, A. J.; Cammi, R.; Pomelli, C.; Ochterski, J. W.; Ayala, P. Y.; Morokuma, K.; Voth, G. A.; Salvador, P.; Dannenberg, J. J.; Zakrzewski, V. G.; Dapprich, S.; Daniels, A. D.; Strain, M. C.; Farkas, O.; Malick, D. K.; Rabuck, A. D.; Raghavachari, K.; Foresman, J. B.; Ortiz, J. V.; Cui, Q.; Baboul, A. G.; Clifford, S.; Cioslowski, J.; Stefanov, B. B.; Liu, G.; Liashenko, A.; Piskorz, P.; Komaromi, I.; Martin, R. L.; Fox, D. J.; Keith, T.; Al-Laham, M. A.; Peng, C. Y.; Nanayakkara, A.; Challacombe, M.; Gill, P. M. W.; Johnson, B.; Chen, W.; Wong, M. W.; Gonzalez, C.; Pople, J. A. *Gaussian 03*, revision C.02; Gaussian Inc.; Wallingford, CT, 2004.
(77) Crawford, T. D.; Sherrill, C. D.; Valeev, E. F.; Fermann, J. T.; King, R. A.; Leininger, M. L.; Brown, S. T.; Janssen, C. L.; Seidl, E. T.; Kenny, J. P.; Allen, W. D. *J. Comput. Chem.* **2007**, *28*, 1610–1616.

Supporting information

S1. Selecting the *s*-Homodesmotic Model

To obtain correct estimates of SEs, the *s*-homodesmotic model should be chosen according to the complexity of the molecule under study, and examples were given that require *s*-homodesmotic models with *s* from 1 to 3. Group additivity methods, which systematize the enthalpy contributions of molecular structural features, provide a straightforward way to check if a chosen *s*-homodesmotic reaction is balanced in all but the strain of the target molecule. For instance, consider reactions 13 and 14, corresponding to $s = 0$ and 1 respectively, which can be used to estimate E_{str} in cyclopentane. Table ST1 displays the Benson group terms corresponding to the reactants and products of each reaction. It is clearly seen that these are perfectly balanced for eq 14 (and the same can be shown for $s \geq 2$), but not for eq 13, which justifies the requirement of using at least $s = 1$ to obtain a correct estimate of the SE in cyclopentane.

$s = 0$ $\qquad 5\ C_2H_6 \rightarrow \text{cyclopentane} + 5\ CH_4$ (13)

$s = 1$ $\qquad 5\ C_3H_8 \rightarrow \text{cyclopentane} + 5\ C_2H_6$ (14)

TABLE ST1. Analysis of Eqs 13 and 14 Using Benson Group Terms

Eq	Reactants	Products
13 ($s = 0$)	$2[C–(C)(H)_3]\times5$	$5[C–(C)_2(H)_2]$
		$[C–(H)_4]\times5$
14 ($s = 1$)	$[C–(C)_2(H)_2]\times5$	$5[C–(C)_2(H)_2]$
	$2[C–(C)(H)_3]\times5$	$2[C–(C)(H)_3]\times5$

An additional and more thorough test is provided by eq 18, after introducing the chemical equations that are used to evaluate each individual term, namely the *s*-homodesmotic equations used for evaluating $E_{str}(R^{\bullet})$ and $E_{str}(RH)$, and eq 9 (with R′ =

strain-free reference) for calculating $\Delta DH^{\circ}(\mathrm{C-H})$. This is exemplified next for the 1-homodesmotic model applied to cyclopentane/cyclopentyl.

The enthalpies of reactions S1 (eq 17) and S2 (the reverse of reaction 14) correspond to $E_{\mathrm{str}}(\mathrm{R}^{\bullet})$ and $-E_{\mathrm{str}}(\mathrm{RH})$, respectively, and the sum, ΔE_{str}, is given by eq S3.

$$\text{isopropyl} + 2\ \text{propyl} + 2\ \text{propane} \rightarrow \text{cyclopentyl} + 2\ \text{ethyl} + 3\ \text{ethane} \qquad \text{(S1)}$$

$$\text{cyclopentane} + 5\ \text{ethane} \rightarrow 5\ \text{propane} \qquad \text{(S2)}$$

$$\text{cyclopentane} + \text{isopropyl} + 2\ \text{propyl} + 2\ \text{ethane} \rightarrow \text{cyclopentyl} + 2\ \text{ethyl} + 3\ \text{propane} \qquad \text{(S3)}$$

On the other hand, $\Delta DH^{\circ}(\mathrm{C-H})$ is given by eq 9 with R′ = propane, eq S4.

$$\text{cyclopentyl} + \text{propane} \rightarrow \text{cyclopentane} + \text{isopropyl} \qquad \text{(S4)}$$

From eq 18, $\Delta DH^{\circ}(\mathrm{C-H}) = \Delta E_{\mathrm{str}}$, i.e., subtracting the last two equations should yield a thermoneutral reaction. Indeed, the resulting reaction corresponds to twice eq S5, whose enthalpy is the difference between the C–H BDE in ethane and the C1–H BDE in propane, which should be very close to zero. This result confirms that the 1-homodesmotic model is adequate to assess the SEs in alkane molecules and the corresponding alkyl radicals. It also justifies the good agreement between the experimental and the theoretical $E_{\mathrm{str}}(\mathrm{R}^{\bullet})$ values for these molecules, obtained with the 1-homodesmotic model.

$$\text{propyl} + \text{ethane} \rightarrow \text{propane} + \text{ethyl} \qquad \text{(S5)}$$

The exercise can be repeated for the remaining parent/radical pairs discussed in the present study. While tedious, it allows gaining considerable insight into what

constitutes an adequate *s*-model for the estimation of the SE of any molecule. For instance, considering the alkene molecules and the corresponding alkyl radicals, the exercise is identical to the example above and the same final result (eq S5) is obtained, proving that the 1-homodesmotic model is also adequate in this case. However, for alkene molecules and the corresponding allyl radicals, the good agreement between experimental and theoretical E_{str} values is somewhat surprising. Table ST2 shows the Benson group analysis of eqs 16 (*s* = 1) and S6 (*s* = 2), corresponding to the application of the *s*-homodesmotic model to cyclopentene.

$$3\ C_3H_8 + 2\ CH_3CH{=}CH_2 \rightarrow \text{cyclopentene} + 4\ C_2H_6 + C_2H_4 \qquad (16)$$

$$2\ \text{1-butene} + 2\ \text{butane} + \text{2-butene} \rightarrow \text{cyclopentene} + 3\ \text{propane} + 2\ \text{propene} \qquad (S6)$$

TABLE ST2. Analysis of Eqs 16 and S6 Using Benson Group Terms

Eq	Reactants		Products	
16	[C–(C$_2$)(H)$_2$]×3	[C–(C$_d$)(H)$_2$]×2	[C–(C$_2$)(H)$_2$]	2[C–(C)(H)$_3$]×4
(*s* = 1)	2[C–(C)(H)$_3$]×3	[C$_d$–(C$_d$)(H)$_2$]×2	2[C–(C$_d$)(C)(H)]	2[C$_d$–(C$_d$)(H)$_2$]
		[C$_d$–(C$_d$)(C)(H)]×2	2[C$_d$–(C$_d$)(C)(H)]	
S6	[C$_d$–(C$_d$)(H)$_2$]×2	2[C–(C)(H)$_3$]×2	[C–(C$_2$)(H)$_2$]	2[C–(C)(H)$_3$]×3
(*s* = 2)	[C$_d$–(C$_d$)(C)(H)]×2	2[C–(C$_2$)(H)$_2$]×2	2[C–(C$_d$)(C)(H)]	[C–(C$_d$)(H)$_2$]×2
	[C–(C$_d$)(C)(H)$_2$]×2	2[C$_d$–(C$_d$)(H)]	2[C$_d$–(C$_d$)(C)(H)]	[C$_d$–(C$_d$)(H)$_2$]×2
	[C–(C)(H)$_3$]×2	2[C$_d$–(C$_d$)(C)(H)]	[C–(C$_2$)(H)$_2$]×3	[C$_d$–(C$_d$)(C)(H)]×2

Table ST2 shows that eq 16 is not balanced, but in eq S6 reactants and products are described by the same number and type of terms. This indicates that the correct model for cyclopentene corresponds to *s* = 2, and that *s* = 1 should *not* have yielded the good estimates displayed in Table 4. The same can be concluded for cyclohexene, and also for cyclopenten-3-yl and cyclohexen-3-yl radicals (Table 5). To clarify this situation

we shall make use again of eq 18. The E_{str} values referred to above were obtained with the 1-homodesmotic model but with eq 18 using 1-methylallyl as the strain-free reference. The analysis of the final result (eq S7) is considerably more difficult than in the previous cases.

allyl + propyl + isopropyl + 2 ethane + 1-butene

$$\rightarrow \text{propene} + 2\ \text{propane} + 2\ \text{ethyl} + \text{1-methylallyl} \qquad \text{(S7)}$$

Fortunately, to justify the model we no longer need to carry out a detailed analysis of the terms involved, but only to prove that eq S7 is thermoneutral. This is a trivial exercise, since we have computed the energies of all the species involved. The results are –4.4 (B3LYP), –1.6 (CBS-Q), –4.4 (CBS-QB3) and –4.9 kJ mol^{-1} (CCSD(T)) for the enthalpy of reaction S7. Therefore, the 1-homodesmotic model can be applied to alkene molecules and allyl radicals, in keeping with the results in Tables 4 and 5.

While the previous conclusion is reassuring, the 2-homodesmotic should be a better model to deal with alkenes and allyl radicals. This is because, as stated, the correct reference molecules are now 1-butene and 1-methylallyl, with $s + 2 = 4$ carbon atoms. Repeating the exercise with the $s = 2$ model and 1-methylallyl as the reference in eq 18, eq S8 is obtained.

buten-1-yl + buten-2-yl + 2 propane + 1-methylallyl + propene

$$\rightarrow \text{propyl} + \text{isopropyl} + 2\ \text{butane} + \text{2-butene} + \text{allyl} \qquad \text{(S8)}$$

Eq S8 can be decomposed into eqs S9 to S11, each one with enthalpies corresponding to the differences between two very similar C–H BDEs: C2–H in butane and propane (S9), C1–H in butane and propane (S10), and C(sp^3)–H in 2-butene and propene (S11).[1] Therefore, one concludes that reaction S9 is thermoneutral.

$$\text{buten-2-yl} + \text{propane} \rightarrow \text{butane} + \text{isopropyl} \qquad \text{(S9)}$$

$$\text{buten-1-yl} + \text{propane} \rightarrow \text{butane} + \text{propyl} \qquad \text{(S10)}$$

1-methylallyl + propene→ 2-butene+ allyl (S11)

As summarized in Table ST3, the application of the 2-homodesmotic model to the alkene/allyl pairs studied in this work shows a general improvement in the agreement between the experimental SE values and those obtained from theoretical methods (particularly the most reliable ones, CBS-QB3 and CCSD(T)). The improvement over the 1-homodesmotic model is however small, and may not justify the increasing complexity of dealing with larger molecules.

We conclude this section by stating that, using the strategy explained in the previous examples for the remaining types of molecules investigated in this study, the conclusions drawn in the main text regarding the selection of the correct *s*-homodesmotic model can be demonstrated. For easy reference, they are compiled in Table ST4.

TABLE ST3. Theoretical Strain Energies (E_{str} ; in kJ mol^{-1}) Calculated by Using *s*-Homodesmotic Reactions (*s* = 1 to 2, from top to bottom) for the Alkene Molecules and Allyl Radicals Studied.

molecule	B3LYP-TZ	CBS-Q	CBS-QB3	CCSD(T)	RSC [a]	"Exp" [b]
cyclopentene	22.1	24.9	25.0	26.4		
	15.5	30.5	23.0	22.2	22.9	23.8
cyclohexene	6.6	4.3	5.9	8.4		
	–0.3	12.0	4.4	4.6	4.7	5.3
cyclopenten-3-yl	18.3	22.8	19.2	20.5		
	18.8	26	23.3	22.2	23.8	22.0
cyclohexen-3-yl	1.2	2.1	–0.9	1.7		
	1.3	7.4	3.7	3.8	3.5	3.0

[a] Ring strain corrections (RSC ≡ E_{str}) of Benson group additivity method from ref 2. [b] "Experimental" E_{str} values for the radicals calculated using eq 18 and the values in Tables 2 and 3.

TABLE ST4. Minimum *s*-Homodesmotic Model that Allows Correct SE Estimation for a Given Parent Molecule/Radical Type

Parent Molecule type	*s*	Radical type	*s*
Alkane	1	Alkyl	1
Alkene	1	Allyl	1
	(2 better)		(2 better)
Unconjugated diene	2	Bis-allyl	
Conjugated diene	3	(from unconjugated diene)	3

Note: Model applicable for molecules with n carbon atoms, $n > s + 2$.

References for S1:

(1) Agapito, F.; Nunes, P. M.; Costa Cabral, B. J.; Borges dos Santos, R. M.; Martinho Simões, J. A. *J. Org. Chem.* **2007**, *72*, 8770-8779.

(2) Sabbe, M. K.; Saeys, M.; Reyniers, M.-F.; Marin, G. B.; Van Speybroeck, V.; Waroquier, M. *J. Phys. Chem. A* **2005**, *109*, 7466-7480.

Bibliography

[1] M. Nic, J. Jirat, B. Kosata, A. Jenkins, and A. McNaughtand A. Wilkinson, *IUPAC Compendium of Chemical Terminology*, IUPAC, 2nd ed., 2009.

[2] M. Gomberg, *An Instance Of Trivalent Carbon: Triphenylmethyl*, J. Am. Chem. Soc. **22**, 757 (1900).

[3] C. Schoepfle and W. Bachmann, *Moses Gomberg 1866-1947*, J. Am. Chem. Soc. **69**, 2921 (1947).

[4] M. B. Smith and J. March, *March's Advanced Organic Chemistry: Reactions, Mechanisms, and Structure*, Wiley-Interscience, Hoboken, NJ, 6th ed., 2007.

[5] D. L. Nelson and M. M. Cox, *Lehninger Principles of Biochemistry*, W. H. Freeman, New York, 4th ed., 2004.

[6] M. Dizdaroglu, P. Jaruga, M. Birincioglu, and H. Rodriguez, *Free Radical-Induced Damage to DNA: Mechanisms and Measurement*, Free Radical Bio. Med. **32**, 1102 (2002).

[7] F. S. Rowland, *Stratospheric Ozone Depletion*, Phil. Trans. R. Soc. B **361**, 769 (2006).

[8] J. K. Donnelly and D. S. Robinson, *Invited Review: Free Radicals in Foods*, Free Rad. Res. **22**, 147 (1995).

[9] F. Gerson and W. Huber, *Electron Spin Resonance Spectroscopy of Organic Radicals*, Wiley-VCH, Weinheim, 2003.

[10] R. A. Moss, M. S. Platz, and M. Jones, *Reactive Intermediate Chemistry*, Wiley, Hoboken, NJ, 2003.

[11] H. Afeefy, J. Liebman, and S. Stein, *Neutral Thermochemical Data in NIST Chemistry WebBook*, NIST Standard Reference Database Number 69, Eds.

P.J. Linstrom and W.G. Mallard, National Institute of Standards and Technology, Gaithersburg MD, `http://webbook.nist.gov` (retrieved December 15, 2009).

[12] Y. Luo, *Comprehensive Handbook of Chemical Bond Energies*, CRC Press, Boca Raton, FL, 2007.

[13] J. A. Martinho Simões and M. E. Minas da Piedade, *Molecular Energetics: Condensed-Phase Thermochemical Techniques*, Oxford University Press, New York, 2008.

[14] J. Cox, D. Wagman, and V. Medvedev, *CODATA Key Values for Thermodynamics*, Hemisphere Publishing, New York, 1989.

[15] J. Berkowitz, G. B. Ellison, and D. Gutman, *Three Methods to Measure RH Bond Energies*, J. Phys. Chem. **98**, 2744 (1994).

[16] R. M. Borges dos Santos, A. L. C. Lagoa, , and J. A. Martinho Simões, *Photoacoustic Calorimetry. An Examination of a Non-Classical Thermochemistry Tool*, J. Chem. Thermodynamics **31**, 1483 (1999).

[17] L. J. J. Laarhoven, P. Mulder, and D. D. M. Wayner, *Determination of Bond Dissociation Enthalpies in Solution by Photoacoustic Calorimetry*, Acc. Chem. Res. **32**, 342 (1999).

[18] J. E. Rudzki, J. L. Goodman, and K. S. Peters, *Simultaneous Determination of Photoreaction Dynamics and Energetics Using Pulsed, Time-Resolved Photoacoustic Calorimetry*, J. Am. Chem. Soc. **107**, 7849 (1985).

[19] L. J. J. Laarhoven and P. Mulder, *α-C—H Bond Strengths in Tetralin and THF: Application of Competition Experiments in Photoacoustic Calorimetry*, J. Phys. Chem. B **101**, 73 (1997).

[20] C. F. Correia, P. M. Nunes, R. M. Borges dos Santos, and J. A. Martinho Simões, *Gas-Phase Energetics of Organic Free Radicals Using Time-Resolved Photoacoustic Calorimetry*, Thermochim. Acta **420**, 3 (2004).

[21] V. S. F. Muralha, R. M. Borges dos Santos, and J. A. Martinho Simões, *Energetics of Alkylbenzyl Radicals: A Time-Resolved Photoacoustic Calorimetry Study*, J. Phys. Chem. A **108**, 936 (2004).

[22] *Sound Analysis (version 1.50D)*, Quantum Northwest, Spokane, WA, 1999.

[23] R. M. Borges dos Santos, B. J. Costa Cabral, and J. A. Martinho Simões, *Bond-Dissociation Enthalpies in the Gas-Phase and in Organic Solvents: Making Ends Meet*, Pure Appl. Chem. **79**, 1369 (2007).

[24] M. Planck, *Üeber das Gesetz der Energieverteilung im Normalspectrum*, Ann. Phys. **309**, 553 (1901).

[25] A. Einstein, *Einstein's Miraculous Year: Five Papers That Changed the Face of Physics*, Princeton University Press, Princeton, NJ, 2005.

[26] N. Bohr, *I. On the Constitution of Atoms and Molecules*, Phil. Mag. (6) **26**, 1 (1913).

[27] E. Rutherford, *LXXIX. The Scattering of α and β Particles by Matter and the Structure of the Atom*, Phil. Mag. (6) **21**, 669 (1911).

[28] L. V. P. R. de Broglie, *Recherches sur la Théorie des Quanta*, PhD thesis, Université de Paris, 1924.

[29] M. Born, W. Heisenberg, and P. Jordan, *Zur Quantenmechanik. II*, Zeit. Phys. **35**, 557 (1926).

[30] M. Born, *Zur Quantenmechanik der Stoßvorgänge*, Zeit. Phys. **37**, 863 (1926).

[31] M. Born and P. Jordan, *Zur Quantenmechanik*, Zeit. Phys. **34**, 858 (1925).

[32] W. Heisenberg, *Über den anschaulichen Inhalt der quantentheoretischen Kinematik und Mechanik*, Zeit. Phys. **43**, 172 (1927).

[33] B. L. van der Waerden, *Sources of Quantum Mechanics*, Dover, Mineola, NY, 2007.

[34] E. Schrödinger, *Collected Papers on Wave Mechanics*, American Mathematical Society, Providence, RI, 3rd ed., 2003.

[35] L. Piela, *Ideas of Quantum Chemistry*, Elsevier, Amsterdam, 2007.

[36] D. Papenfuß, D. Lüst, and W. P. Schleich, *100 Years Werner Heisenberg: Works and Impact*, Wiley-VCH, Weinheim, 2002.

[37] P. A. M. Dirac, *The Principles of Quantum Mechanics*, Oxford University Press, Oxford, 4th ed., 1982.

[38] D. B. Cook, *Handbook of Computational Quantum Chemistry*, Dover, New York, 2005.

[39] A. Szabo and N. S. Ostlund, *Modern Quantum Chemistry*, Dover, Mineola, NY, 1996.

[40] F. Jensen, *Introduction to Computational Chemistry*, Wiley, Hoboken, NJ, 2nd ed., 2006.

[41] J. B. Foresman and A. Frisch, *Exploring Chemistry With Electronic Structure Methods: A Guide to Using Gaussian*, Gaussian, Inc., Pittsburgh, PA, 2nd ed., 1996.

[42] D. A. McQuarrie and J. D. Simon, *Molecular Thermodynamics*, University Science Books, Sausalito, CA, 1999.

[43] P. W. Atkins and R. S. Friedman, *Molecular Quantum Mechanics*, Oxford University Press, Oxford, 3rd ed., 1999.

[44] P. J. Mohr, B. N. Taylor, and D. B. Newell, *CODATA Recommended Values of the Fundamental Physical Constants: 2006*, Rev. Mod. Phys. **80**, 633 (2008).

[45] M. Born and R. Oppenheimer, *Zur Quantentheorie der Molekeln*, Ann. Phys. **389**, 457 (1927).

[46] G. B. Arfken, H. J. Weber, and F. Harris, *Mathematical Methods for Physicists*, Academic Press, London, 5th ed., 2000.

[47] G. E. Uhlenbeck and S. Goudsmit, *Spinning Electrons and the Structure of Spectra*, Nature **117**, 264 (1926).

[48] W. Pauli, *Über den Zusammenhang des Abschlusses der Elektronengruppen im Atom mit der Komplexstruktur der Spektren*, Zeit. Phys. **31**, 765 (1925).

[49] D. R. Hartree, *The Wave Mechanics of an Atom with a Non-Coulomb Central Field. Part I. Theory and Methods*, Mat. Proc. Cambridge Phil. Soc. **24**, 89 (1928).

[50] D. R. Hartree, *The Wave Mechanics of an Atom with a Non-Coulomb Central Field. Part II. Some Results and Discussion*, Mat. Proc. Cambridge Phil. Soc. **24**, 111 (1928).

[51] D. R. Hartree, *The Wave Mechanics of an Atom with a Non-Coulomb Central Field. Part III. Term Values and Intensities in Series in Optical Spectra*, Mat. Proc. Cambridge Phil. Soc. **24**, 426 (1928).

[52] D. R. Hartree, *The Wave Mechanics of an Atom with a Non-Coulomb Central Field. Part IV. Further Results Relating to Terms of the Optical Spectrum*, Mat. Proc. Cambridge Phil. Soc. **25**, 310 (1929).

[53] J. C. Slater, *The Theory of Complex Spectra*, Phys. Rev. **34**, 1293 (1929).

[54] R. Fletcher, *Practical Methods of Optimization*, Wiley, New York, 2nd ed., 1988.

[55] V. Fock, *Näherungsmethode zur Lösung des quantenmechanischen Mehrkörperproblems*, Zeit. Phys. **61**, 126 (1930).

[56] V. Fock, *"Selfconsistent field" mit Austausch für Natrium*, Zeit. Phys. **62**, 795 (1930).

[57] E. U. Condon, *The Theory of Complex Spectra*, Phys. Rev. **36**, 1121 (1930).

[58] C. Roothaan, *New Developments in Molecular Orbital Theory*, Rev. Mod. Phys. **23**, 69 (1951).

[59] G. G. Hall, *The Molecular Orbital Theory of Chemical Valency. VIII. A Method of Calculating Ionization Potentials*, Proc. R. Soc. Lond. A **205**, 541 (1951).

[60] J. A. Pople and R. K. Nesbet, *Self-Consistent Orbitals for Radicals*, J. Chem. Phys. **22**, 571 (1954).

[61] E. Anderson, Z. Bai, J. Dongarra, A. Greenbaum, A. McKenney, J. D. Croz, S. Hammerling, J. Demmel, C. Bischof, and D. Sorensen, LAPACK: a portable linear algebra library for high-performance computers, in *Proceedings of the 1990 ACM/IEEE conference on Supercomputing*, pages 2–11, New York, 1990, IEEE Computer Society Press.

[62] K. L. Schuchardt, B. T. Didier, T. Elsethagen, L. Sun, V. Gurumoorthi, J. Chase, J. Li, and T. L. Windus, *Basis Set Exchange: A Community Database for Computational Sciences*, J. Chem. Inf. Model. **47**, 1045 (2007).

[63] W. J. Hehre, R. Ditchfield, R. F. Stewart, and J. A. Pople, *Self-Consistent Molecular Orbital Methods. IV. Use of Gaussian Expansions of Slater-Type Orbitals. Extension to Second-Row Molecules*, J. Chem. Phys. **52**, 2769 (1970).

[64] W. J. Hehre, R. F. Stewart, and J. A. Pople, *Self-Consistent Molecular-Orbital Methods. I. Use of Gaussian Expansions of Slater-Type Atomic Orbitals*, J. Chem. Phys. **51**, 2657 (1969).

[65] W. J. Hehre, R. Ditchfield, and J. A. Pople, *Self-Consistent Molecular Orbital Methods. XII. Further Extensions of Gaussian-Type Basis Sets for Use in Molecular Orbital Studies of Organic Molecules*, J. Chem. Phys. **56**, 2257 (1972).

[66] T. Kato, *On the Eigenfunctions of Many-Particle Systems in Quantum Mechanics*, Com. Pure App. Math. **10**, 151 (1957).

[67] R. T. Pack and W. B. Brown, *Cusp Conditions for Molecular Wavefunctions*, J. Chem. Phys. **45**, 556 (1966).

[68] D. P. Tew, *Second Order Coalescence Conditions of Molecular Wave Functions*, J. Chem. Phys. **129**, 014104 (2008).

[69] W. Kutzelnigg, *r12-Dependent Terms in the Wave Function as Closed Sums of Partial Wave Amplitudes for Large l*, Theor. Chim. Acta **68**, 445 (1985).

[70] K. Raghavachari and J. B. Anderson, *Electron Correlation Effects in Molecules*, J. Phys. Chem. **100**, 12960 (1996).

[71] I. Shavitt, *The History and Evolution of Configuration Interaction*, Mol. Phys. **94**, 3 (1998).

[72] B. Klahn and W. A. Bingel, *The Convergence of the Rayleigh-Ritz Method in Quantum Chemistry*, Theor. Chim. Acta **44**, 9 (1977).

[73] J. Čížek, *On the Correlation Problem in Atomic and Molecular Systems. Calculation of Wavefunction Components in Ursell-Type Expansion Using Quantum-Field Theoretical Methods*, J. Chem. Phys. **45**, 4256 (1966).

[74] O. Sinanoğlu, *Many-Electron Theory of Atoms and Molecules. I. Shells, Electron Pairs vs Many-Electron Correlations*, J. Chem. Phys. **36**, 706 (1962).

[75] W. Rudin, *Principles of Mathematical Analysis*, McGraw-Hill, New York, 3rd ed., 1976.

[76] C. Møller and M. S. Plesset, *Note on an Approximation Treatment for Many-Electron Systems*, Phys. Rev. **46**, 618 (1934).

[77] K. Raghavachari, G. W. Trucks, J. A. Pople, and M. Head-Gordon, *A Fifth-Order Perturbation Comparison of Electron Correlation Theories*, Chem. Phys. Lett. **157**, 479 (1989).

[78] K. Raghavachari, J. A. Pople, E. S. Replogle, and M. Head-Gordon, *Fifth Order Møller-Plesset Perturbation Theory: Comparison of Existing Correlation Methods and Implementation of New Methods Correct to Fifth Order*, J. Phys. Chem. **94**, 5579 (1990).

[79] A. Halkier, T. Helgaker, P. Jørgensen, W. Klopper, and J. Olsen, *Basis-Set Convergence of the Energy in Molecular Hartree-Fock Calculations*, Chem. Phys. Lett. **302**, 437 (1999).

[80] D. Feller, *The Use of Systematic Sequences of Wave Functions for Estimating the Complete Basis Set, Full Configuration Interaction Limit in Water*, J. Chem. Phys. **98**, 7059 (1993).

[81] J. M. L. Martin, *Ab Initio Total Atomization Energies of Small Molecules – Towards the Basis Set Limit*, Chem. Phys. Lett. **259**, 669 (1996).

[82] D. G. Truhlar, *Basis-Set Extrapolation*, Chem. Phys. Lett. **294**, 45 (1998).

[83] A. Halkier, T. Helgaker, P. Jørgensen, W. Klopper, H. Koch, J. Olsen, and A. K. Wilson, *Basis-Set Convergence in Correlated Calculations on Ne, N2, and H2O*, Chem. Phys. Lett. **286**, 243 (1998).

[84] S. B. Huh and J. S. Lee, *Basis Set and Correlation Dependent Extrapolation of Correlation Energy*, J. Chem. Phys. **118**, 3035 (2003).

[85] F. Jensen, *Estimating the Hartree-Fock Limit From Finite Basis Set Calculations*, Theor. Chem. Acc. **113**, 267 (2005).

[86] D. W. Schwenke, *The Extrapolation of One-Electron Basis Sets in Electronic Structure Calculations: How It Should Work and How It Can Be Made to Work*, J. Chem. Phys. **122**, 014107 (2005).

[87] A. Karton and J. Martin, *Comment on: "Estimating the Hartree-Fock Limit From Finite Basis Set Calculations" [Jensen F. (2005) Theor. Chem. Acc. 113:267]*, Theor. Chem. Acc. **115**, 330 (2006).

[88] D. Bakowies, *Extrapolation of Electron Correlation Energies to Finite and Complete Basis Set Targets*, J. Chem. Phys. **127**, 084105 (2007).

[89] A. J. C. Varandas, *Extrapolating to the One-Electron Basis-Set Limit in Electronic Structure Calculations*, J. Chem. Phys. **126**, 244105 (2007).

[90] T. G. Williams, N. J. DeYonker, and A. K. Wilson, *Hartree-Fock Complete Basis Set Limit Properties for Transition Metal Diatomics*, J. Chem. Phys. **128**, 044101 (2008).

[91] A. J. C. Varandas, *Generalized Uniform Singlet- and Triplet-Pair Extrapolation of the Correlation Energy to the One Electron Basis Set Limit*, J. Phys. Chem. A **112**, 1841 (2008).

[92] T. H. Dunning, Jr., *Gaussian Basis Sets for Use in Correlated Molecular Calculations. I. The Atoms Boron Through Neon and Hydrogen*, J. Chem. Phys. **90**, 1007 (1989).

[93] R. A. Kendall, T. H. Dunning, Jr., and R. J. Harrison, *Electron Affinities of the First-Row Atoms Revisited. Systematic Basis Sets and Wave Functions*, J. Chem. Phys. **96**, 6796 (1992).

[94] D. E. Woon and T. H. Dunning, Jr., *Gaussian Basis Sets for Use in Correlated Molecular Calculations. IV. Calculation of Static Electrical Response Properties*, J. Chem. Phys. **100**, 2975 (1994).

[95] A. K. Wilson, T. van Mourik, and T. H. Dunning, Jr., *Gaussian Basis Sets for Use in Correlated Molecular Calculations. VI. Sextuple Zeta Correlation Consistent Basis Sets for Boron Through Neon*, THEOCHEM **388**, 339 (1996).

[96] R. G. Parr and W. Yang, *Density-Functional Theory of Atoms and Molecules*, Oxford University Press, Oxford, 1994.

[97] W. Koch and M. C. Holthausen, *A Chemist's Guide to Density Functional Theory*, Wiley-VCH, New York, 2nd ed., 2001.

[98] T. S. Koritsanszky and P. Coppens, *Chemical Applications of X-ray Charge-Density Analysis*, Chem. Rev. **101**, 1583 (2001).

[99] P.-O. Löwdin, *Quantum Theory of Many-Particle Systems. I. Physical Interpretations by Means of Density Matrices, Natural Spin-Orbitals, and Convergence Problems in the Method of Configurational Interaction*, Phys. Rev. **97**, 1474 (1955).

[100] P.-O. Löwdin, *Quantum Theory of Many-Particle Systems. II. Study of the Ordinary Hartree-Fock Approximation*, Phys. Rev. **97**, 1490 (1955).

[101] P. Hohenberg and W. Kohn, *Inhomogeneous Electron Gas*, Phys. Rev. **136**, B864 (1964).

[102] R. F. W. Bader, *Atoms in Molecules: A Quantum Theory*, Oxford University Press, Oxford, 1994.

[103] W. Kohn and L. J. Sham, *Self-Consistent Equations Including Exchange and Correlation Effects*, Phys. Rev. **140**, A1133 (1965).

[104] P. A. M. Dirac, *Note on Exchange Phenomena in the Thomas Atom*, Mat. Proc. Cambridge Phil. Soc. **26**, 376 (1930).

[105] J. C. Slater, *A Simplification of the Hartree-Fock Method*, Phys. Rev. **81**, 385 (1951).

[106] S. H. Vosko, L. Wilk, and M. Nusair, *Accurate Spin-Dependent Electron Liquid Correlation Energies for Local Spin Density Calculations: A Critical Analysis*, Can. J. Phys. **58**, 1200 (1980).

[107] A. D. Becke, *Density-Functional Exchange-Energy Approximation With Correct Asymptotic Behavior*, Phys. Rev. A **38**, 3098 (1988).

[108] J. P. Perdew, J. A. Chevary, S. H. Vosko, K. A. Jackson, M. R. Pederson, D. Singh, and C. Fiolhais, *Atoms, Molecules, Solids, and Surfaces: Applications of the Generalized Gradient Approximation for Exchange and Correlation*, Phys. Rev. B **46**, 6671 (1992).

[109] J. P. Perdew, K. Burke, and Y. Wang, *Generalized Gradient Approximation for the Exchange-Correlation Hole of a Many-Electron System*, Phys. Rev. B **54**, 16533 (1996).

[110] C. Lee, W. Yang, and R. G. Parr, *Development of the Colle-Salvetti Correlation-Energy Formula Into a Functional of the Electron Density*, Phys. Rev. B **37**, 785 (1988).

[111] J. P. Perdew, M. Ernzerhof, and K. Burke, *Rationale for Mixing Exact Exchange With Density Functional Approximations*, J. Chem. Phys. **105**, 9982 (1996).

[112] A. D. Becke, *Density-Functional Thermochemistry. III. The Role of Exact Exchange*, J. Chem. Phys. **98**, 5648 (1993).

[113] P. J. Stephens, F. J. Devlin, C. F. Chabalowski, and M. J. Frisch, *Ab Initio Calculation of Vibrational Absorption and Circular Dichroism Spectra Using Density Functional Force Fields*, J. Phys. Chem. **98**, 11623 (1994).

[114] J. A. Pople, M. Head-Gordon, D. J. Fox, K. Raghavachari, and L. A. Curtiss, *Gaussian-1 Theory: A General Procedure for Prediction of Molecular Energies*, J. Chem. Phys. **90**, 5622 (1989).

[115] L. A. Curtiss, C. Jones, G. W. Trucks, K. Raghavachari, and J. A. Pople, *Gaussian-1 Theory of Molecular Energies for Second-Row Compounds*, J. Chem. Phys. **93**, 2537 (1990).

[116] L. A. Curtiss, K. Raghavachari, G. W. Trucks, and J. A. Pople, *Gaussian-2 Theory for Molecular Energies of First- and Second-Row Compounds*, J. Chem. Phys. **94**, 7221 (1991).

[117] L. A. Curtiss, K. Raghavachari, and J. A. Pople, *Gaussian-2 Theory Using Reduced Møller-Plesset Orders*, J. Chem. Phys. **98**, 1293 (1993).

[118] A. G. Baboul, L. A. Curtiss, P. C. Redfern, and K. Raghavachari, *Gaussian-3 Theory Using Density Functional Geometries and Zero-Point Energies*, J. Chem. Phys. **110**, 7650 (1999).

[119] L. A. Curtiss, P. C. Redfern, K. Raghavachari, V. Rassolov, and J. A. Pople, *Gaussian-3 Theory Using Reduced Møller-Plesset Order*, J. Chem. Phys. **110**, 4703 (1999).

[120] L. A. Curtiss, K. Raghavachari, P. C. Redfern, V. Rassolov, and J. A. Pople, *Gaussian-3 (G3) Theory for Molecules Containing First and Second-Row Atoms*, J. Chem. Phys. **109**, 7764 (1998).

[121] L. A. Curtiss, P. C. Redfern, and K. Raghavachari, *Gaussian-4 Theory*, J. Chem. Phys. **126**, 084108 (2007).

[122] L. A. Curtiss, P. C. Redfern, and K. Raghavachari, *Gaussian-4 Theory Using Reduced Order Perturbation Theory*, J. Chem. Phys. **127**, 124105 (2007).

[123] G. A. Petersson, A. Bennett, T. G. Tensfeldt, M. A. Al-Laham, W. A. Shirley, and J. Mantzaris, *A Complete Basis Set Model Chemistry. I. The Total Energies of Closed-Shell Atoms and Hydrides of the First-Row Elements*, J. Chem. Phys. **89**, 2193 (1988).

[124] G. A. Petersson and M. A. Al-Laham, *A Complete Basis Set Model Chemistry. II. Open-Shell Systems and the Total Energies of the First-Row Atoms*, J. Chem. Phys. **94**, 6081 (1991).

[125] G. A. Petersson, T. G. Tensfeldt, and J. Montgomery, *A Complete Basis Set Model Chemistry. III. The Complete Basis Set-Quadratic Configuration Interaction Family of Methods*, J. Chem. Phys. **94**, 6091 (1991).

[126] J. Montgomery, J. W. Ochterski, and G. A. Petersson, *A Complete Basis Set Model Chemistry. IV. An Improved Atomic Pair Natural Orbital Method*, J. Chem. Phys. **101**, 5900 (1994).

[127] J. W. Ochterski, G. A. Petersson, and J. Montgomery, *A Complete Basis Set Model Chemistry. V. Extensions to Six or More Heavy Atoms*, J. Chem. Phys. **104**, 2598 (1996).

[128] J. Montgomery, M. J. Frisch, J. W. Ochterski, and G. A. Petersson, *A Complete Basis Set Model Chemistry. VI. Use of Density Functional Geometries and Frequencies*, J. Chem. Phys. **110**, 2822 (1999).

[129] J. Montgomery, M. J. Frisch, J. W. Ochterski, and G. A. Petersson, *A Complete Basis Set Model Chemistry. VII. Use of the Minimum Population Localization Method*, J. Chem. Phys. **112**, 6532 (2000).

[130] G. P. F. Wood, L. Radom, G. A. Petersson, E. C. Barnes, M. J. Frisch, and J. Montgomery, *A Restricted-Open-Shell Complete-Basis-Set Model Chemistry*, J. Chem. Phys. **125**, 094106 (2006).

[131] J. M. L. Martin and G. de Oliveira, *Towards Standard Methods for Benchmark Quality Ab Initio Thermochemistry—W1 and W2 Theory*, J. Chem. Phys. **111**, 1843 (1999).

[132] S. Parthiban and J. M. L. Martin, *Assessment of W1 and W2 Theories for the Computation of Electron Affinities, Ionization Potentials, Heats of Formation, and Proton Affinities*, J. Chem. Phys. **114**, 6014 (2001).

[133] A. D. Boese, M. Oren, O. Atasoylu, J. M. L. Martin, M. Kállay, and J. Gaüss, *W3 theory: Robust Computational Thermochemistry in the kJ/mol Accuracy Range*, J. Chem. Phys. **120**, 4129 (2004).

[134] A. Karton, E. Rabinovich, J. M. L. Martin, and B. Ruscic, *W4 Theory for Computational Thermochemistry: In Pursuit of Confident Sub-kJ/mol Predictions*, J. Chem. Phys. **125**, 144108 (2006).

[135] S. Grimme, *Semiempirical GGA-Type Density Functional Constructed With a Long-Range Dispersion Correction*, J. Comput. Chem. **27**, 1787 (2006).

[136] S. Grimme, *Semiempirical Hybrid Density Functional With Perturbative Second-order Correlation*, J. Chem. Phys. **124**, 034108 (2006).

[137] T. Schwabe and S. Grimme, *Towards Chemical Accuracy for the Thermodynamics of Large Molecules: New Hybrid Density Functionals Including Non-Local Correlation Effects*, Phys. Chem. Chem. Phys. **8**, 4398 (2006).

[138] T. Schwabe and S. Grimme, *Double-Hybrid Density Functionals With Long-Range Dispersion Corrections: Higher Accuracy and Extended Applicability*, Phys. Chem. Chem. Phys. **9**, 3397 (2007).

[139] H. Iikura, T. Tsuneda, T. Yanai, and K. Hirao, *A Long-Range Correction Scheme for Generalized-Gradient-Approximation Exchange Functionals*, J. Chem. Phys. **115**, 3540 (2001).

[140] T. Yanai, D. P. Tew, and N. C. Handy, *A New Hybrid Exchange-Correlation Functional Using the Coulomb-Attenuating Method (CAM-B3LYP)*, Chem. Phys. Lett. **393**, 51 (2004).

[141] S. Ten-no, *Initiation of Explicitly Correlated Slater-Type Geminal Theory*, Chem. Phys. Lett. **398**, 56 (2004).

[142] W. Klopper, F. R. Manby, S. Ten-No, and E. F. Valeev, *R12 Methods in Explicitly Correlated Molecular Electronic Structure Theory*, Int. Rev. Phys. Chem. **25**, 427 (2006).

[143] G. Knizia, T. B. Adler, and H. Werner, *Simplified CCSD(T)-F12 Methods: Theory and Benchmarks*, J. Chem. Phys. **130**, 054104 (2009).

[144] M. Schütz, G. Hetzer, and H. Werner, *Low-Order Scaling Local Electron Correlation Methods. I. Linear Scaling Local MP2*, J. Chem. Phys. **111**, 5691 (1999).

[145] G. Hetzer, M. Schütz, H. Stoll, and H. Werner, *Low-Order Scaling Local Correlation Methods II: Splitting the Coulomb Operator in Linear Scaling Local Second-Order Møller-Plesset Perturbation Theory*, J. Chem. Phys. **113**, 9443 (2000).

[146] M. Schütz, *Low-Order Scaling Local Electron Correlation Methods. III. Linear Scaling Local Perturbative Triples Correction (T)*, J. Chem. Phys. **113**, 9986 (2000).

[147] M. Schütz and H. Werner, *Low-Order Scaling Local Electron Correlation Methods. IV. Linear Scaling Local Coupled-Cluster (LCCSD)*, J. Chem. Phys. **114**, 661 (2001).

[148] M. Schütz, *Low-Order Scaling Local Electron Correlation Methods. V. Connected Triples Beyond (T): Linear Scaling Local CCSDT-1b*, J. Chem. Phys. **116**, 8772 (2002).

[149] H. Werner and K. Pflüger, *On the Selection of Domains and Orbital Pairs in Local Correlation Treatments*, Ann. Rep. Comput. Chem. **2**, 53 (2006).

[150] F. R. Manby, H. Werner, T. B. Adler, and A. J. May, *Explicitly Correlated Local Second-Order Perturbation Theory With a Frozen Geminal Correlation Factor*, J. Chem. Phys. **124**, 094103 (2006).

[151] H. Werner and F. R. Manby, *Explicitly Correlated Second-Order Perturbation Theory Using Density Fitting and Local Approximations*, J. Chem. Phys. **124**, 054114 (2006).

[152] H. Werner, *Eliminating the Domain Error in Local Explicitly Correlated Second-Order Møller-Plesset Perturbation Theory*, J. Chem. Phys. **129**, 101103 (2008).

[153] T. B. Adler and H. Werner, *Local Explicitly Correlated Coupled-Cluster Methods: Efficient Removal of the Basis Set Incompleteness and Domain Errors*, J. Chem. Phys. **130**, 241101 (2009).

[154] T. B. Adler, H. Werner, and F. R. Manby, *Local Explicitly Correlated Second-Order Perturbation Theory for the Accurate Treatment of Large Molecules*, J. Chem. Phys. **130**, 054106 (2009).

[155] D. A. Mazziotti, Reduced-Density-Matrix mechanics: With application to Many-Electron atoms and molecules, in *Advances in Chemical Physics*, Wiley, Hoboken, NJ, 2007.

[156] Z. Zhao, B. J. Braams, M. Fukuda, M. L. Overton, and J. K. Percus, *The Reduced Density Matrix Method for Electronic Structure Calculations and the Role of Three-Index Representability Conditions*, J. Chem. Phys. **120**, 2095 (2004).

[157] J. J. Foley, IV, A. E. Rothman, and D. A. Mazziotti, *Activation Energies of Sigmatropic Shifts in Propene and Acetone Enolate From the Anti-Hermitian Contracted Schrödinger Equation*, J. Chem. Phys. **130**, 184112 (2009).

[158] L. Greenman and D. A. Mazziotti, *Highly Multireferenced Arynes Studied With Large Active Spaces Using Two-Electron Reduced Density Matrices*, J. Chem. Phys. **130**, 184101 (2009).

[159] A. E. DePrince, III and D. A. Mazziotti, *Open-Shell Molecular Electronic States From the Parametric Two-Electron Reduced-Density-Matrix Method*, J. Chem. Phys. **130**, 164109 (2009).

[160] D. A. Mazziotti, *Realization of Quantum Chemistry Without Wave Functions Through First-Order Semidefinite Programming*, Phys. Rev. Lett. **93**, 213001 (2004).

[161] D. A. Mazziotti, *First-Order Semidefinite Programming for the Direct Determination of Two-Electron Reduced Density Matrices With Application to Many-Electron Atoms and Molecules*, J. Chem. Phys. **121**, 10957 (2004).

[162] P. W. Atkins, *Physical Chemistry*, W.H. Freeman, New York, 6th ed., 1997.

[163] F. Mandl, *Statistical Physics*, Wiley, New York, 2nd ed., 1988.

[164] G. L. Miessler and D. A. Tarr, *Inorganic Chemistry*, Prentice Hall, Englewood Cliffs,NJ, 1991.

[165] J. B. Pedley, *Thermochemical Data and Structures of Organic Compounds, Vol. 1*, Thermodynamics Research Center, College Station, TX, 1994.

[166] P. M. Nunes, F. Agapito, B. J. Costa Cabral, R. M. Borges dos Santos, and J. A. Martinho Simões, *Enthalpy of Formation of the Cyclopentadienyl Radical: Photoacoustic Calorimetry and Ab Initio Studies*, J. Phys. Chem. A **110**, 5130 (2006).

[167] T. Ichino, S. W. Wren, K. M. Vogelhuber, A. J. Gianola, W. C. Lineberger, and J. F. Stanton, *The Vibronic Level Structure of the Cyclopentadienyl Radical*, J. Chem. Phys. **129**, 084310 (2008).

[168] E. F. C. Byrd, C. D. Sherrill, and M. Head-Gordon, *The Theoretical Prediction of Molecular Radical Species: a Systematic Study of Equilibrium Geometries and Harmonic Vibrational Frequencies*, J. Phys. Chem. A **105**, 9736 (2001).

[169] N. X. Wang and A. K. Wilson, *The Behavior of Density Functionals With Respect to Basis Set. I. The Correlation Consistent Basis Sets*, J. Chem. Phys. **121**, 7632 (2004).

[170] F. Agapito, B. J. C. Cabral, and J. A. Martinho Simões, *A Cost-Effective Basis-Set Extrapolation Scheme: Application to the Energetics of Homolytic Bond Dissociation*, THEOCHEM **811**, 361 (2007).

[171] J. P. Perdew, K. Burke, and M. Ernzerhof, *Generalized Gradient Approximation Made Simple*, Phys. Rev. Lett. **77**, 3865 (1996).

[172] J. P. Perdew, K. Burke, and M. Ernzerhof, *Generalized Gradient Approximation Made Simple [Phys. Rev. Lett. 77, 3865 (1996)]*, Phys. Rev. Lett. **78**, 1396 (1997).

[173] A. D. Becke, *Density-Functional Thermochemistry. V. Systematic Optimization of Exchange-Correlation Functionals*, J. Chem. Phys. **107**, 8554 (1997).

[174] H. L. Schmider and A. D. Becke, *Optimized Density Functionals From the Extended G2 Test Set*, J. Chem. Phys. **108**, 9624 (1998).

[175] T. V. Voorhis and G. E. Scuseria, *A Novel Form for the Exchange-Correlation Energy Functional*, J. Chem. Phys. **109**, 400 (1998).

[176] A. D. Boese and N. C. Handy, *A New Parametrization of Exchange-Correlation Generalized Gradient Approximation Functionals*, J. Chem. Phys. **114**, 5497 (2001).

[177] J. Tao, J. P. Perdew, V. N. Staroverov, and G. E. Scuseria, *Climbing the Density Functional Ladder: Nonempirical Meta-Generalized Gradient Approximation Designed for Molecules and Solids*, Phys. Rev. Lett. **91**, 146401 (2003).

[178] G. Ruberto and M. T. Baratta, *Antioxidant Activity of Selected Essential Oil Components in Two Lipid Model Systems*, Food Chem. **69**, 167 (2000).

[179] M. C. Foti and K. U. Ingold, *Mechanism of Inhibition of Lipid Peroxidation by α-Terpinene, an Unusual and Potentially Useful Hydrocarbon Antioxidant*, J. Agric. Food Chem. **51**, 2758 (2003).

[180] F. Agapito, P. M. Nunes, B. J. C. Cabral, R. M. Borges dos Santos, and J. A. Martinho Simões, *Energetics of the Allyl Group*, J. Org. Chem. **72**, 8770 (2007).

[181] F. Agapito, P. M. Nunes, B. J. C. Cabral, R. M. Borges dos Santos, and J. A. Martinho Simões, *Energetics of the Allyl Group.*, J. Org. Chem. **73**, 2480 (2008).

[182] Y. Gao, N. J. DeYonker, E. C. Garrett, A. K. Wilson, T. R. Cundari, and P. Marshall, *Enthalpy of Formation of the Cyclohexadienyl Radical and the C—H Bond Enthalpy of 1,4-Cyclohexadiene: An Experimental and Computational Re-Evaluation*, J. Phys. Chem. A **113**, 6955 (2009).

[183] F. Agapito, P. M. Nunes, B. J. C. Cabral, R. M. Borges dos Santos, and J. A. Martinho Simões, *Energetic Differences Between the Five- and Six-Membered Ring Hydrocarbons: Strain Energies in the Parent and Radical Molecules*, J. Org. Chem **73**, 6213 (2008).

[184] M. Zhao and B. M. Gimarc, *Strain Energies in Cyclic Oxygen O_n, $n = 3$-8*, J. Phys. Chem. **97**, 4023 (1993).

[185] M. Nett, T. A. M. Gulder, A. J. Kale, C. C. Hughes, and B. S. Moore, *Function-Oriented Biosynthesis of β-Lactone Proteasome Inhibitors in Salinispora Tropica*, J. Med. Chem. **52**, 6163 (2009).